TSL/ISV-93-0091
December, 1993

ISSN 0284-2769

Neutrino-induced muon fluxes from neutralino annihilations in the Sun and in the Earth

Joakim Edsjö

Diploma thesis

Department of Radiation Sciences
Uppsala University
Box 535
S-751 21 Uppsala, Sweden

Abstract

The dark matter in the Universe might be composed of neutralinos, which, if supersymmetry exists, probably is the lightest supersymmetric particle. The neutralinos may annihilate two by two producing e.g. fermion–antifermion pairs, gauge bosons and Higgs bosons. These particles will hadronize and/or decay eventually producing muon neutrinos, which can interact with nuclei at a detector producing detectable muons. In this paper, the flux of muons at a detector at the surface of the Earth is calculated through simulations for neutralino annihilations in the Sun and in the Earth for different neutralino masses and annihilation channels. The muon fluxes are integrated with different cuts in energy and muon direction and presented in tables. They are also parametrized and are hence easy to use when calculating event rates in a specific detector. Some examples are included for the AMANDA detector, located at the south pole. The background flux of muons is also considered in some detail, with some specific calculations for the AMANDA detector. The result is that AMANDA should be able to investigate parts of the supersymmetric parameter space and either find a significant muon neutrino flux from neutralino annihilations or put new constraints on the supersymmetric parameters.

Contents

1 Introduction

If one looks at for example galaxies, the amount of visible matter is not enough to account for the rotation of them. The extra matter needed to obtain the correct dynamics as predicted by Newtonian dynamics and the gravitation law is called *dark matter*. Another possibility is of course that the Newtonian dynamics and the gravitation law is not correct at these huge scales (see eg. [1]), but that possibility is not considered further here. If the dark matter particles moved with non-relativistic velocities when they decoupled in the early Universe they are said to be *cold* dark matter and it is believed that they may be neutralinos, which are supersymmetric particles. If they exist, they will get trapped in the Sun and in the Earth and annihilate into different particles, for example quark–antiquark, lepton–antilepton, W^+W^- etc. Which channels that dominate depends on the neutralino mass, the supersymmetric model used and its parameters. The annihilation products will hadronize (if quarks) or decay (if tau leptons for example) and eventually produce energetic muon neutrinos. These muon neutrinos can traverse the Sun or the Earth and enter the detector where they may interact via a charged current interaction producing a muon which can be detected.

One can wonder why just the muon neutrinos are of interest, and the answer is that there are no other known sources of high energy muon neutrinos from the Sun[1] or the core of the Earth. Another reason is that when a muon neutrino interacts with a detector on the Earth it produces muons which have much longer range than electrons and does not decay as tauons does. Hence the muon neutrinos are interesting.

The problems involved with estimating the flux of muons on the Earth from neutralino annihilations can be divided into different subproblems: annihilation processes, stopping of annihilation products, stopping of neutrinos on the way to the detector and interactions in the ice. In sec. 2 the annihilation process is considered, in sec. 3 the interaction of the annihilation products in the Sun and the Earth is considered, in sec. 4 the interaction of neutrinos with the Sun and the Earth is considered and in sec. 5 the muon interactions in the ice is studied. In sec. 6 the muon flux and event rate in the detector is calculated.

This study is performed with the AMANDA detector [2] in mind, but the results are quite general until sec. 6.5. The only assumptions specific for the AMANDA detector made before that section is that the detector medium is ice (i.e. not an isoscalar medium), but if one uses these results for an isoscalar medium (i.e. rock) the error one makes is only of the order of 5%.

2 Capture and annihilation of neutralinos

If supersymmetry exists there will be a lightest stable supersymmetric particle, the LSP. The LSP is most likely the lightest neutralino (see e.g. [3]). If the dark matter is the LSP, the galactic halo will contain a lot of them. As the Sun and the Earth travel through the galactic halo the neutralinos will then get trapped gravitationally and further on annihilate. The capture rate for these neutralinos in the galactic halo depends on the cross section for interaction between the neutralino and the nucleons of the Sun or the Earth. The capture rates have been calculated, e.g. by Kamionkowski [4] using the formulas of Gould [5].

[1] There are at least not any known sources which would give an appreciable flux of high energy muon neutrinos. As will be seen in sec. 7.3 there are other sources of high energy muon neutrinos from the Sun, but these can be neglected.

2.1 Short review of the Minimal SuperSymmetric Model (MSSM)

The Standard Model is an accurate low-energy theory at energy scales up to 100 GeV. In fact, no experimentally confirmed deviations from it have yet been found. However, theorists strongly believe that the success of the Standard Model will not persist to higher energy scales. A theory that would work even at higher energy scales is the supersymmetric extension of the Standard Model, but there is not yet any experimental evidence for it. There exist a lot of different supersymmetric theories of which the Minimal SuperSymmetric Model (MSSM) is the simplest one. Here only the main features are going to be reviewed and for further information, see e.g. ref. [6]. In the MSSM there is one supersymmetric partner for each particle of the standard model. The fermions have integer spin partners whose name is obtained by adding the prefix *s-* to the normal particle name. The bosons have half integer spin partners whose name is obtained by adding the suffix *-ino* to the root of the normal particle name. Hence one gets photinos, squarks, sleptons etc. All supersymmetric particles carry a new quantum number, R, which is believed to be conserved. All ordinary particles have R even and all supersymmetric particles have R odd. According to this it is not possible for a supersymmetric particle to decay into ordinary particles without leaving another supersymmetric particle behind as well. Thus there should exist a lightest supersymmetric particle, the LSP, which all other supersymmetric particles eventually decay into. The LSP is likely to be the lightest neutralino as mentioned above. The neutralinos are Majorana particles which means that they are their own antiparticles. Hence it is possible for them to annihilate two by two producing only ordinary particles. This will be considered in more detail in sec. 2.4.

There are three independent free parameters of the model and they can be chosen to be the ratio of the two vacuum expectation values of the Higgs fields, $\tan\beta = v_2/v_1$, the gaugino mass parameter, M_2, and the Higgsino mass parameter, μ. The mass of one of the neutral Higgs bosons and the top quark mass, m_t, also have to be put into the model.

There are four neutralinos, the $\widetilde{W}_3$, the $\widetilde{B}$, the $\widetilde{H}_1^0$ and the $\widetilde{H}_2^0$, i.e. the partners of the neutral SU(2) and U(1) gauge bosons and of the neutral components of the two Higgs doublets respectively. The first two are called gauginos and the last two Higgsinos. These neutralinos are not the mass eigenstates and in the base ($\widetilde{B}$,$\widetilde{W}_3$,$\widetilde{H}_1^0$,$\widetilde{H}_2^0$) the mass matrix is

$$\begin{pmatrix} M_1 & 0 & -m_Z\cos\beta\sin\theta_W & m_Z\sin\beta\sin\theta_W \\ 0 & M_2 & m_Z\cos\beta\cos\theta_W & -m_Z\sin\beta\cos\theta_W \\ -m_Z\cos\beta\sin\theta_W & m_Z\cos\beta\cos\theta_W & 0 & -\mu \\ m_Z\sin\beta\sin\theta_W & -m_Z\sin\beta\cos\theta_W & -\mu & 0 \end{pmatrix} \tag{1}$$

where m_Z is the mass of the Z^0 and θ_W is the Weinberg angle, which describes the mixing of the fundamental vector fields $W^{(1)}$, $W^{(2)}$, $W^{(3)}$ and B into the physical photon and the gauge bosons W^+, W^- and Z^0. If one assumes that the masses of all the gauginos at some grand unification scale are equal, the $\widetilde{B}$ mass term M_1 is given by $M_1 = \frac{5}{3}M_2\tan^2\theta_W$ [7]. The masses of the neutralinos is then obtained by diagonalising the mass matrix and the lightest neutralino, $\tilde{\chi}$, can then be written as

$$\tilde{\chi} = Z_1\widetilde{B} + Z_2\widetilde{W}_3 + Z_3\widetilde{H}_1^0 + Z_4\widetilde{H}_2^0 \tag{2}$$

where the Z_i's are the appropriate components of the matrix that diagonalizes the mass matrix. The Z_i's of course depend on M_2, μ and $\tan\beta$. In the following, *the neutralino* will be used as short for *the lightest neutralino*. As noted by Olive and Srednicki [8], in much of parameter space where the neutralino is heavier than the W, the gaugino fraction is greater than 0.99 and the neutralino is an almost pure $\widetilde{B}$.

Earlier neutralino searches have resulted in limits on the neutralino mass, which at present is [9] $m_{\tilde{\chi}} > 18$ GeV (with some Grand Unifying Theory assumptions made).

In the MSSM there are five Higgs bosons, three neutral ones (H_1^0, H_2^0 and H_3^0) and two charged ones (H^+ and H^-). To first order, the masses of the Higgs bosons are limited by

$$\begin{cases} m_{H_2^0} \leq |\cos(2\beta)| m_Z \\ m_{H_1^0} \geq m_Z \\ m_{H_2^0} < m_{H_3^0} < m_{H_1^0} \\ m_{H^\pm} \geq m_W \end{cases} \tag{3}$$

where m_Z and m_W are the masses of the Z^0 and the W respectively. To make the simulations simpler, the MSSM parameter dependence of the masses will be neglected and I choose the masses of the Higgs bosons to be

$$\begin{cases} m_{H_2^0} & = & 70 & \text{GeV} \\ m_{H_3^0} & = & 150 & \text{GeV} \\ m_{H_1^0} & = & 200 & \text{GeV} \\ m_{H^\pm} & = & 200 & \text{GeV} \end{cases} . \tag{4}$$

The decay branching ratios of the Higgs bosons depend on the MSSM parameters and in this paper this dependence will also be neglected. I choose the branching ratios, B_i, for the Higgs bosons to be

$$\begin{cases} B_{b\bar{b}} & = & 0.82 \\ B_{c\bar{c}} & = & 0.08 \\ B_{s\bar{s}} & = & 0.01 \\ B_{\tau^+\tau^-} & = & 0.09 \end{cases} \quad \text{for } H_1^0, H_2^0 \text{ and } H_3^0 \tag{5}$$

and

$$B_{\bar{b}t} = 1.00 \quad \text{for } H^\pm. \tag{6}$$

The approximate treatment of the Higgs bosons makes the simulations very much simpler since with these fixed choices of masses and branching ratios, the MSSM parameters do not enter the simulations at all, they only enter when one wants to know the annihilation branching ratios and capture rates. All the simulations where Higgs bosons are considered will use the masses and branching ratios above. As will be seen in sec 6.2 it is possible to calculate approximate muon fluxes from the Higgs channels with the results of the other channels and hence one can calculate the muon fluxes from other choices of masses and branching ratios if one wishes. If the annihilation channels with Higgs bosons are the dominating ones and precise results are needed, it may be necessary to use the actual masses and branching ratios for given MSSM parameters and calculate the muon fluxes as mentioned above. In other cases, the approximate results from the simulations can be used as a guideline.

Another yet unknown mass is the mass of the top quark. Throughout this paper, a top mass of $m_t = 150$ GeV will be used since recent LEP results favour a heavy top quark in this mass region.

2.2 Annihilation rate

Neutralinos accumulate in the Sun and in the Earth by capture from the galactic halo and are depleted by annihilation and evaporation. The equation for the number of neutralinos in the

Sun or the Earth, N, is

$$\frac{dN}{dt} = C - C_A N^2 - C_E N \tag{7}$$

where C is the capture rate of neutralinos from the galactic halo, $C_A N^2$ is twice the annihilation rate (two neutralinos are needed for one annihilation) and $C_E N$ is the evaporation rate. It has been shown [10] that evaporation is only important below a critical neutralino mass of about 4 GeV in case of the Sun, and hence the last term of eq. (7) can be dropped. In case of neutralinos in the Earth, no calculations on the evaporation from the Earth have been found, but if one consideres fig. 1b, where the annihilation profile (which is proportional to the neutralino density squared) in the Earth is shown, one can conclude that hardly no neutralinos at all come far out from the core of the Earth. Hence, it seems reasonable to assume that the evaporation can be neglected also for the Earth.

Solving eq. (7) for the annihilation rate, Γ_A, yields

$$\Gamma_A = \frac{C}{2} \tanh^2(t/\tau_A) \tag{8}$$

where $\tau_A = (CC_A)^{-1/2}$ is the time scale for capture and annihilation to reach equilibrium. If the age of the Sun is much larger than τ_A equilibrium is reached and $\Gamma_A = C/2$.

2.3 Annihilation profile

The annihilation rate per volume element is given by [11]

$$\Gamma = n^2 \langle \sigma v \rangle_A \tag{9}$$

where n is the number density of neutralinos and $\langle \sigma v \rangle_A$ is the thermally averaged annihilation cross section. For neutralinos which move non-relativistically, $\langle \sigma v \rangle_A$ is independent of the temperature [11]. To determine where the annihilation takes place one has to calculate the neutralino density, n, as a function of radius in the Sun and in the Earth. The neutralinos are imagined having a temperature of $T_{\tilde{\chi}}$ which is expected to be independent of radius since the neutralino interacts so weakly with matter and hence will orbit several times between each interaction. If the density of neutralinos is significant only in the core the neutralino temperature can be put to the core temperature to a good approximation. (Ritz and Seckel actually concluded that $T_{\tilde{\chi}} \simeq T_C$ (T_C is the temperature in the core of the Sun) for neutralino masses of 10 and 20 GeV and thus the approximatin seems satisfactory.)

To calculate the density of neutralinos a bit of statistical mechanics is needed. According to classical statistical mechanics (see e.g. sec. 7.9 of [12]) the probability of finding a classical system of ν degrees of freedom in a state $q_1, q_1 + dq_1, \ldots q_\nu, q_\nu + dq_\nu, p_1, p_1 + dp_1, \ldots p_\nu, p_\nu + dp_\nu$ is given by

$$p\, dq_1 \ldots dp_\nu = \frac{f(q_1, \ldots p_\nu) \exp(-\beta H(q_1, \ldots p_\nu))\, dq_1 \ldots dp_\nu}{\int f(q_1, \ldots p_\nu) \exp(-\beta H(q_1, \ldots p_\nu))\, dq_1 \ldots dp_\nu} \tag{10}$$

where $q_1, \ldots q_\nu$ and $p_1, \ldots p_\nu$ are the generalized coordinates and their conjugate momenta, $f(q_1, \ldots p_\nu)$ is the density of states in phase space, $\beta = 1/(k_B T)$ and $H(q_1, \ldots p_\nu)$ is the Hamiltonian (total energy) of the system. Since the density of states is constant in phase space, i.e. $f = const.$, eq. (10) reduces to

$$p\, dq_1 \ldots dp_\nu = \frac{\exp(-\beta H(q_1, \ldots p_\nu))\, dq_1 \ldots dp_\nu}{\int \exp(-\beta H(q_1, \ldots p_\nu))\, dq_1 \ldots dp_\nu}. \tag{11}$$

Now imagine a system of N neutralinos in the gravitational potential of the Sun or the Earth. If the number of neutralinos is small enough not to change the gravitational potential significantly the Hamiltonian can be written as $H = H_1 + H_2 + \cdots + H_N$ where each term H_i only depends on the generalized coordinates and conjugate momenta of neutralino number i. In this case the Boltzmann factor factorizes as $\exp(-\beta H) = \exp(-\beta H_1) \cdots \exp(-\beta H_N)$. Now consider one neutralino with generalized coordinates and conjugate momenta q_1, q_2, q_3 and p_1, p_2, p_3. The probability of finding this particle in a state $q_1, q_1 + dq_1, \ldots p_3, p_3 + dp_3$ is then given by integration of eq. (11) over the coordinates and momenta for the other particles. Since the Boltzmann factor factorizes the probability becomes

$$p \, dq_1 dq_2 dq_3 dp_1 dp_2 dp_3 = \frac{\exp(-\beta H_1(q_1, q_2, q_3, p_1, p_2, p_3)) \, dq_1 dq_2 dq_3 dp_1 dp_2 dp_3}{\int \exp(-\beta H_1(q_1, q_2, q_3, p_1, p_2, p_3)) \, dq_1 dq_2 dq_3 dp_1 dp_2 dp_3}. \tag{12}$$

Since the gravitational potential of the Sun or the Earth only depends on radial distance from the core it is wise to use polar coordinates, $q_1 = r$, $q_2 = \theta$ and $q_3 = \phi$. If the gravitational potential is called $\Phi(r)$ the potential energy of a neutralino of mass $m_{\tilde{\chi}}$ is $m_{\tilde{\chi}} \Phi(r)$ and the Hamiltonian becomes $H_1 = K_1 + m_{\tilde{\chi}} \Phi(r)$ where K_1 is the kinetic energy of the particle. Since the Hamiltonian is independent of θ and ϕ, the probability of finding a neutralino at a radius r is also independent of θ and ϕ. The probability of finding a neutralino in $q_1, q_1 + dq_1$ is then given by

$$\begin{aligned} p \, dq_1 &= \frac{\int \exp(-\beta K_1(q_1, q_2, q_3, p_1, p_2, p_3)) \, dp_1 dp_2 dp_3 \int dq_2 \int dq_3 \exp(-\beta m_{\tilde{\chi}} \Phi(q_1))}{\int \exp(-\beta K_1(q_1, q_2, q_3, p_1, p_2, p_3)) \, dp_1 dp_2 dp_3 \int dq_2 \int dq_3 \int \exp(-\beta m_{\tilde{\chi}} \Phi(q_1)) \, dq_1} \\ &= \frac{\exp(-\beta m_{\tilde{\chi}} \Phi(q_1))}{\int \exp(-\beta m_{\tilde{\chi}} \Phi(q_1)) \, dq_1} = const. \; \exp(-\beta m_{\tilde{\chi}} \Phi(r)). \end{aligned} \tag{13}$$

The potential energy as a function of radius can be calculated by noting that the force on a particle of mass $m_{\tilde{\chi}}$ at a radius of r is

$$\boldsymbol{F} = -\frac{G m_{\tilde{\chi}} M(r)}{r^2} \hat{\boldsymbol{r}} \tag{14}$$

where G is the gravitational constant and $M(r)$ is the mass of the Sun or the Earth up to the radius r and is given by

$$M(r) = \int_0^r \rho(r') 4\pi r'^2 \, dr' \tag{15}$$

where $\rho(r)$ is the density at radius r. Since the force is equal to $\boldsymbol{F} = -\boldsymbol{\nabla} m_{\tilde{\chi}} \Phi(r)$ one can integrate eq. (14) to get the potential. Doing that yields

$$\Phi(r) = \int_0^r \frac{G M(r')}{r'^2} \, dr' \tag{16}$$

where the arbitrary constant of the potential is chosen to be zero at $r = 0$. By introducing a new dimensionless paramter $x = r/R$ where R is the radius of the Sun or the Earth and putting the potential in eq. (16) into eq. (13) one obtains

$$n(x) = n_C \exp \left[-\frac{m_{\tilde{\chi}} \Phi(x)}{k_B T_{\tilde{\chi}}} \right] = n_C \exp \left[-\frac{m_{\tilde{\chi}}}{k_B T_{\tilde{\chi}}} \frac{1}{R} \int_0^x \frac{G M(x)}{x^2} \, dx \right]. \tag{17}$$

The annihilation probability is proportional to n^2 as given by eq. (9). The interesting thing here is how far out from the center of the Sun or the Earth that a significant amount of annihilation

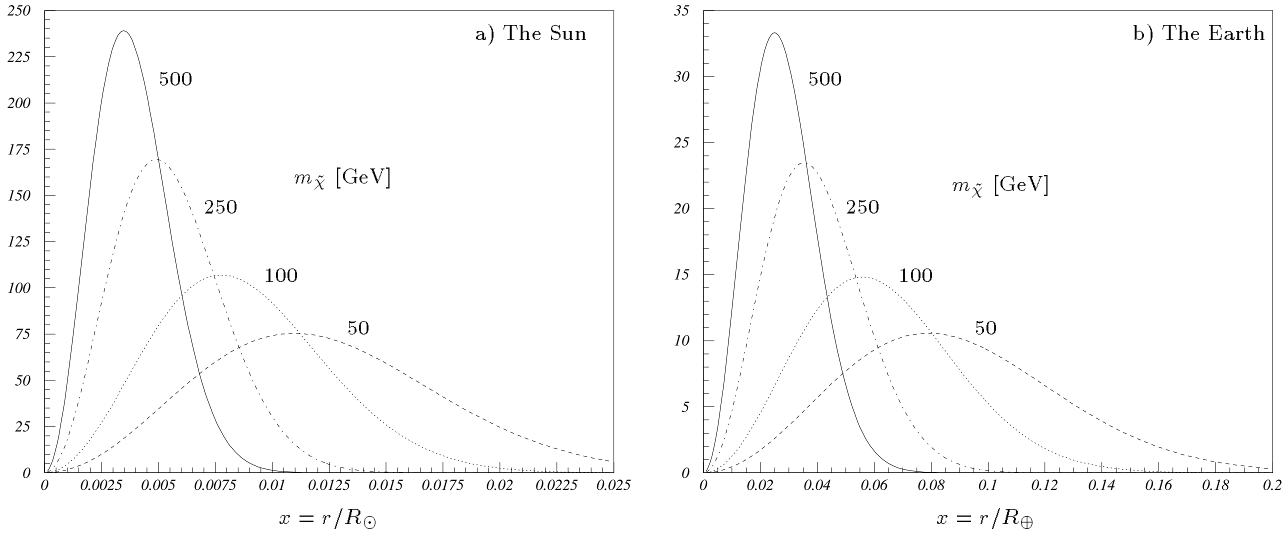

Figure 1: *The annihilation profile (eq. (18)) for neutralinos of the specified masses. The scale on the y-axis is arbitrary and the curves are normalized to have equal area. The neutralino density is calculated with a) eq. (19) in the Sun and b) eq. (22) in the Earth.*

takes place. The probability that annihilation takes place in a spherical shell of radius x and thickness dx is given by

$$dp_A \propto n^2(x)x^2\,dx \tag{18}$$

and the total probability that annihilation takes place within a certain radius x_{max} is of course proportional to $\int_0^{x_{max}} n^2(x)x^2dx$.

To calculate $n(x)$, the density of the Sun and the Earth is needed as a function of radius. At first, annihilation in the Sun will be considered. The density function and temperature in the core of the Sun is obtained from the solar model of Bahcall et al. [13]. They obtained a core temperature of $T_C = 1.56 \times 10^7$ K. An important assumption here is that the presence of neutralinos in the Sun *does not* change the Bahcall results significantly. If the annihilation takes place mainly in the region where the density is approximately constant the integration in eq. (15) becomes very simple. Assuming that the density is constant and equal to the core density of the Sun, $\rho \approx \rho_{core} = 148$ g/cm^3 gives

$$n(x) = n_C \exp(-82.93\,x^2 m_{\tilde{\chi}}) \tag{19}$$

where the mass of the neutralino should be given in GeV. By using this equation and eq. (18) the annihilation profile can be calculated. In fig. 1a the annihilation profile is shown for some different neutralino masses and in table 1 the amount of annihilation within certain radii is shown. As can be seen, most of the annihilation takes place within $x = 0.02$ and according to the solar model of Bahcall the density in this region is nearly constant. Hence the approximation of constant density is justified. A more detailed analysis has been performed where the actual density from Bahcall has been used. The neutralino density has then been calculated and compared with the approximate eq. (19). The result is that eq. (19) is accurate to within 5% in the region where 99% of the annihilation takes place. The error is largest for a neutralino mass of 50 GeV and at high x whereas at lower x-values and higher masses the accuracy is much better then 5%. Since the error is so small in the interesting region, eq. (19) can be used as a good approximation.

$m_{\tilde{\chi}}$ [GeV]	Fraction of annihilation taking place up to x_{max} =							
	0.0010	0.0025	0.0050	0.0075	0.0100	0.0150	0.0200	0.0500
50	0.001	0.009	0.063	0.183	0.354	0.708	0.915	1.000
100	0.002	0.024	0.158	0.399	0.655	0.941	0.996	1.000
150	0.003	0.042	0.258	0.576	0.826	0.989	1.000	1.000
200	0.004	0.063	0.354	0.708	0.915	0.998	1.000	1.000
250	0.006	0.085	0.443	0.802	0.960	1.000	1.000	1.000
500	0.017	0.208	0.754	0.975	0.999	1.000	1.000	1.000

Table 1: *The annihilation of neutralinos in the Sun taking place up to different fractions of the radius of the Sun for different neutralino masses. The results are obtained by integration of eq. (18) with the approximate neutralino density of eq (19).*

It is now necessary to estimate the density of neutralinos in the Sun to see if the assumption that it is small enough not to change the Bahcall results and the gravitational potential is correct. The total rate of annihilations is given by integration of eq. (9)

$$\Gamma_A = 4\pi \langle \sigma v \rangle_A n_C^2 R_\odot^3 \int_0^1 \frac{n^2(x)}{n_C^2} x^2 \, dx \tag{20}$$

The thermally averaged cross section is for photinos [14] given by

$$\langle \sigma v \rangle_A \simeq \frac{0.88 \times 10^{-26}}{1 + 0.04 m_{\tilde{\chi}}^2} \ \mathrm{cm^3/s} \tag{21}$$

For a neutralino mass of 50 GeV one then gets $\Gamma_A \simeq 0.22 n_C^2$. Assuming that the annihilation rate, Γ_A, is of the order of 10^{24} s^{-1} [4] one gets $n_C \simeq 2.1 \times 10^{12}$ cm^{-3} which corresponds to a mass density of $\rho_{\tilde{\chi}} \simeq 1.9 \times 10^{-10}$ g/cm^3. With the same assumptions one gets for a neutralino mass of 500 GeV that $n_C \simeq 1.2 \times 10^{14}$ cm^{-3} and $\rho_{\tilde{\chi}} \simeq 1.1 \times 10^{-7}$ g/cm^3. These densities should be compared with the calculated core density of 148 g/cm^3 in the Bahcall model. Hence the neutralinos do not contribute much at all to the mass density in the Sun and it is thus probable that the calculations of Bahcall without neutralinos can be used as was done. This estimate was quite rough, but the annihilation rate is probably not much higher than 10^{24} s^{-1} so a change in this number would not change the mass density to higher values. If, however, the thermally averaged cross section for other neutralinos than a pure photino is significantly smaller than that given by eq. (21), the density of neutralinos will increase and become larger but it will probably still be negligible compared to the density of other elements in the core of the Sun. The neutralino can also interact weakly with the solar medium, but it is reasonable to assume that these interactions will not change the Bahcall results significantly.

Now consider annihilation in the Earth. The density function and core temperature is obtained from [15]. In the Earth as well, one has to assume that the presence of neutralinos does not change the density profile significantly. The core density is $\rho_{core} = 13.09$ g/cm^3 and the temperature in the core is $T_C \approx 6000$ K. Again assuming that the annihilation takes place in the region where the density is approximately constant and equal to the core density, one obtains

$$n(x) = n_C \exp(-1.601\, x^2 m_{\tilde{\chi}}) \tag{22}$$

$m_{\tilde{\chi}}$ [GeV]	Fraction of annihilation taking place up to x_{max} =							
	0.010	0.020	0.030	0.040	0.050	0.075	0.100	0.150
50	0.002	0.012	0.038	0.084	0.151	0.387	0.642	0.939
100	0.004	0.032	0.098	0.205	0.341	0.692	0.907	0.998
150	0.008	0.057	0.166	0.326	0.507	0.856	0.978	1.000
200	0.012	0.084	0.236	0.438	0.639	0.934	0.995	1.000
250	0.016	0.113	0.304	0.536	0.739	0.971	0.999	1.000
500	0.044	0.266	0.590	0.837	0.954	1.000	1.000	1.000

Table 2: *The annihilaton of neutralinos in the Earth taking place up to different fractions of the radius of the Earth for different neutralino masses. The results are obtained by integration of eq. (18) with the approximate neutralino density of eq. (22).*

where the neutralino mass should be given in GeV. By using this equation and eq. (18) the annihilation profile can be calculated for the Earth. In fig. 1b the annihilation profile is shown for some different neutralino masses and in table 2 the amount of annihilation within certain radii is shown. As can be seen, most of the annihilation takes place within $x = 0.15$ where the density is almost equal to the core density. Hence the approximation of constant density is justified. A more detailed analysis has been performed where the actual density from [15] has been used. The neutralino density has then been calculated and compared with the approximate eq. (22). The result is that eq. (22) is accurate to within 2% in the region where 99% of the annihilation takes place. The error is largest for a neutralino mass of 50 GeV and at high x whereas at lower x-values and higher masses the accuracy is much better then 2%. Since the error is so small in the interesting region, eq. (22) can be used as a good approximation.

By assuming that the capture rate in the Earth is of the order of 10^{14} s^{-1} one can calculate the mass density of neutralinos in the Earth in the same way as it was done in the Sun above. The result is that the mass density of neutralinos is totally negligible compared to the mass density from ordinary matter. Hence, the assumption that the neutralino density is small enough not to change the results in [15] is justified.

2.4 Annihilation channels

As mentioned in sec. 2.1 two neutralinos can annihilate into different channels, for example [4] $f\bar{f}$, where f is a fermion, W^+W^-, Z^0Z^0, $H_1^0H_3^0$, $Z^0H_1^0$, $Z^0H_2^0$, W^+H^- and W^-H^+. The lowest order annihilation diagram into $f\bar{f}$ is shown in fig. 2. The annihilation cross section into fermions is essentially proportional to the fermion mass squared. Hence, annihilation into quarks will be dominated by the heavy quarks (c, b and t). Therefore only these quarks will be considered. According to a recent calculation by M. Drees et al. [16] the annihilation into gg and $gq\bar{q}$ is not negligible and must also be taken account of. For a pure $\widetilde{B}$ they obtained

$$\frac{\sigma_{gg}}{\sigma_{f\bar{f}}} \simeq \left(\frac{m_{\tilde{\chi}}}{50\text{ GeV}}\right)^2, \tag{23}$$

when $m_b \ll m_{\tilde{\chi}} \ll m_t, m_{\tilde{q}}$ where m_b is the mass of the bottom quark, m_t is the mass of the top quark and $m_{\tilde{q}}$ is the mass of the squarks. Roughly speaking one can conclude that these

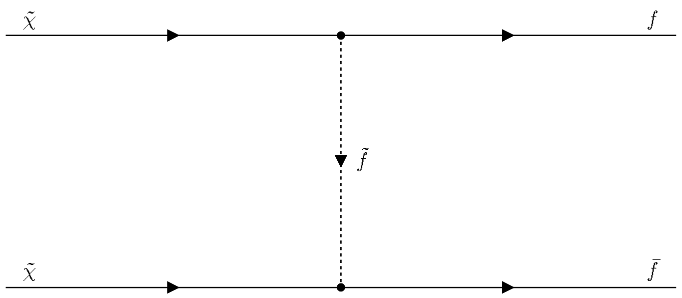

Figure 2: *The lowest order diagram for annihilation of two neutralinos into two fermions.*

two new channels decrease the branching ratios into the other channels by a factor of ~ 2. The gg-channel gives essentially no energetic neutrinos while the $gq\bar{q}$-channel can give some energetic neutrinos from the $q\bar{q}$-pair. According to Drees et al. [16] 2/3 or less of the available energy goes into the $q\bar{q}$-pair and less than 50% of the $q\bar{q}$-pairs produced are heavy quarks. Furthermore, if the branching ratio into $gq\bar{q}$ is large, less than 2/3 of the available energy goes into the $q\bar{q}$-pair. Hence this channel will in general not give many high energy neutrinos either. Thus, the effect of these two channels is to decrease the muon flux by about the same amount as the branching ratios into the other channels are decreased.

2.5 Numerical examples of branching ratios and capture rates

L. Bergström [17] are calculating branching ratios to different neutralino annihilation channels. In table 5 (in sec. 6.6) some examples are shown for different MSSM parameters. Kamionkowski [4] has calculated the capture rate in the Sun for different MSSM parameters (and with the assumption that the density in the Universe is exactly critical and that all dark matter is made up of neutralinos) and using his graphs, the capture rates in the Sun for the examples in the table are also shown. M. Mori et al. [18] have calculated the capture rates in the Earth (with the same assumptions) and the values obtained from their graphs are also shown in the table. These capture rates are, however, only approximate since both Kamionkowski and Mori et al. have used another mass of the H_2^0 (50 and 45 GeV) than chosen here. The capture rate for the Earth when $\tan\beta = 25$ is obtained form Mori et al.'s graph for $\tan\beta = 8$, but they claim that it is qulitatively correct also at higer values of $\tan\beta$. Also shown is the approximate gaugino fraction of the neutralino which is also obtained from the graphs of Kamionkowski. The examples in table 5 will be used in sec. 6.6 where asolute event rates are calculated for the AMANDA detector (which is also shown in the table).

L. Bergström and K. Mellbourn[19] are about to present results on both branching ratios and capture rates in the Sun and in the Earth. Those results can than be used to predict event rates over a larger range of MSSM parameters than those in table 5.

2.6 Conclusions

Of course the mixing of the neutralinos to get the lightest neutralino is important in many aspects. For example the cross section for scattering off nuclei in the Sun or in the Earth depends on the mixing and hence the capture rate does. Also the branching ratios into different channels depend on the mixing and doing these calculations for different parameter values is a big task in itself and hence it can not be covered in this paper. The examples in table 5 will be used in sec. 6.6 to calculate examples of event rates in the AMANDA detector. Until then only the process from the primary annihilation products and onwards will be considered channel by channel.

3 Interactions of the annihilation products

According to sec. 2.3, the annihilation can be considered to take place primarily in the core of the Sun or the Earth where the density is approximately $\rho_{core} = 148$ g/cm^3 in the Sun and $\rho_{core} = 13.09$ g/cm^3 in the Earth. This is quite a dense environment for particles to travel in. If the annihilation products are quarks, hadronic jets will form and some of the produced hadrons and leptons will eventually decay producing muon neutrinos. In some cases these particles will be able to interact with the surrounding medium before they decay and hence lose part of their energy. The problem has been studied by Ritz and Seckel [11] and their approach will partly be followed here.

3.1 Stopping of light hadrons

If the annihilation products are quarks, the heavy quarks (c, b or t) will dominate as mentioned in sec. 2.4. One will get a heavy $q\bar{q}$-pair going off back-to-back. These will hadronize which usually results in two back-to-back jets of light hadrons (i.e. containing only u, d or s quarks) plus one leading heavy hadron (containing the heavy quark) in each jet. Firstly, the light hadrons will be considered.

The interaction time scale is given by [11]

$$\tau_{int} = [n\sigma v]^{-1} = 5.5 \times 10^{-35} [\rho\sigma\beta]^{-1} \text{ s} \tag{24}$$

where ρ is the density of the medium in g/cm^3, σ is the cross section in cm^2 and β is the hadron velocity. $\pi^\pm$ and K's can decay to muon neutrinos (directly or indirectly) and for them the interaction cross section is $\sigma \approx 20$ mb [20] in the relativistic regime. Since the density in the core of the Sun is about 148 g/cm^3 [13] the interaction time scale is $\tau_{int} \approx 1.9 \times 10^{-11}$ s in the Sun. The density in the core of the Earth is 13.09 g/cm^3 [15] which gives the interaction time scale $\tau_{int} \approx 2.1 \times 10^{-10}$ s in the Earth. The life times of π's and K's are about 10^{-8} s and hence they will be stopped before they decay both in the Sun and in the Earth.

A collision of a light hadron with a nucleus produces more light hadrons and some heavier hadrons if the energy is high enough. The energy of the products are of course smaller than the π or K energy and thus the energy of π's and K's are soon distributed among a lot of non-relativistic particles which are of no interest in this study. The conclusion is then that the lighter hadrons in the jets can be ignored as producers of high energy muon neutrinos.

3.2 Stopping of heavy hadrons

Concerning the heavy hadrons (i.e. hadrons containing c, b or t quarks) the situation is different. One will get two back-to-back jets of hadrons with a heavy hadron as the leading, most energetic particle. The lifetimes for hadrons containing c- or b-quarks are of the order of $\tau_{dec} \approx 10^{-12}$–$10^{-13}$ s. The cross sections for scattering off a nucleon can be estimated as follows. B. Povh et al. [20] have concluded that the total cross section for scattering of a hadron on a proton is

$$\sigma^{tot}_{hadron\ p} \simeq 6 \langle r^2_{st} \rangle_{hadron} \tag{25}$$

where $\langle r_{st}^2 \rangle_{hadron}$ is the mean squared strong interaction radius of the hadron. They also concluded that the value of $\langle r_{st}^2 \rangle_{hadron}$ decreases by nearly constant steps as the number of strange valence quarks increases by one unit (while keeping the total number of valence quarks constant). I assume that this is also the case when the number of c and b-quarks are increased. B. Povh et al. calculated (from experiments) the following mean squared radii for Λ, π and J/Ψ

$$\left\{ \begin{array}{rcl} \langle r_{st}^2 \rangle_\Lambda & = & 0.58 \pm 0.02 \text{ fm}^2 \\ \langle r_{st}^2 \rangle_\pi & = & 0.41 \pm 0.02 \text{ fm}^2 \\ \langle r_{st}^2 \rangle_{J/\Psi} & = & 0.04 \pm 0.02 \text{ fm}^2 \end{array} \right. \tag{26}$$

which would give that the constant decrease in $\langle r_{st}^2 \rangle$ for each c-quark is

$$\Delta \langle r_{st}^2 \rangle \simeq \frac{\langle r_{st}^2 \rangle_\pi - \langle r_{st}^2 \rangle_{J/\Psi}}{2} = 0.19 \text{ fm}^2 \tag{27}$$

since the J/Ψ contains two c-quarks. The radii for c-hadrons are then approximately given by

$$\left\{ \begin{array}{rcl} \langle r_{st}^2 \rangle_{c-meson} & \simeq & \langle r_{st}^2 \rangle_\pi - \Delta \langle r_{st}^2 \rangle = 0.23 \text{ fm}^2 \\ \langle r_{st}^2 \rangle_{c-baryon} & \simeq & \langle r_{st}^2 \rangle_\Lambda - \Delta \langle r_{st}^2 \rangle = 0.40 \text{ fm}^2 \end{array} \right. \tag{28}$$

which with eq. (25) gives

$$\left\{ \begin{array}{rcl} \sigma_{c-meson\ p} & \simeq & 14 \text{ mb} \\ \sigma_{c-baryon\ p} & \simeq & 24 \text{ mb} \end{array} \right. \tag{29}$$

Since the b-quarks are heavier than the c-quarks, the radius of the Υ (which is a $b\bar{b}$-system) is expected to be less than the radius of the J/Ψ, but even the radius of the J/Ψ is negligible compared to the radius of the π in eq. (27). Hence $\Delta \langle r_{st}^2 \rangle$ is expected to be approximately equal for c- and b-hadrons. Therefore it is expected that the mean squared radii for the b-mesons and b-baryons will be approximately the same as that for c-mesons and c-baryons respectively. Thus the cross sections in eq. (29) are expected to be approximately valid also for b-hadrons. Since neutrons and protons have similar strong interactions the cross sections above should be valid for scattering off neutrons as well.

Eq. (24) then gives the interaction time scale in the Sun as $\tau_{int} \approx 2.8 \times 10^{-11}$ s for c- and b-mesons and $\tau_{int} \approx 1.6 \times 10^{-11}$ s for c- and b-baryons. In the Earth the interaction time scales are $148/13.09 = 11.3$ times longer due to the lower density. To compare the time scales of interaction and decay one must also consider that the hadrons are relativistic and hence their decay times should be multiplied with the relativistic gamma factor, $\gamma = 1/\sqrt{1-\beta^2}$. If γ is in excess of τ_{int}/τ_{dec} interactions are a more likely than decay. To take the interaction into account one can notice that, at the energies involved here, the two time scales τ_{dec} and τ_{int} are of the same order and hence one can not assume that the energy loss is a continous process. Instead one can calculate the effective mean time for any of the two processes interaction or decay to occur. It is given by

$$\frac{1}{\tau_{eff}} = \frac{1}{\tau_{int}} + \frac{1}{\gamma \tau_{dec}}. \tag{30}$$

The probability that anything (interaction or decay) happens sometimes between 0 and t is

$$p_{int}(t) = 1 - e^{-t/\tau_{eff}} \tag{31}$$

This is in fact the cumulative distribution function if one normalizes over the region $t \in [0, \infty]$. Hence one can choose a number Y from a uniform distribution ($Y \in]0,1[$) and extract the time of interaction, T, as

$$T = -\tau_{eff} \ln(1 - Y). \tag{32}$$

To determine if interaction or decay has occured one has to look at the probability at each instant for either of them to occur. The probability for an interaction to occur in the interval $t, t + dt$ is $p_{int}\, dt = 1/\tau_{int}\, dt$ and the probability for decay to occur in $t, t + dt$ is $p_{dec}\, dt = 1/(\gamma \tau_{dec})\, dt$. If a uniformly chosen number on the interval]0,1[is smaller than the ratio $p_{int}/(p_{int} + p_{dec})$ an interaction has thus taken place. When this interaction has been taken care of, the procedure is gone through over and over again until the particle has decayed.

The interaction of a heavy hadron with a nucleon in the Sun can be seen like this: The hadron containing the heavy quark produces a jet of new hadrons whose leading hadron contains the heavy quark. This is the only hadron that will be considered in such a jet. The leading hadron takes an energy fraction, z, from the initial heavy hadron. Ritz and Seckel [11] have calculated $\langle z \rangle$ with the result

$$\begin{cases} \langle z \rangle \approx 0.6 \frac{m_c}{m_i} & \text{for } c\text{-hadrons} \\ \langle z \rangle \approx 0.7 & \text{for } b\text{-hadrons} \end{cases} \tag{33}$$

where m_i is the mass of the initial c-hadron and m_c is the mass of the c-quark. Assuming that the resulting neutrino suffers from the same fractional energy loss as the hadrons do one can simulate the hadronisation and decay of unstable particles as if the surrounding medium were not present and then look at the muon neutrinos to see if they originate from b- or c-hadron decay. If that is the case the probability for interaction(s) is calculated with the above method and for each interaction the neutrino energy is multiplied by $\langle z \rangle$ in eq. (33) above. If the considered hadron itself originated from the decay of another heavy hadron the same procedure is repeated with that one. This iterative procedure is continued until a non-interacting parent (e.g. W, Z, τ etc.) or the string from which all hadrons originate is found.

It would now be interesting to know how many interactions the parent hadrons in total participate in before producing a muon neutrino. In fig. 3 the total number of interactions for all parent hadrons in the Sun is shown for the $b\bar{b}$-channel when the neutralino mass is 50 and 500 GeV respectively. At 50 GeV, the $b\bar{b}$-channel is expected to be the dominating annihilation channel and hence it is an intersting example. At 500 GeV, the $b\bar{b}$-channel will not be the dominating one (except possibly for some specially chosen MSSM parameters) but with this neutralino mass the number of interactions will be as high as possible (since the decay is suppressed due to a high γ-factor). As seen in the figure less than 50% of the parent hadrons interact when $m_{\tilde{\chi}} = 50$ GeV. This means that more than 50% of the events are not affected at all of the way the interactions are treated. Hence the approximate treatment above is justified. When $m_{neu} = 500$ GeV, approximately one fourth of the hadrons do not participate in any interactions at all before producing a muon neutrino. For the high-energy tail of the spectrum the non-interacting fraction is expected to be even lower than one fourth. Hence this approximate treatment is not very good for this high neutralino masses. As mentioned above the $b\bar{b}$-channel is not expected to dominate at these high energies anyway and therefore, for a given set of branching ratios into the different channles the total flux of muon neutrinos is going to be calculated accurately enough.

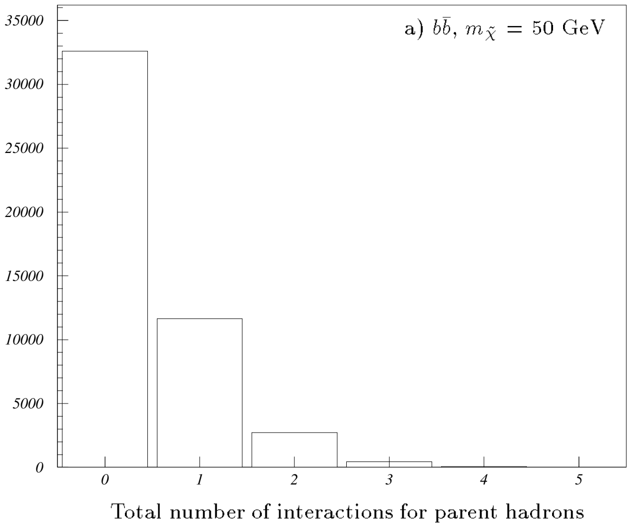

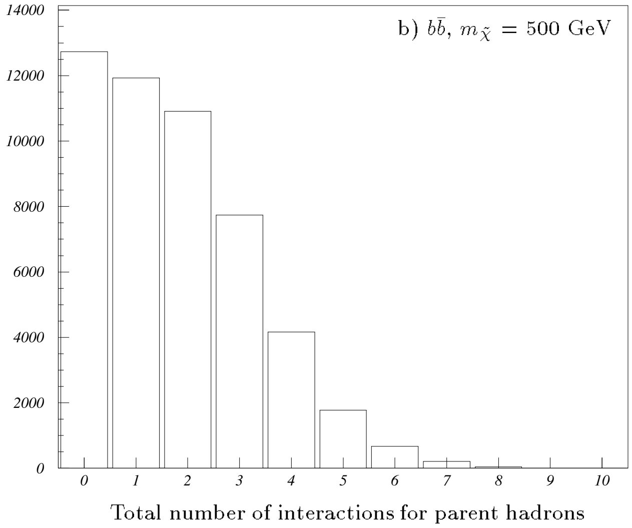

Figure 3: *The total number of interactions in the Sun for all parent hadrons of a muon neutrino.* 10^5 *events are simulated in each case.*

3.3 Stopping of charged leptons

For moderately relativistic charged particles the mean energy loss in ordinary matter is given by the Bethe-Bloch equation [9]

$$\frac{dE}{dx} = -4\pi N_A r_e^2 m_e c^2 \rho z^2 \frac{Z}{A}\frac{1}{\beta^2}\left[\ln\left(\frac{2m_e c^2\gamma^2\beta^2}{I}\right) - \beta^2\right] \tag{34}$$

where the particle has charge ze and Z, A, ρ are the atomic number, atomic weight and density of the stopping material, m_e and r_e are the mass and the classical radius of the electron and the product $4\pi N_A r_e^2 m_e c^2 = 0.3071$ MeV cm^2 g^{-1}. $\beta = v/c$ and $\gamma = 1/\sqrt{1-\beta^2}$ refers to the incident particle. I is the ionization constant and is approximately equal to

$$I \simeq 16\, Z^{0.9} \text{ eV for } Z > 1. \tag{35}$$

Eq. (34) is valid in the core of the Earth which consists of mainly liquid iron, for which eq. (35) gives $I \simeq 300$ eV. With $\rho = 13.09$ g/cm^3 [15] one then obtains

$$\left(-\frac{dE}{dx}\right)_{min}^{Earth} \simeq 0.020 \text{ GeV/cm (for } \gamma = 3.2) \tag{36}$$

For the core of the Sun, which is a plasma, eq. (34) is not correct and it has to be replaced by [21]

$$\frac{dE}{dx} = -\frac{e^2}{4\pi\epsilon_0}\frac{\omega_p^2}{(\beta c)^2}\ln\left(\frac{\Lambda m_e c^2\gamma\beta^2}{\omega_p \hbar}\right) \tag{37}$$

where ω_p is the plasma frequency and Λ is a number of order unity. The plasma frequency is given by

$$\omega_p = \sqrt{\frac{e^2 n_0}{m_e \epsilon_0}} \tag{38}$$

where n_0 is the density of electrons in the plasma. The core of the Sun consists of approximately 34% hydrogen and 64% helium-4 [13] which together with the core density $\rho = 148$ g/cm^3 gives the density of electrons as $n_0 = 5.89 \times 10^{25}$ cm^{-3}. Eq. (38) then gives $\omega_p = 4.3 \times 10^{17}$ s^{-1}. By putting $\Lambda = 1$ in eq. (37) the minimum of the mean energy loss becomes

$$\left(-\frac{dE}{dx}\right)^{Sun}_{min} \simeq 0.28 \text{ GeV/cm (for } \gamma = 4.1) \tag{39}$$

Multiplication by the velocity of the particle ($\sim c$) in eqs. (36) and (39) yields

$$\begin{cases} \left(-\frac{dE}{dt}\right)^{Earth}_{min} & \simeq \quad 5.9 \times 10^8 \text{ GeV/s} \\ \left(-\frac{dE}{dt}\right)^{Sun}_{min} & \simeq \quad 8.5 \times 10^9 \text{ GeV/s} \end{cases} . \tag{40}$$

Thus the mean stopping time for a charged particle of energy E is at most $\tau_{stop} = E/(dE/dt)$. The life time of the muon is $\tau_{dec} = 2.2 \times 10^{-6}$ s which in the lab system is boosted to $\gamma\tau_{dec} = E\tau_{dec}/m_\mu$. The ratio between the stopping time and the decay time in the lab system then becomes $m_\mu/(\tau_{dec}\, dE/dt)$ which yields

$$\begin{cases} \tau_{stop} \lesssim 8.2 \times 10^{-5}\, \gamma\tau_{dec} & \text{in the Earth} \\ \tau_{stop} \lesssim 5.7 \times 10^{-6}\, \gamma\tau_{dec} & \text{in the Sun} \end{cases} . \tag{41}$$

Since the stopping time is so much smaller than the decay time, muons will get stopped well before they decay in both the Earth and in the Sun and they will thus not produce any high energy muon neutrinos.

In the case of tauons with a life time of $\tau_{dec} = 3.4 \times 10^{-13}$ s one observes that these particles will probably decay before interactions. To estimate an upper bound on the energy loss of a tauon one has to calculate the maximum of the mean energy loss which (for relativistic particles) is obtained when γ is as large as possible. For a 500 GeV tauon the maximum of the energy loss equations (34) and (37) (multiplied by c) is[2]

$$\begin{cases} \left(-\frac{dE}{dt}\right)^{Earth}_{max} & \simeq \quad 1.0 \times 10^9 \text{ GeV/s} \\ \left(-\frac{dE}{dt}\right)^{Sun}_{max} & \simeq \quad 1.2 \times 10^{10} \text{ GeV/s} \end{cases} . \tag{42}$$

The mean energy loss for a 500 GeV tauon is then given by $dE/dt\, \gamma\tau_{dec}$ which is 1.1 GeV in the Sun and 0.098 GeV in the Earth. For relativistic particles at lower energies the energy loss is even smaller and thus the tauons can be considered as decaying before they lose any significant amount of energy.

3.4 Stopping of other annihilation products

Among the other annihilation products are the gauge bosons, W^+, W^- and Z^0. These have lifetimes of the order of $\tau = \hbar/\Gamma \simeq 3 \times 10^{-25}$ s, during which they reach about 0.1 fm and hence their interactions can be neglected. One also has the Higgs bosons, H_1^0, H_2^0, H_3^0, H^- and H^+ which have lifetimes of the same order as the gauge bosons. Hence they will also not interact before they decay.

[2]At these high energies eq. (34) overestimates the energy loss and hence the obtained maximum is too large. The actual energy loss in the Earth is then less than 0.098 GeV which further justifies the stopping of tauons to be neglected.

3.5 Conclusions

As seen above the same general behaviour of the stopping is obtained in the Sun and in the Earth. The only difference is that the stopping is a larger effect in the Sun than in the Earth. To conclude, light hadrons and muons get stopped while heavy hadrons may or may not lose energy. Tauons lose hardly no energy at all and the W^+, W^-, Z^0 and Higgs bosons will not lose any energy. The way the energy loss of heavy hadrons is treated is not expected to be of big importance since when the energy loss of heavy hadrons is large in one channel, that channel is not expected to dominate the annihilation branching ratio. E.g. when the neutralino mass is large, the heavy hadrons in the $b\bar{b}$-channel lose much energy before they decay, but at the same time the $b\bar{b}$-channel is not expected to dominate. However, one should be aware of that there may exist such MSSM parameters that make the neutralino mass large and at the same time channels whose neutrino flux is dominated by heavy hadron decay ($c\bar{c}$, $b\bar{b}$ and $H_1^0 H_3^0$) are dominating. In that case, the resulting fluxes may have large errors.

4 Neutrino interactions in the Sun and in the Earth

When the neutrinos are created they are created almost in the core of the Sun or the Earth (see sec. 2.3). Before reaching the detector they have to travel through certain amounts of matter. In sec. 4.1 neutrino interactions with nuclei are described and in the following sections absorption and energy loss specific for neutrinos from the Sun and the Earth will be considered.

4.1 Neutrino interactions with nuclei

The diagrams for charged and neutral current interactions of a neutrino with a nucleon are shown in fig. 4. The charged current cross section is given by [22]

$$\frac{d^2\sigma^{\nu N,\bar{\nu}N}}{dx\,dQ^2} = \frac{G^2}{2\pi}\left[(1-y)\frac{F_2^{\nu N}(x)}{x} + \frac{y^2}{2}\frac{2xF_1^{\nu N}(x)}{x} \pm y\left(1-\frac{y}{2}\right)\frac{xF_3^{\nu N}(x)}{x}\right] \tag{43}$$

where G is the Fermi constant, $F_i(x)$ are the structure functions of the nucleon, x is the Bjorken x, y is the energy fraction of the incoming neutrino that goes into the hadronic system and Q^2 is the squared momentum transfer. The Bjorken x is given by

$$x = \frac{Q^2}{2MyE} \tag{44}$$

where M is the mass of the nucleon and E is the energy of the incoming neutrino.

In the energy range (1 GeV $< E_\nu <$ 1 TeV) the total cross section for the charged current interaction $\nu + N \to \mu + X$ is approximately given by

$$\sigma_{CC} \simeq aE_\nu \times 10^{-39}\ \mathrm{cm}^2 \tag{45}$$

where a is a constant that depends on projectile and target. If one now thinks about the detector one wants to be able to make a cut in the angle of the muon relative to the direction to the core of the Sun or the Earth since the background can be reduced in that way. Hence it is the events with a small scattering angle that is the most interesting ones. The scattering angle is small when Q^2 is small and hence it is interesting to go down to as low Q^2 as possible. Glück, Reya and Vogt [23] claims that their new structure functions (HO) from 1992 are applicable

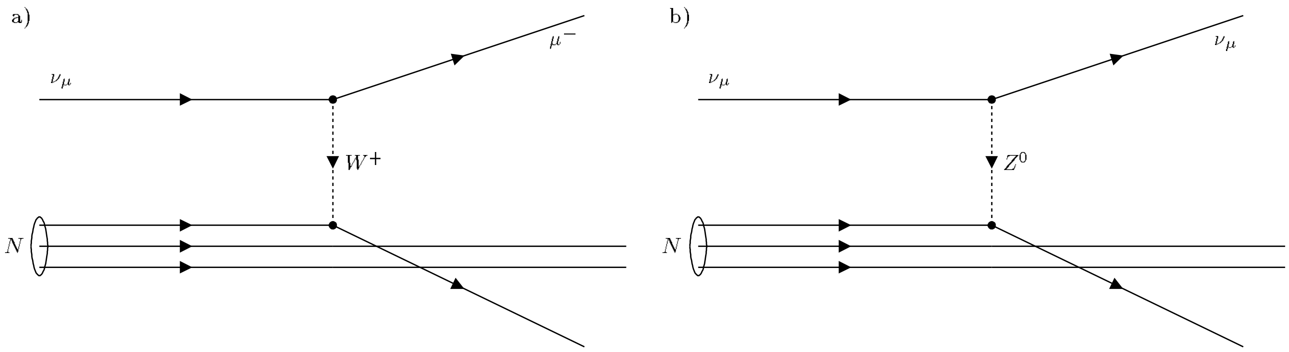

Figure 4: *The lowest order diagrams for neutrino nucleon (N) deep inelastic scattering. a) charged current. b) neutral current.*

down to $Q^2 = 0.3$ GeV^2. Using their structure functions and integrating the differential cross section one can calculate a in eq. (45) above. With a lower cut at $Q^2 = 0.3$ GeV^2 the result is

$$a_{\nu n} = 8.81 \quad ; \quad a_{\nu p} = 4.51 \quad ; \quad a_{\bar{\nu} n} = 2.50 \quad \text{and} \quad a_{\bar{\nu} p} = 3.99 \tag{46}$$

when the neutrino energy, E_ν, is given in GeV.

The cross section for the neutral current interaction $\nu + N \rightarrow \nu + X$ is

$$\sigma_{NC} \simeq b E_\nu \times 10^{-39} \text{ cm}^2 \tag{47}$$

where integration of the differential neutral current cross section yields

$$b_{\nu n} = 2.20 \quad ; \quad b_{\nu p} = 1.97 \quad ; \quad b_{\bar{\nu} n} = 1.15 \quad \text{and} \quad b_{\bar{\nu} p} = 1.14. \tag{48}$$

when the neutrino energy, E_ν, is given in GeV. The values of the coefficients are calculated at a neutrino energy of 100 GeV. To check the accuracy of the linearized cross sections the differential cross sections have been integrated at other energies and in the region 1–500 GeV the accuracy is quite good ($\sim 5\%$).

One can now wonder if it is good to use the GRV structure functions to a value of Q^2 as low as 0.3 GeV^2. The total charged current cross section constants for neutrino scattering off an isoscalar medium are $a_{\nu N} = 6.67$ and $a_{\bar{\nu} N} = 3.25$ for the GRV structure functions and experiments [9] give $a_{\nu N} = 6.7$ and $a_{\bar{\nu} N} = 3.4$. Hence the calculated cross sections are only slightly lower than the experimental ones. At low Q^2 there can also be resonant scattering and π production described by a vector dominance model and this is not included in the above calculated cross sections but are included in the experimental cross sections and hence they are expected to be larger. Since the difference is so small between the calculated coefficients and the measured ones one can assume that the contribution from these other reactions is small and can be neglected.

4.2 Mean free path of neutrinos in the Sun

The annihilation and decay processes in the core of the Sun give, as dicsussed, rise to muon neutrinos traversing the solar medium. On their way out of the Sun they can interact with the solar medium, either by being "absorbed" via a charged current process or by losing energy via a neutral current scattering off nucleons. Energy loss due to scattering off electrons will be neglected since this is smaller by a factor of 10^3 [11]. The approach here will not follow that of Ritz and Seckel since this can be made in more detail.

The mean free path of the neutrinos in the Sun has to be calculated, but since the Sun is not homogenous this is a quantity that depends on where in the Sun the neutrino is. Instead, the effective thickness of the Sun is calculated by using the solar model of Bahcall et al. [13]. Since the thickness coming from neutron and proton are needed separately one can note that all nuclei in the Sun except hydrogen contains almost equal amounts of protons and neutrons. The integral of the solar density and the hydrogen density over the dimensionless variable $x = r/R_\odot$, is then

$$I_0 = \int_0^1 \rho(x)\, dx = 21.4 \text{ g/cm}^3 \tag{49}$$

$$I_H = \int_0^1 \rho(x) X_H(x)\, dx = 11.0 \text{ g/cm}^3 \tag{50}$$

where $R_\odot$ is the solar radius and X_H is the hydrogen mass fraction. The effective thickness is then given by $R_\odot I$. The integrals of protons and neutrons separately is given by

$$I_p = \frac{1}{2}(I_0 + I_H) = 16.2 \text{ g/cm}^3 \tag{51}$$

$$I_n = \frac{1}{2}(I_0 - I_H) = 5.2 \text{ g/cm}^3 \tag{52}$$

One can now use these integrals to consider passage of neutrinos through a homogenous block of material with the thickness $R_\odot I_0$ g/cm^2. The error one makes when assuming that the block is homogeneous is that the density of protons will be overestimated at the beginning and underestimated at the end. Thus the ratio of the macroscopic cross sections, Σ_{CC}/Σ_{NC}, will be too small at the beginning and too large at the end for neutrinos and the other way around for antineutrinos. This approximation should however be acceptable since the number of interactions is so small. In fig. 5 the number of interactions of a neutrino on the way out of the Sun is shown for the W^+W^--channel with a neutralino mass of 500 GeV. This channel is chosen because it has a very hard neutrino energy spectrum and hence the number of interactions is expected to be as large as possible for this channel (since the cross section is proportional to the neutrino energy). As can be seen almost half of the neutrinos escape the Sun without any interaction at all. For other channels and smaller neutralino mass even more neutrinos do not interact at all. To make the simulation program simpler, interactions has been considered with protons and neutrons separately which means that a single neutrino interacts only with protons or only with neutrons. This should though not give rise to a large error since it is very few neutrinos ($\sim 7\%$) that interact more than once and and it is only these neutrinos that are affected by this approximate treatment.

As pointed out in sec. 2.3, the annihilation takes place mainly in the core of the Sun at x-values smaller than 0.02. That the annihilation does not take place exactly in the core yields a smearing of the effective thickness that has to be traversed. This smearing can be estimated by integration of the solar density from 0 to 0.02 which yields

$$\Delta I_0 = \int_0^{0.02} \rho(x)\, dx = 2.9 \text{ g/cm}^3 \tag{53}$$

$$\Delta I_H = \int_0^{0.02} \rho(x) X_H(x)\, dx = 1.0 \text{ g/cm}^3. \tag{54}$$

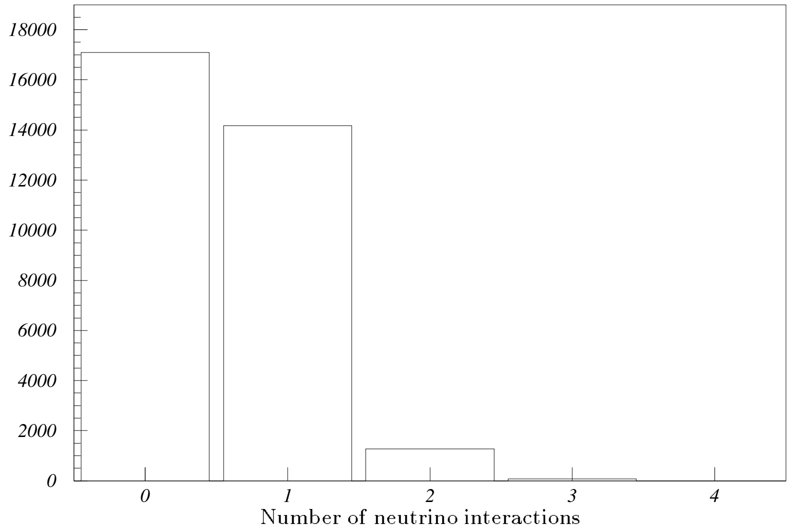

Figure 5: *The number of interactions (neutral and charged current) that a neutrino participates in on the way out of the Sun, obtained from a simulation of* 10^5 *events in the* W^+W^-*-channel with a neutralino mass of 500 GeV.*

Expressing this in terms of protons and neutrons gives

$$\Delta I_p = \frac{1}{2}(\Delta I_0 + \Delta I_H) = 2.0 \text{ g/cm}^3 \quad (55)$$

$$\Delta I_n = \frac{1}{2}(\Delta I_0 - \Delta I_H) = 1.0 \text{ g/cm}^3. \quad (56)$$

which yields an error of up to 19% in the effective thickness. The difference in neutrino spectrum from neutrinos created at $x = 0.02$ (towards the Earth) and neutrinos created in the core is shown in fig. 6.

The macroscopic cross section for neutral and charged current interactions of neutrinos is given by

$$\Sigma_\nu = N_A \frac{A}{M_A} E_\nu \times 10^{-39} \{(a_{\nu p} + b_{\nu p})I_p + (a_{\nu n} + b_{\nu n})I_n\} \quad (57)$$

and similarly for antineutrinos. N_A is Avogadro's number, A is the atomic mass number and M_A is the atomic mass. The mean free path is then given by $\lambda = 1/\Sigma$. The probability for interaction somewhere between 0 and $x = r/R_\odot$ is then

$$p_{int}(x) = 1 - e^{-xR_\odot \Sigma} \quad (58)$$

As pointed out in sec. 3.2 this is the cumulative distribution function normalized over the region $x \in [0, \infty]$. Hence one can choose a uniform number $Y \in]0,1[$ and extract X as

$$X = -\frac{\ln(1-Y)}{R_\odot \Sigma} \quad (59)$$

X will then have the appropriate distribution of how far the neutrino gets before it interacts. If $X > 1$ the neutrino will of course have escaped from the Sun. If $X < 1$ the type of interaction (charged or neutral current) that is going to take place has to be chosen. The probability for a charged current interaction is equal to $\Sigma_{CC}/(\Sigma_{CC} + \Sigma_{NC}) = (a_{\nu p} I_p + a_{\nu n} I_n)/(a_{\nu p} I_p + a_{\nu n} I_n +$

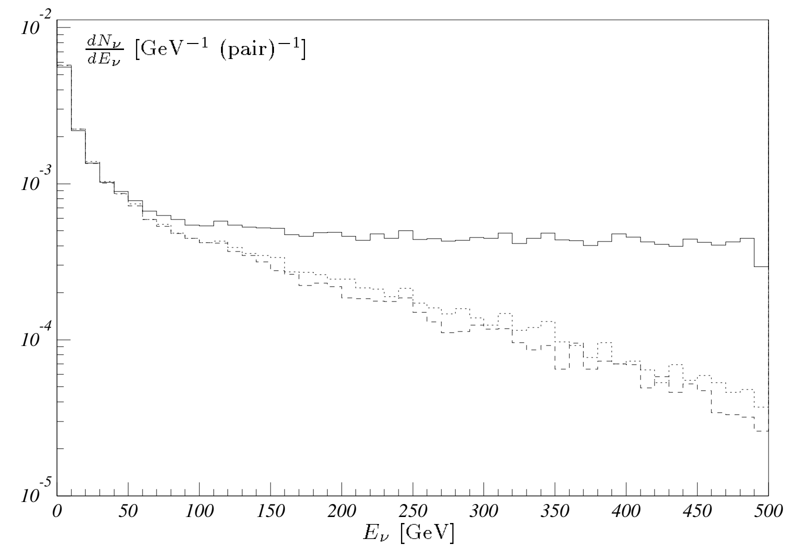

Figure 6: *The neutrino spectra from neutrinos created in the core of the Sun (long-dashed line) and at $x = 0.02$ towards the Earth (short-dashed line). For comparison the energy spectra without interactions is also shown (solid line). These data are taken from a simulation of* 10^5 *events in the W^+W^--channel with a neutralino mass of 500 GeV.*

$b_{\nu p} I_p + b_{\nu n} I_n$) for neutrinos and similarly for antineutrinos. If a uniformly chosen number is smaller than this fraction a charged current interaction has occured, in which case the neutrino is absorbed. If, on the other hand, the interaction is a neutral current, it is simulated with PYTHIA 5.6 [24] and the new neutrino energy is extracted from the simulation. With this new energy the procedure is started over again to see if the neutrino interacts on the way still left out of the Sun.

In this way the treatment is correct for both low energy neutrinos as well as high energy ones. The approach of Ritz and Seckel was to separate the absorption probability and the energy loss. The energy loss was considered to be continous, which is correct if the number of interactions on the way out of the Sun is large. The separation of the two processes, on the other hand, is correct if the energy loss is small and these two assumptions (many interactions and small energy loss) can *never* be met at the same time since if the neutrino interacts many times it also loses a large amount of its energy. Therefore, that treatment is not very good. On the average, about the same mean energy of the neutrinos that escape the Sun will be obtained by the two methods[3], but *the distribution* of energies, dN_ν/dE_ν, will be different. In sec. 6.1 it will be shown that the rate is an integral over events and the integrand is proportional to the energy squared and hence the high energy part of the distribution is more important. In fig. 7 the neutrino energy spectrum at the surface of the Sun with the two methods is shown. Clearly seen is that the spectrum at high energies differ with the two methods. For other channels and lower neutralino masses the difference is smaller. To be noted is that the Ritz and Seckel method used here is updated with the new values of I_0 and I_H as well as the new cross sections.

[3]If the energy is small, the mean energy of the neutrinos that escape the Sun will be approximately the same, but if the energy is higher the absorption probability is overestimated with the method of Ritz and Seckel since it is calculated with the neutrino energy before any energy losses. Actually, those neutrinos that undergo a neutral current interaction loses energy and this lowers the probability for absorption on the way left out of the Sun. The result is that with the new method, fewer high energy neutrinos will get absorbed.

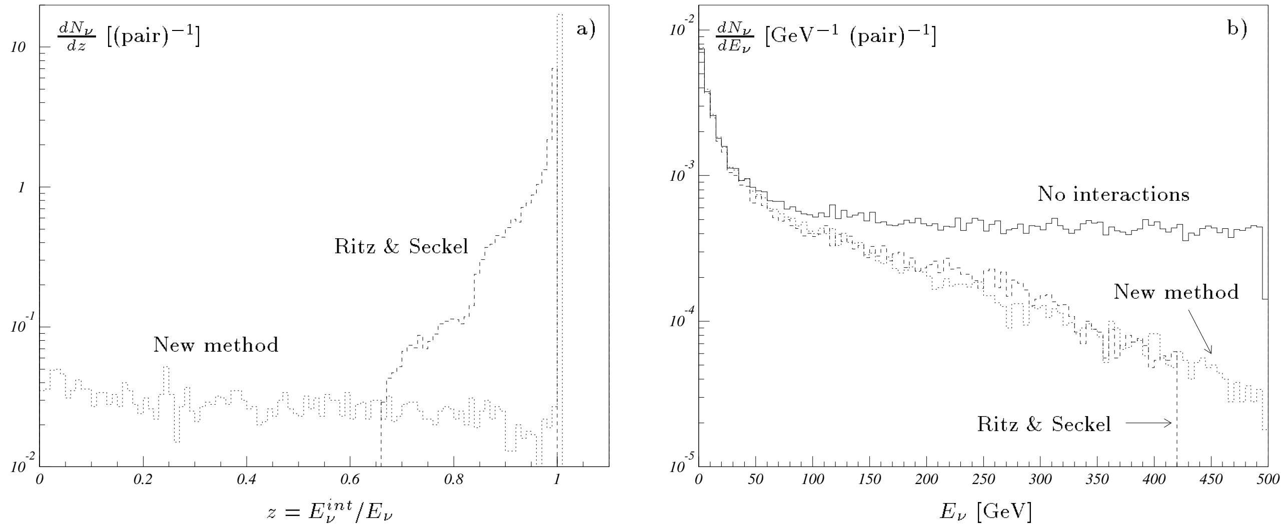

Figure 7: *a) Distribution of the ratio between the neutrino energy after interaction in the Sun and before interaction, as calculated with the method of Ritz and Seckel [11] and with the new method. b) The neutrino energy spectrum with no interactions turned on, with the method of Ritz and Seckel and with the new method. The data are from a simulation of* 10^5 *events in the* W^+W^-*-channel with a neutralino mass of 500 GeV.*

4.3 Interactions during the passage through the Earth

Imagine a flux of neutrinos that have to traverse a certain distance in the Earth of density ρ_{Earth}. The traversed matter can be considered as a block of materia with an effective thickness T g/cm^2. Using the dimensionless variable y which is the fraction of the block that is traversed one gets the differential equation for the flux in the block as

$$d\Phi = -\Phi \frac{TAN_A}{M_A} \sigma y \, dy \tag{60}$$

which has the solution (for $y = 1$)

$$\Phi = \Phi_0 e^{-TAN_A \sigma / M_A}. \tag{61}$$

The effective thickness between the core and the surface of the Earth is given by

$$T = R_\oplus I = R_\oplus \int_0^1 \rho(x) \, dx \tag{62}$$

where $x = r/R_\oplus$ and $R_\oplus$ is the radius of the Earth. By putting in the density function for the Earth [15] in eq. (62) the value of I is calculated to be

$$I = 8.60 \text{ g/cm}^3 \tag{63}$$

The maxiumum effective thickness that has to be traversed is $2IR_\oplus$ and both for neutrinos from the Sun and for the Earth the actual effective thickness is smaller. From sec. 4.1 one obtains that the total cross sections (neutral and charged current) are $\sigma_\nu = 8.8 \times 10^{-39} E_\nu$ cm^2 and $\sigma_{\bar{\nu}} = 4.4 \times 10^{-39} E_{\bar{\nu}}$ cm^2 for neutrinos and antineutrinos respectively with the energies in GeV. Eq. (61) with $T = 2IR_\oplus$ and eq. (63) gives

$$\begin{cases} \Phi = \Phi_0 \exp(-5.8 \times 10^{-5} E_\nu) & \text{for neutrinos} \\ \Phi = \Phi_0 \exp(-2.9 \times 10^{-5} E_{\bar{\nu}}) & \text{for antineutrinos} \end{cases} \tag{64}$$

where the energies should be given in GeV. For muon neutrinos of 500 GeV the fraction of neutrinos that traverse the entire Earth without interacting is $\Phi/\Phi_0 = 0.971$ and similarly $\Phi/\Phi_0 = 0.986$ for antineutrinos. Hence the interaction of muon neutrinos in the Earth can be neglected to a good approximation.

4.4 Muon neutrinos from tau neutrinos

Of course, there may also be tau neutrinos produced in the decay of the annihilation products. These may interact via a charged current on the way out of the Sun or the Earth producing tauns which eventually may decay to muon neutrinos. The energy distribution of these indirectly produced muon neutrinos will be very soft even if the tau neutrino spectrum is hard (as is the case from the $\tau^+\tau^-$-channel), since there are two more steps of energy losses involved here. Firstly, not all of the tau neutrino's energy goes into the tauon and secondly not all of the tauons energy goes into the muon neutrino. Hence, these indirectly produced muon neutrinos will be neglected in this paper.

4.5 Neutrino fluxes from simulations

Simulation of the hadronisation and/or decay of annihilation products in the Sun and the Earth, stopping of annihilation products and in case of the Sun subsequent neutrino interactions yield the muon neutrino fluxes from different channels. Jetset 7.3 [24] is used for the simulation of the hadronisation/decay of the annihilation products and Pythia 5.6 is used for the simulation of the neutral current neutrino-nucleon interactions on the way out of the Sun. In fig. 8 the neutrino fluxes at the surface of the Earth are shown for some different channels and for annihilation in the Sun and in the Earth. The fluxes are calculated from the neutrino yield divided by $4\pi D^2$ where D is the distance from the annihilation point to the detector. In case of the Sun, D equals approximately the distance from the Sun to the Earth. In the Earth the distance varies a lot with the point of annihilation and in sec. 5.3 the actual distance from the point of annihilation will be calculated. Thus, eq. (80) is used for the distance when annihilation in the Earth is considered.

As can be seen in the fig. 8, the spectra approximately scale with neutralino mass. The effect of neutrino interactions on the way out of the Sun is clearly seen if one compares fig. 8c with 8d. In d) the spectra scale since the neutrino ineractions in the Earth are neglected while in c) the neutrinos can interact on the way out of the Sun. Also seen is that spectra from $\tau^+\tau^-$ and W^+W^- are much harder than those from $b\bar{b}$ which of course depends on the fact that the τ and the W can decay directly to muon neutrinos while the b-quarks must hadronize first and later decay to muon neutrinos. In e) and f) a bump is seen for $m_{\tilde{\chi}} = 100$ GeV. This bump corresponds to prompt decay of W's to muon neutrinos, $W^+ \to \mu^+\nu_\mu$, while the smooth background slope corresponds to indirectly produced muon neutrinos from W decay to quarks or tauons which eventually has given rise to muon neutrinos.

4.6 Conclusions

The neutrinos created in the core of the Sun may well interact on the way out of the Sun, while the interactions of neutrinos during the passage through the Earth can be neglected.

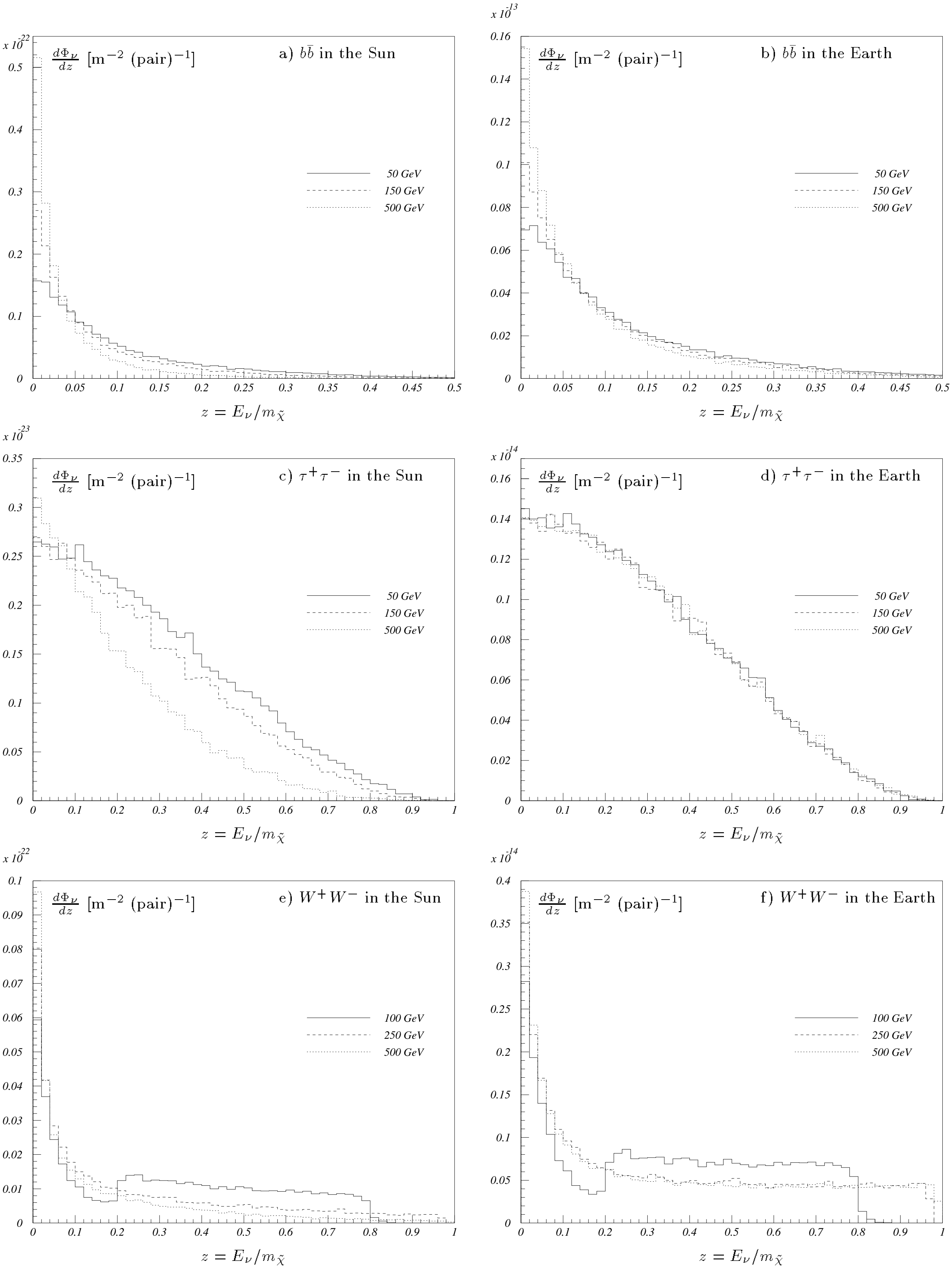

Figure 8: *Neutrino ($\nu_\mu + \bar{\nu}_\mu$) fluxes at the surface of the Earth for the indicated neutralino masses and annihilation channels.*

5 Muon interactions in the ice

The observable muons are created by charged current neutrino interactions in the ice. The muons can interact with the ice on their way to the detector and this is analysed in detail in the following.

5.1 Stopping of muons

For the energy loss of muons one can use [25]

$$\frac{dE_\mu}{dx} \simeq -\alpha - \beta E_\mu \tag{65}$$

where α [GeV/cm] corresponds to ionization losses and β [cm^{-1}] corresponds to the energy loss due to bremsstrahlung, pair production and photonuclear interactions. W. Lohmann et al. [26] have calculated the energy loss, dE_μ/dx, in water for muons in the energy range 1–10^4 GeV. Fitting α and β to their results in the region 1–500 GeV yields

$$\left\{ \begin{array}{l} \alpha/\rho \approx 0.0025 \ \mathrm{GeV/(g/cm^2)} \\ \beta/\rho \approx 4.0 \times 10^{-6} \ \mathrm{(g/cm^2)^{-1}} \end{array} \right. . \tag{66}$$

This parametrization gives an accuracy of better than 4% in the energy region 10–500 GeV and slightly worse below 10 GeV. For the needs of this project this accuracy is good enough. In the ice one can use the density $\rho_{ice} \simeq 1.0$ g/cm^3 which yields

$$\left\{ \begin{array}{l} \alpha \approx 0.0025 \ \mathrm{GeV/cm} \\ \beta \approx 4.0 \times 10^{-6} \ \mathrm{cm^{-1}} \end{array} \right. . \tag{67}$$

By integration of eq. (65) one can derive an expression for the range of muons,

$$L_\mu \simeq \frac{1}{\beta} \ln \left[\frac{E_\mu + \alpha/\beta}{\alpha/\beta} \right] \tag{68}$$

5.2 Muon energy at the detector

Imagine a plane in the ice, perpendicular to the source of neutrinos. As the muons are created they have to pass a certain amount of ice before reaching this plane. The muons can have been created anywhere between the plane and a distance $L_\mu(E_\mu)$ away from it. The probability for creation at a specific point is proportional to the neutrino flux at that point.

As mentioned in section 4.3 the attenuation of the neutrino flux due to interactions in the Earth can be neglected. The flux of neutrinos is then proportional to $1/D^2$ where D is the distance from the source. Consider a 500 GeV muon. According to eqs. (67) and (68) such a muon has a range of approximately $L_\mu = 1500$ m. The variation of the flux over this range from neutrinos created in the core of the Earth is then given by $[\Phi(R_\oplus - L_\mu) - \Phi(R_\oplus)]/\Phi(R_\oplus) \approx 0.0005$ and hence it can be neglected. In the case of neutrinos from the Sun the variation is even smaller since the distance to the Sun is larger. Thus, the flux of neutrinos is approximately constant over the range of the produced muons. Therefore the point of creation can be chosen according to a uniform distribution between the plane and a distance $L_\mu(E_\mu)$ away from it. The energy loss of the muon as it passes the ice on the way to the detector can then be calculated. Integration of eq. (65) gives the energy of the muon at the plane as

$$E_\mu^{det}(x) = (E_\mu + \frac{\alpha}{\beta})e^{-\beta x} - \frac{\alpha}{\beta} \tag{69}$$

where x is the traversed distance in the ice.

5.3 Direction of muons at the detector

When a muon reaches the detector it does not in general have a direction pointing directly from the core of the Sun or the Earth towards the detector. There are many reasons for this:

1. The muon undergoes multiple Coulomb scattering in the ice.
2. In the charged current scattering process the angle of the muon relative to the incoming neutrino is not zero.
3. The annihilation of neutralinos does not take place exactly in the core of the Sun or the Earth.

The first effect is not dependent on from where (the Sun or the Earth) the neutrinos come and hence it can be considered in general. The RMS-value of the multiple Coulomb scattering angle, θ_{rms}^{space}, is given by [9]

$$\theta_{rms}^{space} = \sqrt{2}\frac{0.0136 \text{ GeV}}{\beta c p} z\sqrt{x/X_0}\,[1 + 0.038\ln(x/X_0)] \tag{70}$$

where p, βc and z are the momentum, velocity and charge number of the incident particle and x/X_0 is the thickness of the scattering medium measured in radiation lengths, X_0. The radiation length can be approximated by [9]

$$X_0 = \frac{716.4 \text{ g cm}^{-2} A}{Z(Z+1)\ln(287/\sqrt{Z})} \tag{71}$$

where Z and A are the atomic number and weight of the medium. For a muon incident on ice, X_0 can be calculated according to

$$\frac{1}{X_0} = \frac{1}{X_0(Hydrogen)} + \frac{1}{X_0(Oxygen)} \tag{72}$$

where

$$X_0(Hydrogen) = \frac{716.4 \text{ g cm}^{-2} A}{Z(Z+1)\ln(287/\sqrt{Z})}\frac{1}{2/18\rho_{ice}} = 379.8 \text{ cm} \tag{73}$$

$$X_0(Oxygen) = \frac{716.4 \text{ g cm}^{-2} A}{Z(Z+1)\ln(287/\sqrt{Z})}\frac{1}{16/18\rho_{ice}} = 38.8 \text{ cm} \tag{74}$$

with $\rho_{ice} = 1.0$ g/cm^3. Eqs. (72) to (74) yield $X_0 = 35.2$ cm. A muon of 10 GeV has a range of approximately 4000 cm according to eq. (68). Hence $x/X_0 \approx 114$ and putting this in eq. (70) gives $\theta_{rms}^{space} \approx 1.4°$. Since both x/X_0 and p rises linearly with energy the angle decreases with energy approximately as $1/\sqrt{E_\mu}$. Hence the effect decreases as the energy increases.

The angle between the direction of the neutrino and the direction of the produced muon can be extracted from the simulation. This angle is of the order of a few degrees (see θ' in fig. 9) and hence it is more important than the multiple Coulomb scattering. To a first approximation, the multiple Coulomb scattering can be neglected and that is done in this paper.

Now consider the last effect, that the annihilation does not take place exactly in the middle of the Sun or the Earth. According to sec. 2.3 most of the annihilation takes place within a fractional radius of $x = 0.02$ in case of the Sun. Since the diameter of the Sun is about $0.5°$ large as viewed from the Earth the difference in angle from neutralino annihilations in the core and at $x = 0.02$ away from it can be totally neglected compared to the scattering angle mentioned above.

In case of the Earth, however, the annihilation can take place up to $x = 0.15$–0.20 and this corresponds to an angle of about $10°$. Hence, this angle can be of the same order or larger than the scattering angle. In the following, the resulting direction of the muon when the last two processes are considered will be calculated.

Consider the Earth as a sphere with radius 1. Introduce a coordinate system S where the detector is situated at $z = 1$ along the z-axis (the detector is approximated as being situated at the surface which is justified as long as the depth of the detector is small compared with the radius of the Earth). A neutrino on the way to the detector can have been produced anywhere in the Earth with the distribution in fractional radius given by eq. (18). Here r will be used instead of x for the fractional radius since the cartesian coordinate x will be used in the derivation below. The radius, r, will then be chosen according to the distribution of eq. (18). Then choose the coordinate system in such a way that the annihilation point lies in the xz-plane. To determine the polar angle θ_A of the annihilation point one has to notice that the annihilation profile should be isotropic which means that the probability for annihilation in a certain direction (as seen from the core) is proportional to the solid angle $d\Omega = sin\theta_A d\theta_A d\phi_A$ in that direction. Hence the polar angle θ_A has to be chosen according to the distribution $f(\theta_A) = \frac{1}{2}\sin\theta_A$. The cumulative distribution function is then given by $F(\theta_A) = \frac{1}{2}(1-\cos\theta_A)$ and if θ_A is chosen as $\theta_A = \arccos(1-2Y)$ where Y is a uniformly chosen number on the interval $[0,1]$, θ_A will have the appropriate distribution. The coordinates x and z are then

$$\left\{ \begin{array}{lcl} x & = & r\sin\theta_A \\ z & = & r\cos\theta_A \end{array} \right. . \tag{75}$$

The angle between the direction of the neutrino and the z-axis is then given by

$$\beta = \arctan\left[\frac{x}{1-z}\right]. \tag{76}$$

The muon is then created with an angle of θ' relative to the direction of the neutrino. Let the direction of the neutrino be described by the vector $p_\nu = (\sin\beta, 0, \cos\beta)$ and let the direction of the muon be p_μ. Now introduce a new coordinate system S' with the z'-axis along p_ν. In this coordinate system the directions of the neutrino and muon are $p'_\nu = (0,0,1)$ and $p'_\mu = (\sin\theta'\cos\phi', \sin\theta'\sin\phi', \cos\theta')$. The angle θ' is obtained from the simulation of the charged current interaction $\nu + N \to \mu + X$. The angle ϕ' should be chosen according to a uniform distribution in the interval $[0, 2\pi]$. The transformation between the coordinate system S' and S is given by a rotation around the y-axis with the angle β. This rotation is given by the matrix

$$R = \begin{pmatrix} \cos\beta & 0 & \sin\beta \\ 0 & 1 & 0 \\ -\sin\beta & 0 & \cos\beta \end{pmatrix}. \tag{77}$$

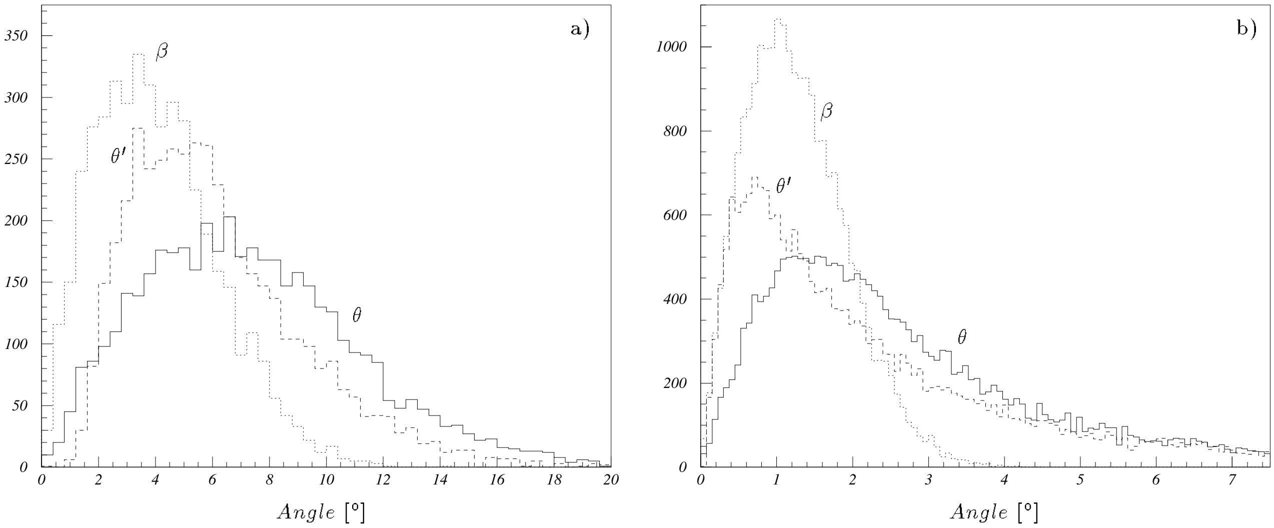

Figure 9: *The distributions of the angles θ, θ' and β where θ is the angle of the muon relative to the direction from the core of the Earth to the detector, θ' is the angle of the muon relative to the neutrino direction and β is the angle of the neutrino relative to the direction from the core of the Earth to the detector. A cut in the muon energy at the detector is applied as $E_\mu^{det} > 5$ GeV. a) From a simulation of 10^5 events in the $b\bar{b}$-channel with a neutralino mass of 50 GeV. b) From a simulation of 10^5 events in the W^+W^--channel with a neutralino mass of 500 GeV.*

The direction of the muon in the system S is then given by

$$p_\mu = Rp'_\mu = (\cos\beta\sin\theta'\cos\phi' + \sin\beta\cos\theta', \sin\theta'\sin\phi', -\sin\beta\sin\theta'\cos\phi' + \cos\beta\cos\theta'). \quad (78)$$

The angle of the muon with respect to the z-axis is thus given by

$$\theta = \arccos\left[\cos\beta\cos\theta' - \sin\beta\sin\theta'\cos\phi'\right]. \quad (79)$$

This is the angle of the muon relative to the direction from the core of the Earth to the detector if multiple Coulomb scattering is neglected. In fig. 9 the angle of the muon relative to the neutrino, θ', and relative to the direction from the core of the Earth to the detector, θ, is shown. Also shown is the angle of the neutrino relative to the direction from the core of the Earth to the detector, β.

As will be seen in sec. 6.1 the distance, D, from the annihilation place to the detector is also needed. In the variables used above it is given by

$$D = R_\oplus\sqrt{x^2 + (1-z)^2}. \quad (80)$$

6 Flux and rate calculations

6.1 How to simulate the muon flux at the detector

Neutrinos are created in the Sun and in the Earth and when they reach the detector they have a certain probability to participate in a charged current interaction producing a muon. The charged current interaction is simulated with PYTHIA 5.6 [24] and the muon energy and direction relative to the neutrino direction can be extracted from the simulation. Now imagine a plane in the ice, perpendicular to the direction to the source of neutrinos (the Sun or the core of the Earth). The probability that a neutrino of energy E_ν interacts via a charged current interaction in the ice and that the produced muon passes a unit area of this plane is given by

$$p_{det} = \frac{\sigma_{CC}(E_\nu) N L_\mu(E_\mu)}{4\pi D^2} \tag{81}$$

where N is the number of nucleons per cm^3 in the ice, D is the distance from the neutrino source to the detector and σ_{CC} is the charged current cross section for neutrino-nucleon interactions in ice.

For neutralino annihilations in the Sun one can use the mean distance from the core of the Sun to the core of the Earth, D_{Earth}, as D in eq. (81). One then makes a small error due to the eccentricity of the orbit of the Earth, which is $e = 0.017$. This yields that $D_{max}/D = 1.017$ and $D_{min}/D = 0.983$. The maximum errors of $1/D^2$ if one takes $D = D_{Earth}$ is thus 3.5%. To be correct one should of course use the average of $1/D^2$ over the period of the year that one is looking at the Sun. As will be shown in sec. 7.2 below, the background of muons will be too high in the antartic summer and it is during the summer (january) that the Earth is closest to the Sun. If one would like to use the correct average one has to apply appropriate cuts in time of the year to use the detector and the result would be a slightly higher value of D in eq. (81). This correction has not been used in the calculations since the error is so small compared with other errors and at the end it is still possible to correct the results by multiplication of $\langle 1/D^2\rangle/(1/D^2_{Earth})$ if so desired.

Another source of error is the approximation that the detector is at the same distance from the Sun as the center of the Earth is. If one compares the radius of the Earth, $D_\oplus = 6.4 \times 10^6$ m with the error in the above approximation, $0.017 D_{Earth} = 2.5 \times 10^9$ m, it is obvious that the error in the last approximation is negligible compared to the first one.

For neutralino annihilations in the Earth one can use the radius of the Earth, $R_\oplus$, as D in eq. (81), but as mentioned in sec. 2.3 annihilations can take place as far out as at a fractional radius of $x = 0.15$. If one then uses $D = R_\oplus$ one makes a maximum error in $1/D^2$ of nearly 40%! In sec. 5.3 the actual distance between the annihilation place and the detector, D, was calculated (see eq. (80)). By using this value in eq. (81) one obtains a more accurate calculation.

To get a feeling of the dependence of p_{det} on neutrino energy, E_ν, one can notice that the cross section σ_{CC} is propotional to the neutrino energy, E_ν, and that the range of the muon is proportional to the muon energy, E_μ. On the average E_μ will be proportional to E_ν and hence the probability in eq. (81) is essentially proportional to the neutrino energy squared, i.e. $p_{\rm det} \propto E_\nu^2$. This is the reason why the high energy tail of the neutrino spectrum is most important.

If one now generates neutralino annihilation products (e.g. b-quarks) in the Sun or in the Earth and follow the resulting muon neutrinos all the way to the detector and their subsequent interactions in the ice one can add all the detection probabilities given by eq. (81) and at the end divide by the number of generated parent particle pairs. The obtained number is actually the flux of muons in the ice per m^2 and parent pair.

6.2 Muon fluxes from simulations

The hadronisation and/or decay of annihilation products are simulated with Jetset 7.3 [24] and the neutrino-nucleon interactions on the way out of the Sun and in the ice are simulated with Pythia 5.6. The neutrino-nucleon interactions at the detector are simulated as if the detector medium is ice (as in AMANDA), but if one uses the results for an isoscalar detector medium (e.g. rock), the error one makes is only of the order of 5%. The muon flux is then calculated with eq. (81). Since the neutrino-nucleon interactions at low energies ($\lesssim 5$ GeV) are very time-consuming to simulate and probably not simulated in a good way either, only neutrinos with an energy above 5 GeV are simulated. For neutrinos with less energy a parametrization of the energy distribution, $d\sigma/dE_\mu$, is used and the muon angle is chosen as a fixed value depending on neutrino energy, $\theta = 15^\circ/\sqrt{E_\nu/2 \text{ GeV}}$. Hence the neutrinos with an energy of less than 5 GeV are not treated very accurately and the calculated muon fluxes at these low energies are expected to have larger errors than at higher energies. Especially when angular cuts are applied below 5 GeV, the results are not that accurate, due to the simple θ-equation above.

Concerning the Higgs bosons, they all decay into other particles from which the muon fluxes are simulated. Hence it is possible to approximately calculate the muon fluxes from channels containing Higgs particles from the fluxes from other channels. Nevertheless, simulations are done for Higgs bosons as well since in that way it is possible to check how accurately one can calculate the fluxes from Higgs boson channels and also the simulation results can be used as a guideline. Remember though, that the results for the channels containing Higgs bosons are based on the chosen Higgs masses and branching ratios in sec. 2.1. Depending on the MSSM parameters they may differ significantly from those used here and in that case it is better to calculate the muon flux from Higgs boson channels from the other channels. How that can be done is explained in an example below.

In fig. 10 the differential flux of muons in ice at the surface of the Earth is shown for some different neutralino masses and different channels. Integration of the differential flux above a threshold energy for the muon gives the total muon flux above that threshold. In table 9 to 22 (in appendix A) the muon fluxes above different thresholds and for different annihilation channels are shown for annihilation in the Sun and in the Earth. To be able to decrease the background, the fluxes are shown with different cuts in θ, the angle between the muon direction and the direction from the core of the Sun or the Earth to the detector.

If there were no energy loss of heavy hadrons before decay and no energy loss of the neutrinos on the way to the detector, the muon fluxes for a given channel are expected to scale approximately. As mentioned in sec. 6.1 above, the detection probability is approximately proportional to the neutrino energy squared. Hence the total flux should be approximately proportional to the neutralino mass squared. Thus, the fluxes in fig. 10 are divided by m_χ^2 and in d) and f) where the dominant flux are from prompt decay of τ's and W's and the neutrino absorption on the way to the detector can be neglected, the scaling hypothesis is seen to be correct. In b) the scaling is broken due to energy losses of heavy hadrons and in c) and e) the scaling is broken due to neutrino interactions on the way out of the Sun, whereas in a) both effects enter.

As can be seen in the tables, the highest fluxes are obtained from channels where the annihilation products directly can decay into muon neutrinos, i.e. τ's, W's and Z's. In the channels $Z^0H_1^0$, $Z^0H_2^0$, W^+H^- and W^-H^+, the main contribution to the muon flux comes from the Z's and the W's. As mentioned earlier, the Higgs masses are chosen as examples and it is now time to show that it is possible to approximately calculate the fluxes from the channels containing Higgs particles from the fluxes from other channels. Actually, the fluxes from the W^+H^- and W^-H^+-channels cannot be calculated separately from the other channels, since the Higgs boson decays into $\bar{b}t$ and the contribution to the flux from $\bar{b}$ is not equal to one half of that from $b\bar{b}$ because the ratio of neutrinos to antineutrinos is different in the flux from the b and from the $\bar{b}$. The same argument is of course valid for the t-quark and the W. However, the

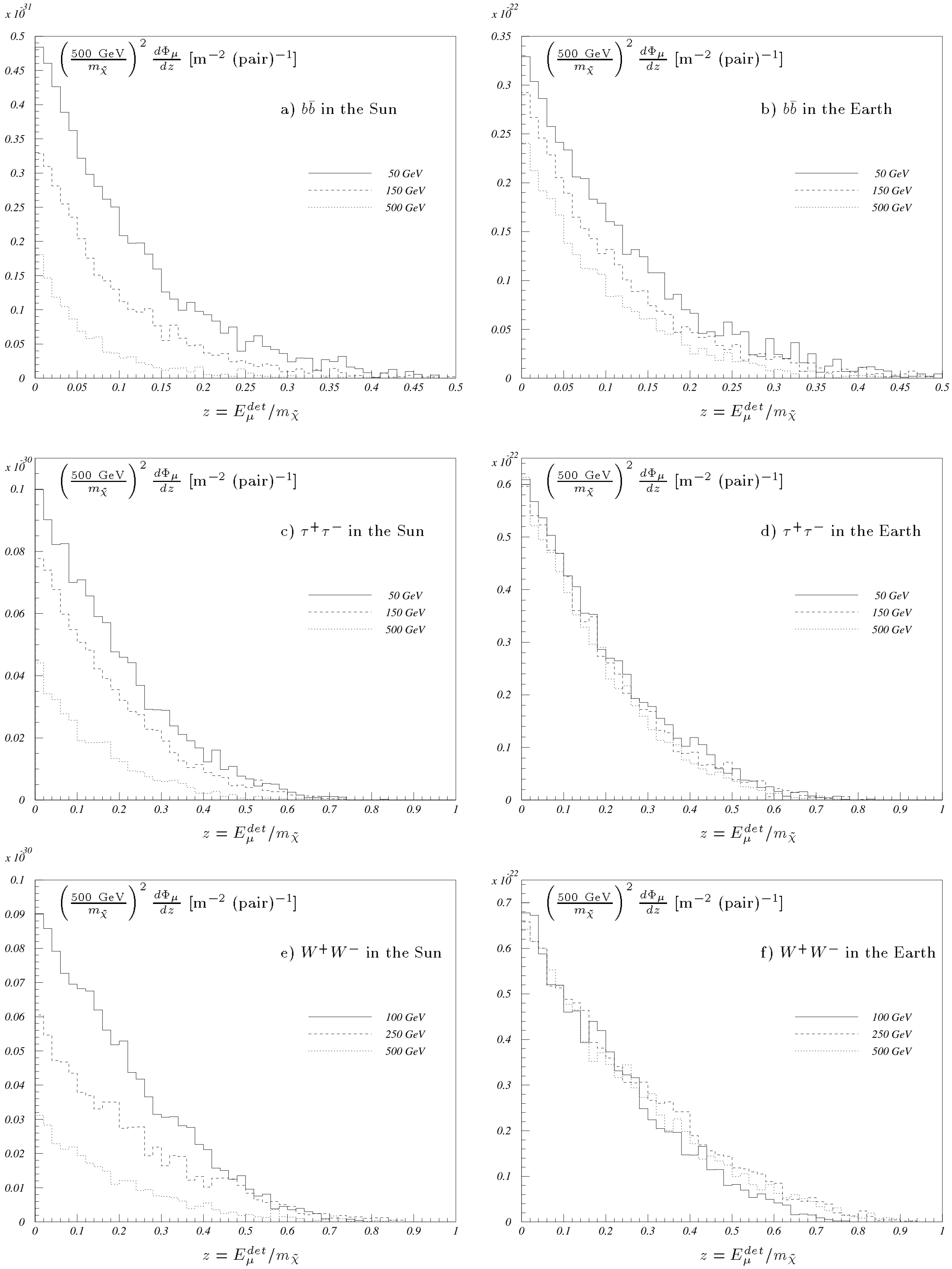

Figure 10: *Muon fluxes ($\mu^+ + \mu^-$) in ice at the surface of the Earth for the indicated neutralino masses and annihilation channels.*

sum of the two channels can be calculated approximately since here both b and $\bar{b}$, t and $\bar{t}$ and W^+ and W^- enters. The annihilation of neutralinos is of course equal into the two channels and hence it is anyway the sum of the two channels that is interesting. Thus, this limitation is of no importance.

Consider annihilation of two neutralinos of masses $m_{\tilde{\chi}}$ into two particles of masses m_1 and m_2. Since the neutralinos are assumed to be at rest when annihilating the total momentum of the two outgoing particles are equal in magnitude and opposite in direction. The total energy of particle 1 can be shown to be

$$E_1 = \frac{(2m_{\tilde{\chi}})^2 - m_2^2 + m_1^2}{4m_{\tilde{\chi}}} \tag{82}$$

where the masses are to be given in GeV. Thus, one can calculate the energy that goes to each of the two particles and use the tables in appendix A to get the flux from each of the two particles separatly. As an example, take the $Z^0H_2^0$-channel in the Sun with $m_{\tilde{\chi}} = 150$ GeV. $m_Z = 91.2$ GeV and $m_{H_2^0} = 70$ GeV yields $E_Z = 156$ GeV and $E_{H_2^0} = 144$ GeV. Interpolation of the fluxes in tables 11 and 12 yield that the total flux in the Z^0Z^0-channel is 240×10^{-35} m^{-2} (pair)$^{-1}$ when $m_{\tilde{\chi}} = 156$ GeV. In the $Z^0H_2^0$-channel there is only one Z^0 while there are two in the Z^0Z^0-channel and hence the contribution to the flux from that Z^0 is approximately $240/2 \times 10^{-35}$ m^{-2} (pair)$^{-1}$. If one assumes that the H_2^0 decays to $b\bar{b}$ in 82% of the cases the flux from it can approximately be calculated as 82% of the flux from the $b\bar{b}$-channel at $m_{\tilde{\chi}} = 72$ GeV. Interpolation between the muon flux tables yields that the flux from $b\bar{b}$ at this neutralino mass is approximately 12×10^{-35} m^{-2} (pair)$^{-1}$. Hence the total flux from the $Z^0H_2^0$-channel can be approximated by $(240/2 + 0.82 \times 12) \times 10^{-35} = 130 \times 10^{-35}$ m^{-2} (pair)$^{-1}$ which should be compared with the value obtained in the simulation, which is 137×10^{-35} m^{-2} (pair)$^{-1}$. The agreement is quite good. If one chooses other masses and branching ratios for the Higgs bosons than those chosen here, it is thus possible to calculate the muon fluxes approximately with the method described.

6.3 Parametrization of the muon fluxes

To increase the ease of use, the muon fluxes obtained from the simulations have been fitted to a parametrization according to the following

$$\frac{d\Phi_\mu}{dz}(m_{\tilde{\chi}}, z) = \frac{p_1 + p_2 m_{\tilde{\chi}} + p_3 m_{\tilde{\chi}}^2}{1 + \exp\left[\frac{z - p_4 \exp(-p_5 m_{\tilde{\chi}}^\alpha)}{p_6}\right]} \exp\left[-p_7\left(\frac{z}{m_{\tilde{\chi}}}\right)^2\right] \tag{83}$$

where $m_{\tilde{\chi}}$ is the mass of the neutralino in GeV and $z = E_\mu^{det}/m_{\tilde{\chi}}$. Only the fluxes with the cut $\theta < 5°$ have been fitted since this cut keeps the background down without reducing the signal too much. The fits have been made to the fluxes from the channels $c\bar{c}$, $b\bar{b}$, $t\bar{t}$, $\tau^+\tau^-$, W^+W^- and Z^0Z^0, since the fluxes from the other channels can be calculated from these as described in sec. 6.2. The results of the fits for different channels are shown in tables 3 and 4. The parameter α has been chosen to 1, except for the $b\bar{b}$-channel in the Earth where $\alpha = -1/2$ has been chosen to obtain a better fit. In general, the quality of the fits is quite good. In figure 11 a typical fit and the three worst fits are shown. Special concern has been taken to obtain good agreement in the high energy tail of the fluxes, since if one integrates the fluxes from a given threshold energy and upwards it may be just the tail that enters. A disagreement of this kind is seen in c) and d). The disagreement at the low energy part in b) is less severe since this part

Channel	p_1	p_2	p_3	p_4	p_5	p_6	p_7	α	Bad fit at $m_{\tilde{\chi}}$ =
$c\bar{c}$	1.97	−0.116	0.00235	0.244	0.00389	0.0464	0	1	
$b\bar{b}$	6.39	−0.351	0.00735	0.324	0.00472	0.0551	-1.16×10^4	1	
$t\bar{t}$	−469	3.91	0.0123	0.558	0.00470	0.115	1.75×10^5	1	150 GeV
$\tau^+\tau^-$	−48.4	0.690	0.0188	0.390	0.00279	0.103	244	1	
W^+W^-	−231	3.52	0.00964	0.706	0.00392	0.143	3.97×10^4	1	
Z^0Z^0	−324	5.18	0.00912	0.657	0.00387	0.153	5.01×10^4	1	

Table 3: *Parametrization of the muon fluxes for different channels and annihilation in the Sun. The fluxes are fitted to a parametrization according to eq. (83) and with these values the unit of the flux in eq. (83) is* $10^{-35} m^{-2} (pair)^{-1}$. *An angular cut of* $\theta < 5°$ *has been applied.*

Channel	p_1	p_2	p_3	p_4	p_5	p_6	p_7	α	Bad fit at $m_{\tilde{\chi}}$ =
$c\bar{c}$	1.36	−0.0445	0.000420	0.167	0.00229	0.0560	0	1	
$b\bar{b}$	3.58	−0.117	0.00110	0.0297	−21.7	0.0706	3.15×10^4	−1/2	100 GeV
$t\bar{t}$	115	−1.43	0.00553	2.06	0.00795	0.157	3.33×10^5	1	150 GeV
$\tau^+\tau^-$	5.77	−0.216	0.00272	0.272	0.000790	0.109	-4.17×10^3	1	
W^+W^-	7.98	−0.222	0.00291	0.392	0.000800	0.147	2.20×10^4	1	
Z^0Z^0	14.6	−0.329	0.00363	0.464	0.00120	0.145	4.30×10^4	1	

Table 4: *Parametrization of the muon fluxes for different channels and annihilation in the Earth. The fluxes are fitted to the parametrization according to eq. (83) and with these values the unit of the flux in eq. (83) is* $10^{-25} m^{-2} (pair)^{-1}$. *An angular cut of* $\theta < 5°$ *has been applied.*

of the spectra only enters when one calculates the total flux above a small threshold energy and the error is never larger than $\sim 10\%$. All other fits are better than those in c) and d) and if one calculates the total flux of muons above a given threshold energy, the accuracy of the fits is in general of the order $\lesssim$ 5–10% when the threshold energy is in the range 0–50 GeV. The only big disagreement is for a high threshold energy and the $t\bar{t}$-channel at 150 GeV as can be seen in c) and d). The parametrization in eq. (83) is a smoothly varying function which should not give rise to any surprises when interpolating to intermediate masses. Thus it should be justified to use the parametrization in the range 50 GeV $\leq m_{\tilde{\chi}} \leq$ 500 GeV.

As mentioned earlier, the method described in sec. 6.2 can be used to calculate the fluxes from other channels than those parametrized here. As an example, take the $Z^0H_2^0$-channel in the Sun at $m_{\tilde{\chi}} = 150$ GeV as studied earlier (but now with the cut $\theta < 5°$). In this case 156 GeV goes into the Z^0 and 144 GeV goes into the H_2^0. Integration of the fluxes, $d\Phi_\mu/dz$, from $z = 0$ to $z = 1$ yields the total flux from each channel. With the branching ratios of the H_2^0 from sec. 2.1 (with the $s\bar{s}$-channel neglected) the contributions to the flux from the different

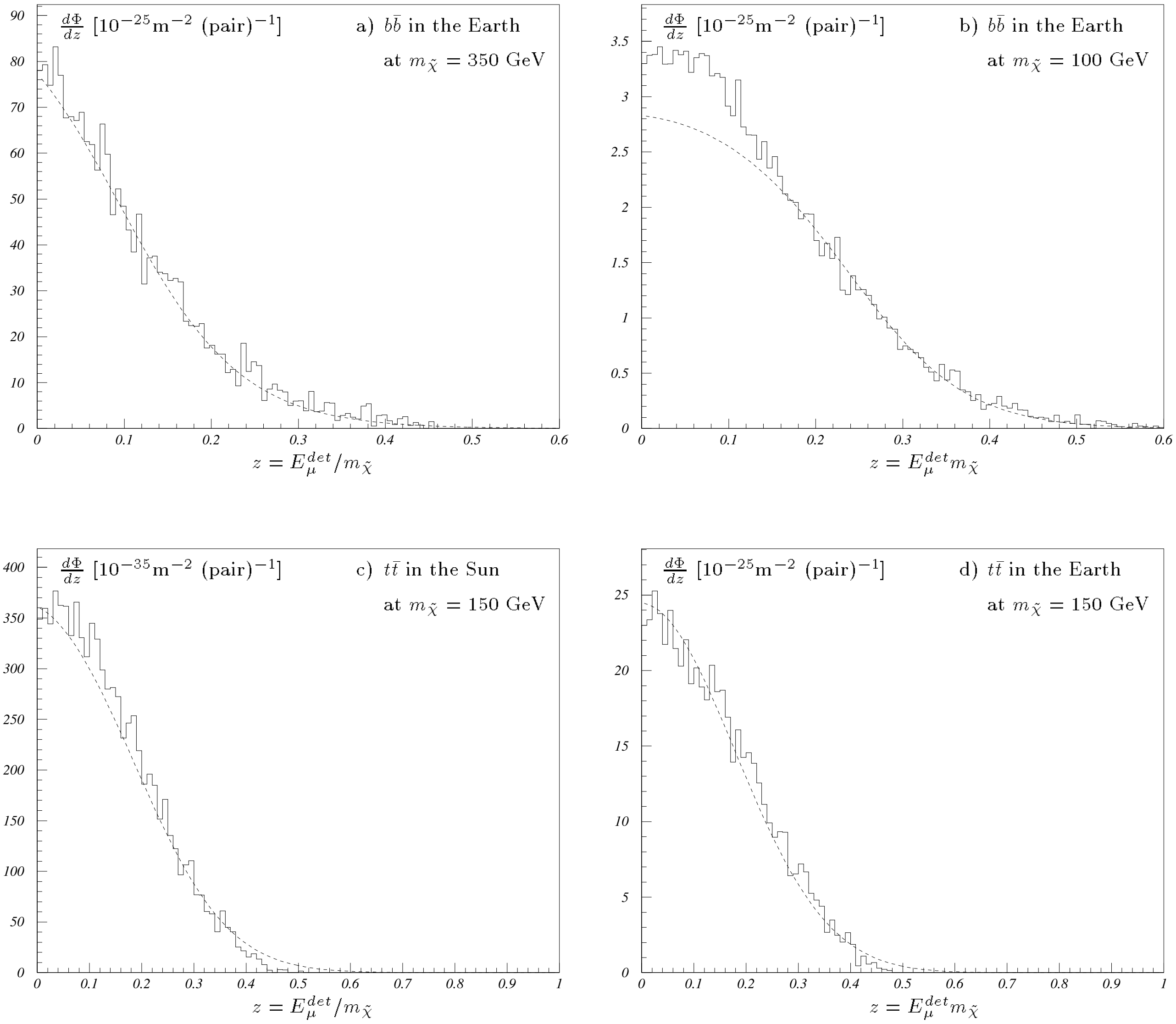

Figure 11: *Example of fits to the muon fluxes. a) A typical fit ($b\bar{b}$ in the Earth at 350 GeV). b) The worst obtained fit ($b\bar{b}$ in the Earth at 100 GeV). c) A moderate fit ($t\bar{t}$ in the Sun at 150 GeV). d) A moderate fit ($t\bar{t}$ in the Earth at 150 GeV). The fits in b)–d) are the worst ones obtained.*

channels become

$$\left\{ \begin{array}{lll} Z^0 Z^0 & \text{at } m_{\tilde{\chi}} = 156 \text{ GeV} & \Rightarrow \quad \Delta\Phi_{ZZ} = 0.5 \times 217.13 = 108.57 \\ b\bar{b} & \text{at } m_{\tilde{\chi}} = 72 \text{ GeV} & \Rightarrow \quad \Delta\Phi_{b\bar{b}} = 0.82 \times 4.75 = 3.90 \\ c\bar{c} & \text{at } m_{\tilde{\chi}} = 72 \text{ GeV} & \Rightarrow \quad \Delta\Phi_{c\bar{c}} = 0.08 \times 1.07 = 0.09 \\ \tau^+\tau^- & \text{at } m_{\tilde{\chi}} = 72 \text{ GeV} & \Rightarrow \quad \Delta\Phi_{\tau\tau} = 0.09 \times 31.83 = 2.87 \end{array} \right. \tag{84}$$

in units of 10^{-35} m^{-2}(pair)$^{-1}$. This yields the total flux $\Phi = 115 \times 10^{-35}$ m^{-2}(pair)$^{-1}$ which should be compared with the flux obtained from the simulations, $\Phi = 116 \times 10^{-35}$ m^{-2}(pair)$^{-1}$. The agreement is quite good.

6.4 Absolute rate of events

The absolute rate of events at the detector is given by

$$\Gamma_{events} = \Gamma_A A_{eff} \sum_i B_i \Phi_i \tag{85}$$

where Γ_A is the annihilation rate, A_{eff} is the effective area of the detector in the direction of the Sun, B_i is the branching ratio for annihilation channel i and Φ_i is the muon flux (over threshold for the detector) per unit area and parent pair.

6.5 The AMANDA detector

It is now time to apply the results to the AMANDA detector [2]. The AMANDA detector is a neutrino detector situated at the south pole. The detector consists of strings with photomultiplier tubes that are put down in the ice at a depth of about 1 km. At this depth the antarctic ice is clear and bubblefree (i.e. transparent). It is also very pure with a very small amount of radioactive material in it. When a neutrino enters the ice it can interact via a charged current reaction and produce a muon. Since the speed of light in the ice will be lower than it is in vacuum the produced muon will, if it is energetic enough, move with a speed greater than the speed of light in the ice. Hence the muon will emit Čerenkov radiation which can be detected by the photomultiplier tubes. With careful timing of the signals it is possible to reconstruct the muon direction with an accuracy of about 1°. Hence it is possible to apply cuts in the angle of the muon relative to the direction from the source to the detector.

The present plan for the detector [27] is to use 10 strings with 20 photomultipliers on each with one string in the middle and the other nine symmetrically on a circle of radius 30 m around it. With this configuration the effective area in the direction of the Sun is approximately $A_{eff} = 2000$ m^2 and downwards in the direction of the core of the Earth it is approximately $A_{eff} = 10000$ m^2. The energy threshold for detection of muons is not exactly known yet, but considering eq. (68) a muon of 10 GeV has a range of about 40 m which is nearly the diameter of the detector. Hence the threshold is expected to be in this region, $E_\mu^{th} \sim 10$ GeV.

6.6 Absolute rate examples

By using the examples of branching ratios and capture rates in table 5, the absolute rate of events can be calculated with eq. (85). The results are shown in the same table. As can be seen, in many of the examples the event rate is high enough for detection to be possible.

7 Background flux of muons

The background flux of muons has different origin, e.g. neutrinos created in the Earth's atmosphere by cosmic rays may produce muons in the detector and muons created by cosmic rays may penetrate the Earth and reach the detector. There is also a possibility for neutrinos created by cosmic rays in the Sun's corona to reach the detector. These processes will be considered in the following sections.

Example number	1	2	3	4	5	6	7	8	9	10	11
$m_{\tilde{\chi}}$ [GeV]	38.9	117.9	250.3	352.6	192.5	146.0	60.1	234.4	466.4	492.6	494.1
μ [GeV]	100	200	300	400	200	500	100	300	500	500	600
M_2 [GeV]	200	300	600	800	1500	300	200	500	1000	1500	1000
$\tan\beta$	2.0	2.0	2.0	2.0	2.0	2.0	25.0	25.0	25.0	25.0	25.0
Gaugino fraction	~ 0.5	~ 0.5	~ 0.5	~ 0.5	~ 0.01	~ 0.99	~ 0.5	~ 0.5	~ 0.5	~ 0.01	~ 0.9
$B_{c\bar{c}}$	3.36	0.01	0.00	0.00	0.00	0.00	0.00	0.00	0.00	0.00	0.00
$B_{b\bar{b}}$	90.48	5.89	0.05	0.01	0.02	1.05	94.68	6.22	0.04	0.00	0.02
$B_{t\bar{t}}$	0.00	0.00	3.87	5.49	16.05	0.00	0.00	22.09	19.06	32.86	14.19
$B_{\tau^+\tau^-}$	4.72	0.30	0.00	0.00	0.00	0.02	4.88	0.31	0.00	0.00	0.00
$B_{W^+W^-}$	0.00	13.97	3.18	1.68	38.10	0.17	0.00	1.59	1.73	16.22	0.13
$B_{Z^0Z^0}$	0.00	3.98	2.13	1.23	31.25	0.01	0.00	0.88	1.32	13.22	0.09
$B_{H_1^0H_3^0}$	0.00	63.54	3.92	1.87	2.94	50.59	0.00	3.84	1.07	3.49	1.23
$B_{Z^0H_1^0}$	0.00	0.00	82.62	86.52	10.29	29.39	0.00	63.66	75.67	28.19	82.78
$B_{Z^0H_2^0}$	0.00	10.41	1.55	1.59	0.00	5.23	0.00	0.00	0.01	0.98	0.08
$B_{W^\pm H^\mp}$	0.00	0.00	2.55	1.56	1.16	11.42	0.00	1.24	0.76	3.01	0.90
B_{gg}	1.24	1.89	0.13	0.07	0.17	2.10	0.24	0.14	0.17	0.98	0.30
$B_{gq\bar{q}}$	0.00	0.00	0.00	0.00	0.00	0.00	0.00	0.00	0.16	1.06	0.29
C_A^{Sun} [10^{24} s^{-1}]	5	0.8	0.2	0.1	0.02	0.02	700	70	20	2	9
C_A^{Earth} [10^{14} s^{-1}]	200	8	1	0.4	0.1	0.1	1000	4	1	0.1	0.2
Γ_{events}^{Sun} [yr^{-1}]	1.4	19	21	18	2.4	0.31	990	6300	4800	580	2300
Γ_{events}^{Earth} [yr^{-1}]	12	45	62	60	5.9	0.58	460	190	280	37	63

Table 5: *Gaugino fractions [4], branching ratios B_i [17] in %, capture rates [4, 18] C and event rates Γ (eq. (85)) in* AMANDA *for different choices of the parameters in the MSSM. The effective areas used are A_{eff} = 2000 m^2 in the direction of the Sun and A_{eff} = 10000 m^2 in the direction of the Earth's core. The fluxes, Φ_i, are obtained from the tables in appendix A and the cuts made are $\theta < 5°$ and $E_\mu > 10$ GeV. The parameters for examples 7, 8 and 9 are excluded by the Kamiokande experiment [18] but included anyway as illustrative examples.*

E_μ^{min} [GeV]	$\Phi_b(E_\mu > E_\mu^{min})$ $[10^{-9}\ \mathrm{m}^{-2}\ \mathrm{s}^{-1}\ \mathrm{sr}^{-1}]$	Absolute rate of events, Γ [yr^{-1}] $\theta < 10°$	$\theta < 7.5°$	$\theta < 5°$
2	2.03	12.2	6.9	3.1
4	1.71	10.3	5.8	2.6
7	1.46	8.8	5.0	2.2
10	1.31	7.9	4.4	2.0

Table 6: *Muons from atmospheric neutrinos in the near horizontal direction, corresponding to background when one looks towards the Sun. The fluxes are from Gaisser et al. [28] and the absolute rates are calculated with an effective area of A_{eff} = 2000 m^2.*

E_μ^{min} [GeV]	$\Phi_b(E_\mu > E_\mu^{min})$ $[10^{-9}\ \mathrm{m}^{-2}\ \mathrm{s}^{-1}\ \mathrm{sr}^{-1}]$	Absolute rate of events, Γ [yr^{-1}] $\theta < 10°$	$\theta < 7.5°$	$\theta < 5°$
2	3.37	102	57	25
4	2.90	87	49	22
7	2.52	76	43	19
10	2.28	69	39	17

Table 7: *Muons from upgoing atmospheric neutrinos in the near vertical direction, corresponding to background when one looks towards the core of the Earth. The fluxes are from Gaisser et al. [28] and the absolute rates are calculated with an effective area of A_{eff} = 10000 m^2.*

7.1 Background of muons from atmospheric neutrinos

Gaisser and Stanev [28] have calculated underground muon fluxes by using the neutrino fluxes calculated by Volkova [29]. In table 6 the fluxes they obtained in the near horizontal direction is shown for different cuts in the muon energy. These muons contribute to the background when one looks towards the Sun. Also shown is the absolute rate of background events for different cuts in the angle θ, which is the angle beteen the muon direction and the direction from the Sun to the detector.

In table 7 the same but for the vertical direction is shown. These muons contribute to the background when one looks towards the center of the Earth. Also shown is the absolute rate of background events for different cuts in the angle θ, which is the angle beteen the muon direction and the direction from the core of the Earth to the detector.

7.2 Background of atmospheric muons

For atmospheric muons to reach the detector they have to traverse a certain amount of matter. If one looks towards the center of the Earth they have to pass the entire Earth and that penetration can be neglected. If one however looks towards the Sun, the amount of matter that has to be traversed depends on where the Sun is compared to the horizon. In case of AMANDA this depends only on season since the Sun's height above (or below) horizon is constant over one day. When the Sun is as high as it can be above the horizon there are only some kilometers of ice for the muons to traverse and hence muons can reach down to the detector. One wants to look at the Sun for as large fraction of the year as possible and hence the flux of muons

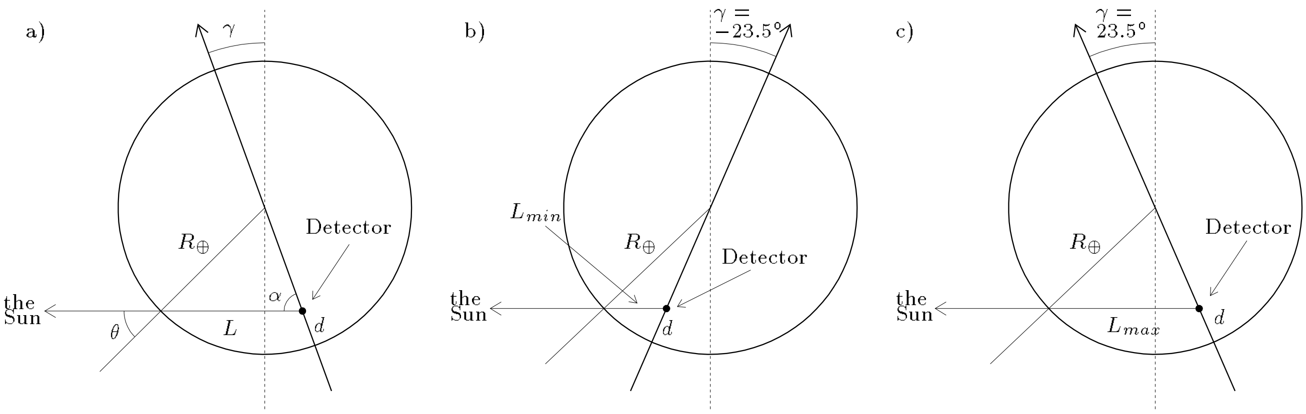

Figure 12: *The geometry of the* AMANDA *detector [2] in the Earth and relevant distances and angles for the calculation of L, the distance the atmospheric muons has to pass in the Earth before reaching the detector. In the figures $d = 1$ km is the depth of the detector, $R_\oplus = 6.38 \times 10^3$ km is the radius of the Earth, γ is the projected tilt angle of the Earth axis as seen from the Sun and θ is the impact angle of the muon as it penetrates the surface of the Earth. The distance d is greatly exaggerated in the figure. a) general case. b) summer at* AMANDA *when $L = L_{min}$. c) winter at* AMANDA *when $L = L_{max}$.*

that reach down to the detector as a function of season has to be calculated. In figure 12 the geometry of the detector in the Earth is shown. The wanted thickness is the distance called L in the figure, which can be written as

$$L = R_\oplus \cos\theta + R_\oplus \sin\theta \tan\gamma \tag{86}$$

The angle θ can be obtained by noting that

$$\cos\alpha = \frac{R_\oplus \sin\theta \tan\gamma}{R_\oplus - d} \tag{87}$$

Further on one has $\alpha = 90° - \gamma$ which yields

$$\theta = \arcsin\left(\frac{R_\oplus - d}{R_\oplus}\cos\gamma\right) \tag{88}$$

The angle γ is the tilt of the Earth axis away from the Sun. The Earth axis tilt compared to a line perpendicular to the orbital plane is called the *obliquity* and it is [30] $\gamma_\oplus = 23.5°$. The projected angle, γ, can then be written as

$$\tan\gamma = \tan\gamma_\oplus \cos\varphi \tag{89}$$

where φ is the azimutal angle of the Earth along its orbit around the Sun. $\varphi = 0°$ corresponds to winter at AMANDA and $\varphi = 180°$ corresponds to summer. With these equations it is possible to calculate the thickness of the Earth that the muons have to pass through as a function of φ, i.e. as a function of season.

In reality one has to accept muons that come from a certain solid angle centered on the Sun. If one uses a cut in this angle, ψ, of $\pm 5°$ one has to calculate the distance L for different directions in this solid angle. If one looks in a direction ψ from the center of the Sun, and the part of that angle that is pointing "upwards" is called ψ', one can note that the distance L

only changes significantly when ψ' changes and not when the other part of the angle ψ changes. This is also true for the angle θ. By assuming that L and θ only depend on ψ' and not on the other part of ψ they can be calculated approximately by substituting γ with $\gamma + \psi'$ in eqs. (86) to (88).

Now consider a muon that has to traverse a distance L to reach the detector. Inversion of eq. (68) yields that it must have at least an energy of

$$E_\mu^{min} = \frac{\alpha}{\beta} [\exp(L\beta) - 1] \qquad (90)$$

to reach the detector. The flux of muons from this direction can then be calculated by integration of the differential flux at the surface from this minimum to infinity. Integration of this flux over the solid angle around the Sun yields the total flux of muons from this solid angle at the detector. Lipari [31] has calculated the differential fluxes of muons at the surface of the Earth for energies in the interval 1–10^6 GeV and for different zenith angles, θ. For energies above 10^6 GeV an extrapolation has been done by assuming that the differential flux follows a power law, $d\Phi/dE_\mu \propto E_\mu^{-\gamma}$ where γ has been estimated from the differential flux at 3.16×10^5 and 10^6 GeV. By using these fluxes it is possible to calculate the total flux and event rate as a function of season. This is shown in table 8.

Since the background muons from atmospheric neutrinos is about 2 events/yr the background from atmospheric muons can be neglected for roughly one half of the year, i.e. during the antarctic winter. However, during the antarctic summer the flux of atmospheric muons at the detector is huge compared with both the signal and the background rates and observation in the direction of the Sun is thus not possible when the Sun is above the horizon. Note that this is not included neither in the rate examples in table 5 nor in the background rates in table 6. In practice, one thus has to divide these event rates by two when one looks towards the Sun.

7.3 Cosmic ray-induced muon neutrinos from the Sun

I.V. Moskalenko et al. [32] have recently calculated the flux of cosmic ray-induced muon neutrinos from the Sun's corona. They calculated the total flux above certain energy thresholds in a solid angle of $\pm 0.25°$ around the Sun and compared it with the corresponding neutrino flux from the Earth's atmosphere. The result is that up to 200 GeV the two sources (Sun's corona and Earth's atmosphere) are of the same order, but above 200 GeV the total flux from the Sun is higher. By differentiating their total flux, the differential flux can be obtained. In fig. 13 the differential muon neutrino flux from the Sun's corona is shown together with the differential neutrino flux from the Earth's atmosphere as calculated by Lipari [31]. An angular cut of $\pm 5°$ around the Sun is made and since this solid angle is larger than that used by Moskalenko et al. the flux from the Earth's atmosphere is increased while the flux from the Sun's corona is kept constant. Hence the background from the Earth's atmosphere dominates as can be seen in the figure. The total rate of events is proportional to an integral of the differential flux times the neutrino energy squared (sec. 6.1) and hence the high energy part of the differential flux is quite important. At higher energies than those shown in the figure, the fluxes will probably decrease even faster and hence the part of the spectrum shown will give the main contribution to the rate. Since the differential flux from the Sun's corona is less than that from the Earth's atmosphere, the background rate from the Sun's corona will be less than the background rate from atmospheric neutrinos. The background of muon neutrinos from the Sun's corona can thus be neglected compared to the background of muon neutrinos from the Earth's atmosphere.

φ [°]	L_{min} [cm]	$(E_\mu^{min})_{min}$ [GeV]	Φ_{max} [cm^{-2} s^{-1} sr^{-1}]	Φ_{tot} [cm^{-2} s^{-1}]	Γ [yr^{-1}]
0	4.05×10^8	$> 10^{60}$	$< 10^{-134}$	$< 10^{-138}$	$< 10^{-124}$
45	2.74×10^8	$> 10^{60}$	$< 10^{-134}$	$< 10^{-138}$	$< 10^{-124}$
75	3.53×10^7	$> 10^{60}$	$< 10^{-134}$	$< 10^{-138}$	$< 10^{-124}$
80	6.02×10^6	2.1×10^{13}	7.0×10^{-35}	3.0×10^{-39}	1.9×10^{-24}
82	3.39×10^6	5.4×10^8	1.7×10^{-22}	8.9×10^{-27}	5.6×10^{-12}
84	2.29×10^6	6.4×10^6	2.5×10^{-17}	2.2×10^{-21}	1.4×10^{-6}
86	1.72×10^6	6.2×10^5	1.2×10^{-14}	2.0×10^{-18}	1.2×10^{-3}
87	1.52×10^6	2.8×10^5	1.0×10^{-13}	2.0×10^{-17}	1.3×10^{-2}
88	1.37×10^6	1.5×10^5	5.2×10^{-13}	1.4×10^{-16}	8.7×10^{-2}
89	1.24×10^6	9.1×10^4	2.0×10^{-12}	6.7×10^{-16}	4.2×10^{-1}
90	1.14×10^6	5.9×10^4	6.1×10^{-12}	2.5×10^{-15}	1.6×10^0
91	1.05×10^6	4.1×10^4	1.6×10^{-11}	7.9×10^{-15}	5.0×10^0
92	9.71×10^5	3.0×10^4	3.5×10^{-11}	2.1×10^{-14}	1.4×10^1
93	9.05×10^5	2.3×10^4	6.9×10^{-11}	5.1×10^{-14}	3.2×10^1
94	8.48×10^5	1.8×10^4	1.3×10^{-10}	1.1×10^{-13}	6.9×10^1
95	7.97×10^5	1.4×10^4	2.1×10^{-10}	2.1×10^{-13}	1.4×10^2
96	7.53×10^5	1.2×10^4	3.4×10^{-10}	3.9×10^{-13}	2.5×10^2
98	6.77×10^5	8.8×10^3	7.5×10^{-10}	1.1×10^{-12}	7.1×10^2
100	6.16×10^5	6.8×10^3	1.4×10^{-9}	2.7×10^{-12}	1.7×10^3
105	5.04×10^5	4.1×10^3	4.4×10^{-9}	1.4×10^{-11}	8.7×10^3
120	3.37×10^5	1.8×10^3	2.7×10^{-8}	2.0×10^{-10}	1.3×10^5
135	2.66×10^5	1.2×10^3	6.3×10^{-8}	6.8×10^{-10}	4.3×10^5
150	2.31×10^5	9.4×10^2	1.0×10^{-7}	1.3×10^{-9}	8.0×10^5
165	2.14×10^5	8.5×10^2	1.3×10^{-7}	1.7×10^{-9}	1.1×10^6
180	2.09×10^5	8.2×10^2	1.3×10^{-7}	1.9×10^{-9}	1.2×10^6

Table 8: *Background of atmospheric muons as a function of φ, the azimutal angle of the Earth along its orbit around the Sun. The values of L_{min} and $(E_\mu^{min})_{min}$ are the minimum values in a solid angle of $\pm 5°$ around the Sun. Φ_{max} is the maximum of the integrated flux above E_μ^{min} in the solid angle around the Sun. Φ_{tot} is the total flux in the whole solid angle and Γ is the corresponding rate of events with the assumption that A_{eff} = 2000 m^2. The differential fluxes used are from Lipari [31].*

7.4 Conclusions

As can be seen from the previous sections, the background of muons from atmospheric neutrinos is the most important background source. When one looks towards the Sun, the background of atmospheric muons is far too high during the antarctic summer, but during the winter it can be neglected. The flux of muon neutrinos from the Sun's corona is also negligible compared to the flux of muon neutrinos from the Earth's atmosphere. Hence, if the Sun is observed only during the antarctic winter, the main contribution to the background flux of muons are coming from atmospheric neutrinos, table 6. When the core of the Earth is observed, the background flux of muons coming from atmospheric neutrinos, table 7, is always the most important background.

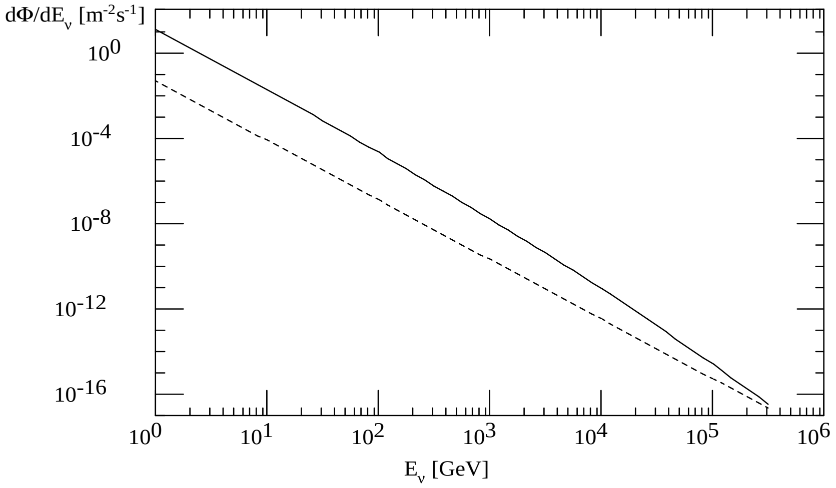

Figure 13: *The differential muon neutrino fluxes from the Earth's atmosphere (solid) and the Sun's corona (dashed) in a solid angle of $\pm 5°$ around the Sun. The flux from the Earth's atmosphere is calculated by Lipari [31] and the flux from the Sun's corona is obtained by differentiating the total flux calculated by Moskalenko et al. [32].*

8 Comparison between signal and background rates

As mentioned in sec. 7.4, the main background of muons are coming from atmospheric neutrinos which interact in the ice producing muons. One can compare the signal event rates for the examples in table 5 with the background event rates in tables 6 and 7. The result is that for low neutralino masses ($\lesssim$ 100 GeV) and low $\tan\beta$ (~ 2), the signal rate is of the same size or less than the background rate. If the absolute rates were high, this would not be a problem, but since the absolute rates are so low it will not be possible to separate signal from background for these cases. If, on the other hand, the neutralino mass is higher, the signal rate is higher and sometimes much higher than the background rate. In these cases one would clearly be able to observe a signifcant muon flux above the background flux. In fig. 14 the expected event rate (signal and background) is shown in concentric angular bins centered on the Sun for the third example in table 5. The first bin corresponds to an angular cut of $\pm 5°$ around the Sun and the next ones are concentric and of the same size in solid angle. The signal rate is calulated with eq. (85) and the data in tables 5 and 13. The dashed line corresponds to the expected background rate. It is clearly seen that it should be possible to see an increased flux in the first bin if the parameters were those of this example.

The conclusion is that in parts of parameter space (high neutralino mass or high $\tan\beta$), it is possible for Amanda to search for neutralino annihilations and find a significant signal if the MSSM parameters are in that region and supersymmetry exists. If Amanda would not see a significant signal in these regions of parameter space, it is possible to put constraints on the parameteres in the MSSM. To be noted is that for some examples in the table where Amanda clearly is able to search for a neutralino, Kamiokande [18] has not been able to search (due to too low signal rates). Hence Amanda will be able to investigate *new* parts of the parameter space.

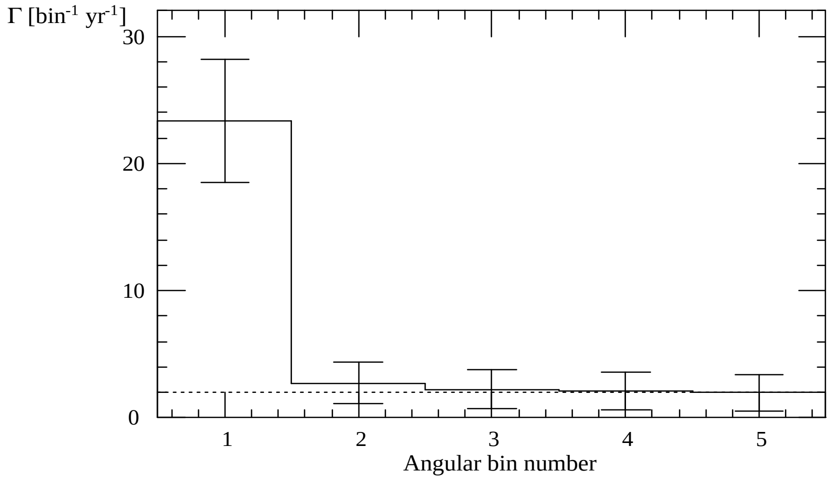

Figure 14: *The expected event rate in concentric angular bins around the Sun for the third example in table 5. The solid line corresponds to the total event rate (signal + background) and the dotted line is the background flux of muons from atmospheric neutrinos (table 6). The first bin corresponds to an angular cut of* $\pm 5^\circ$ *around the Sun and the next ones are concentric and of the same size in solid angle. The errors shown is just the square root of the number of events in each bin. A cut of* $E_\mu^{det} > 10$ *GeV is applied.*

9 Conclusions

As shown in table 5 there is some possibility of observing an enhanced flux of muons in the direction from the Sun or the Earth, and in many cases the fluxes are larger than the background flux of muons (tables 6 and 7). In this section the possible errors made and changes that could be done are discussed.

First of all, the rate examples all consider specific choices of the MSSM parameters. There may well be some other suitable choices that make the rates higher or lower. As mentioned in sec. 8 it is possible for AMANDA to investigate the MSSM parameter space in those regions where the rate is high (roughly where $m_{\tilde{\chi}} \gtrsim 100$ GeV or $\tan\beta \gtrsim 2$). If the MSSM parameters are in those regions where the rate is high, AMANDA will be able to detect a significant muon flux form neutralino annihilations. On the other hand, if AMANDA would not see a significant flux of muon neutrinos from the Sun or the Earth it should be possible to make new constraints on the MSSM parameters.

When Kamionkowski [4] and Mori et al. [18] have calculated the capture rates they have assumed that the density in the Universe is exactly critical and that all dark matter is made up of neutralinos. The first assumption is reasonable, but the second one is dubious since some parts of the dark matter may have been discovered recently, namely the Brown dwarfs. However, these will probably not make up all the mass of the dark matter and presumably a substantial fraction of the dark matter will be composed of other objects, e.g. neutralinos.

The effective area of the AMANDA detector is calculated from simulations of muons with much higher energies than those considered here. Hence it is probable that the effective areas change when going down in energies. One way to obtain very accurate results would be to use the muon fluxes calculated here and then simulate the interaction with the detector using GEANT as was done when the effective area was calculated.

In this paper, the configuration with ten strings in the AMANDA detector has been used as an example. During the winter of 1993/1994 the first six strings will be put down in the ice and with this set-up the effective areas are smaller than those used here, but of course it will be possible to start searching for neutralino annihilations even with this smaller detector. If the AMANDA detector is successful, it can be supplemented with a lot of more strings which would give a detector with much higher effective areas than those obtained with ten strings and this would be a very powerful detector in the search for neutralinos (if they are not found earlier).

Acknowledgements

I would like to thank my supervisor Gunnar Ingelman for the idea of the project and for giving me valuable support and help when I encountered problems. I also want to thank Lars Bergström for theoretical guidance in supersymmetry and helpful discussions. Thanks also to the people in the AMANDA group for discussions and help. At last, but not least, thanks also to Mats Thunman, Anders Edin and Johan Rathsman for valuable discussions, help with computer problems etc.

This report was written in LaTeX and the figures were made with PAW and TOPDRAW.

References

[1] D.H. Eckhardt, Phys. Rev. **D48** (1993) 3762.

[2] R.M. Morse et al., AMANDA proposal. For an overview of high energy neutrino telescopes, see e.g. F. Halzen, *Astroparticle Physics with High Energy Neutrino Telescopes*, Madison preprint MAD/PH/785.

[3] H.E. Haber , *Introductory low-energy supersymmetry*, U.C. Santa Cruz, SCIPP-92-33.

[4] M. Kamionkowski, Phys. Rev. **D44** (1991) 3021.

[5] A. Gould, Astrophys. Journal **321** (1987) 571, A. Gould, Astrophys. Journal **368** (1991) 610, A. Gould, Astrophys. Journal **388** (1992) 338.

[6] H.E. Haber and G.L. Kane, Phys. Rep. **117** (1985).

[7] G.B. Gelmini, P. Gondolo and E. Roulet, Nucl. Phus. **B351** (1991) 623.

[8] K.A. Olive and M. Srednicki, Phys. Lett. **B230** (1989) 78

[9] Particle Data Group, Phys. Rev. **D45** (1992).

[10] T.K. Gaisser, G. Steigman and S. Tilav, Phys. Rev. **D34** (1986) 2206.

[11] S. Ritz and D. Seckel, Nucl. Phys. **B304** (1988) 877.

[12] F. Mandl, *Statistical Physics*, 2nd Ed., John Wiley & Sons (1988).

[13] J.N. Bahcall and R.K. Ulrich, Rev. Mod. Phys. **60** (1988) 297.

[14] M. Srednicki, K. A. Olive and J. Silk, Nucl. Phys. **B279** (1987) 804.

[15] *The New Encyclopædia Britannica*, 15th Ed., 1991.

[16] M. Drees, G. Jungman, M. Kamionkowski and M.M. Nojiri, *Neutralino Annihilation into Gluons*, Madison preprint MAD-PH-766 (EFI-93-38, IASSNS-HEP-93/37).

[17] L. Bergström, private communication.

[18] M. Mori et al., KEK Preprint 93-77, submitted to Phys. Rev. **D**.

[19] L. Bergström and K. Mellbourn, private communication. Report in preparation.

[20] B. Povh and J. Hüfner, Phys. Lett. **B245** (1990) 653.

[21] J.D. Jackson, *Classical Electrodynamics*, 2nd Ed., John Wiley & Sons, 1975.

[22] D.H. Perkins, *Introduction to High Energy Physics*, 3rd Ed., Addison-Wesley Publishing Company, Inc. (1987).

[23] M. Glück, E. Reya and A. Vogt, Z. Phys **C53** (1992) 127.

[24] T. Sjöstrand, *PYTHIA 5.6 and JETSET 7.3. Physics and Manual*, CERN-TH.6488/92, T. Sjöstrand, Computer Physics Commun **39** (1986) 347, T. Sjöstrand and M. Bengtsson, Computer Physics Commun **43** (1987) 367, H.-U. Bengtsson and T. Sjöstrand, Computer Physics Commun **46** (1987) 43.

[25] T. Gaisser, *Cosmic Rays and Particle Physics*, Cambridge University Press, 1990.

[26] W. Lohmann, R. Kopp and R. Voss, *Energy loss of muons in the energy range 1–10000 GeV*, CERN Report 85-03 (1985).

[27] S. Carius and P.-O. Hulth, private communication.

[28] T.K. Gaisser and T. Stanev, Phys. Rev. **D30** (1984) 985.

[29] L.V. Volkova, Yad. Fiz. **31** (1980) 784 [Sov. J. Nucl. Phys **31** (1980) 1510]; in *Proceedings of the 1978 DUMAND Summer Workshop, LaJolla, California*, edited by A. Roberts (Scripps Institute of Oceanography, LaJolla, 1979), Vol. 1, p. 75.

[30] G.O. Abell, D. Morrison and S.C. Wolff, *Exploration of the Universe*, 5th Ed., CBS College Publications, 1987.

[31] P. Lipari, Astropart. Phys. **1** (1993) 195.

[32] I.V. Moskalenko and S. Karakula, J. Phys. G: Nucl. Part. Phys: **19** (1993) 1399.

A Tables of muon fluxes

In the following two sections the muon fluxes above different thresholds and for different annihilation channels are shown for annihilation in the Sun and in the Earth. The masses and branching ratios of the Higgs bosons are those chosen in sec. 2.1 and the mass of the top quark is set to 150 GeV.

A.1 Muon fluxes from neutralino annihilations in the Sun

Channel	θ cut	Φ_μ [$\times 10^{-35}$ m^{-2}(parent pair)$^{-1}$] E_μ^{det} [GeV] $>$									
		0	3	5	7	10	15	20	25	30	50
$c\bar{c}$	no cut	1.90	0.983	0.612	0.369	0.161	(0.036)	(0.0075)	(0.0021)	(0)	0
	$\theta < 10°$	1.20	0.796	0.561	0.359	0.161	(0.036)	(0.0075)	(0.0021)	(0)	0
	$\theta < 7.5°$	0.874	0.634	0.477	0.322	0.159	(0.036)	(0.0075)	(0.0021)	(0)	0
	$\theta < 5°$	0.481	0.366	0.293	0.216	0.116	(0.035)	(0.0075)	(0.0021)	(0)	0
$b\bar{b}$ †	no cut	6.39	3.79	2.62	1.79	0.967	0.310	0.0830	(0.016)	(0.0014)	0
	$\theta < 10°$	4.48	3.20	2.41	1.73	0.959	0.310	0.0830	(0.016)	(0.0014)	0
	$\theta < 7.5°$	3.52	2.66	2.09	1.57	0.913	0.306	0.0830	(0.016)	(0.0014)	0
	$\theta < 5°$	2.19	1.74	1.44	1.15	0.733	0.279	0.0810	(0.016)	(0.0014)	0
$\tau^+\tau^-$	no cut	22.2	16.8	13.7	11.0	7.73	4.03	1.83	0.698	(0.19)	0
	$\theta < 10°$	19.0	15.4	13.1	10.7	7.68	4.03	1.83	0.698	(0.19)	0
	$\theta < 7.5°$	16.6	13.8	11.9	9.98	7.32	3.97	1.83	0.698	(0.19)	0
	$\theta < 5°$	12.3	10.5	9.23	7.96	6.13	3.59	1.76	0.692	(0.19)	0

Table 9: *Muon fluxes at Earth for different annihilation channels and for annihilation in the Sun. A neutralino mass of $m_{\tilde{\chi}}$ = 50 GeV is used. Values in paranthesis are calculated from less than 100 events and have thus large errors. In each channel* 10^5 *events are simulated except in † where* 10^6 *events are simulated.*

Channel	θ cut	Φ_μ [$\times 10^{-35}$ m^{-2}(parent pair)$^{-1}$] E_μ^{det} [GeV] $>$									
		0	3	5	7	10	15	20	25	30	50
$c\bar{c}$	no cut	5.44	3.77	2.99	2.32	1.60	0.827	0.471	(0.25)	(0.15)	(0)
	$\theta < 10°$	4.30	3.37	2.81	2.25	1.58	0.822	0.471	(0.25)	(0.15)	(0)
	$\theta < 7.5°$	3.63	2.97	2.55	2.10	1.53	0.821	0.471	(0.25)	(0.15)	(0)
	$\theta < 5°$	2.58	2.19	1.96	1.68	1.30	0.753	0.450	(0.25)	(0.15)	(0)
$b\bar{b}$ †	no cut	18.0	13.5	11.0	9.05	6.72	3.99	2.24	1.23	0.648	(0.024)
	$\theta < 10°$	15.2	12.4	10.5	8.84	6.66	3.98	2.24	1.23	0.648	(0.024)
	$\theta < 7.5°$	13.4	11.2	9.70	8.31	6.42	3.94	2.24	1.22	0.648	(0.024)
	$\theta < 5°$	9.98	8.59	7.68	6.79	5.49	3.57	2.11	1.19	0.645	(0.024)
$\tau^+\tau^-$	no cut	75.8	65.6	59.3	53.5	45.9	35.1	26.2	19.2	13.7	2.78
	$\theta < 10°$	71.7	63.5	58.1	52.7	45.6	35.0	26.2	19.2	13.7	2.78
	$\theta < 7.5°$	67.7	60.5	55.8	51.0	44.6	34.6	26.1	19.2	13.7	2.78
	$\theta < 5°$	58.3	52.8	49.2	45.5	40.5	32.2	24.8	18.7	13.4	2.78
W^+W^-	no cut	94.1	83.4	76.6	70.8	62.3	48.9	37.8	28.5	21.3	3.91
	$\theta < 10°$	90.5	81.4	75.4	70.0	61.9	48.8	37.8	28.5	21.3	3.91
	$\theta < 7.5°$	86.3	78.1	72.7	67.9	60.6	48.2	37.6	28.4	21.3	3.91
	$\theta < 5°$	75.6	69.0	64.7	60.9	55.1	45.0	35.8	27.6	20.9	3.91
Z^0Z^0	no cut	111	97.1	89.0	81.1	70.3	54.2	40.2	29.2	20.3	2.44
	$\theta < 10°$	106	94.4	87.5	80.2	69.8	54.2	40.2	29.2	20.3	2.44
	$\theta < 7.5°$	100	90.5	84.3	77.7	68.2	53.5	40.0	29.2	20.2	2.44
	$\theta < 5°$	87.2	79.4	74.6	69.4	61.7	49.6	38.2	28.4	20.0	2.44
$Z^0H_2^0$	no cut	71.3	62.1	56.7	51.8	44.7	35.3	27.4	21.0	15.8	3.39
	$\theta < 10°$	67.2	60.2	55.6	51.2	44.5	35.3	27.4	21.0	15.8	3.39
	$\theta < 7.5°$	63.9	57.8	53.8	49.9	43.7	35.0	27.3	21.0	15.8	3.39
	$\theta < 5°$	55.5	50.9	47.8	44.8	40.1	32.8	26.1	20.4	15.6	3.39

Table 10: *Muon fluxes at Earth for different annihilation channels and for annihilation in the Sun. A neutralino mass of $m_{\tilde{\chi}}$ = 100 GeV is used. Values in paranthesis are calculated from less than 100 events and have thus large errors. In each channel* 10^5 *events are simulated except in* † *where* 10^6 *events are simulated.*

Channel	θ cut	Φ_μ [$\times 10^{-35}$ m^{-2}(parent pair)$^{-1}$] E_μ^{det} [GeV] $>$									
		0	3	5	7	10	15	20	25	30	50
$c\bar{c}$	no cut	9.40	7.21	6.01	4.98	3.91	2.48	1.57	1.03	(0.70)	(0.083)
	$\theta < 10°$	8.15	6.76	5.83	4.91	3.89	2.48	1.57	1.03	(0.70)	(0.083)
	$\theta < 7.5°$	7.25	6.17	5.44	4.66	3.76	2.45	1.57	1.03	(0.70)	(0.083)
	$\theta < 5°$	5.52	4.84	4.37	3.86	3.25	2.28	1.48	0.997	(0.69)	(0.083)
$b\bar{b}$	no cut	30.0	24.3	20.9	18.0	14.5	10.1	7.04	4.76	3.11	(0.62)
	$\theta < 10°$	26.8	23.0	20.3	17.7	14.4	10.1	7.04	4.76	3.11	(0.62)
	$\theta < 7.5°$	24.4	21.4	19.1	17.0	14.0	9.99	7.04	4.76	3.11	(0.62)
	$\theta < 5°$	19.4	17.4	15.9	14.4	12.2	9.12	6.63	4.58	3.06	(0.61)
$t\bar{t}$	no cut	109	94.5	85.9	78.0	67.5	52.4	39.4	29.2	20.7	3.35
	$\theta < 10°$	102	91.5	84.3	77.0	67.1	52.3	39.4	29.2	20.7	3.35
	$\theta < 7.5°$	96.8	87.4	81.1	74.6	65.5	51.7	39.2	29.2	20.7	3.35
	$\theta < 5°$	82.8	75.7	71.0	66.0	59.0	47.9	37.2	28.2	20.3	3.35
$\tau^+\tau^-$	no cut	146	132	123	114	103	85.9	70.9	58.1	47.1	18.0
	$\theta < 10°$	142	130	121	113	102	85.9	70.9	58.1	47.1	18.0
	$\theta < 7.5°$	136	126	118	111	101	85.2	70.6	58.0	47.1	18.0
	$\theta < 5°$	123	114	108	102	93.8	80.5	67.7	56.4	46.2	18.0
W^+W^-	no cut	188	173	164	156	144	125	109	94.2	81.1	42.5
	$\theta < 10°$	184	171	163	155	143	125	109	94.2	81.1	42.5
	$\theta < 7.5°$	180	168	160	153	142	124	109	94.1	81.1	42.5
	$\theta < 5°$	166	157	150	144	135	119	105	91.9	79.9	42.5
Z^0Z^0	no cut	227	210	199	189	175	152	133	115	98.1	48.0
	$\theta < 10°$	223	207	198	188	174	152	133	115	98.1	48.0
	$\theta < 7.5°$	217	203	194	185	172	151	132	115	98.0	48.0
	$\theta < 5°$	201	189	182	174	164	145	128	113	97.0	47.9
$Z^0H_1^0$	no cut	73.4	62.3	55.8	50.2	42.1	31.2	22.9	16.0	10.6	(1.0)
	$\theta < 10°$	68.3	59.9	54.5	49.4	41.8	31.2	22.9	16.0	10.6	(1.0)
	$\theta < 7.5°$	63.7	56.6	51.9	47.5	40.7	30.8	22.8	16.0	10.6	(1.0)
	$\theta < 5°$	53.4	48.2	44.7	41.5	36.2	28.4	21.5	15.5	10.4	(1.0)
$Z^0H_2^0$	no cut	137	125	117	110	101	86.1	73.9	63.6	54.3	28.7
	$\theta < 10°$	132	122	115	109	100	86.1	73.9	63.6	54.3	28.7
	$\theta < 7.5°$	128	119	113	107	99.2	85.6	73.8	63.5	54.3	28.7
	$\theta < 5°$	116	110	104	99.8	93.4	81.9	71.6	62.2	53.4	28.7
W^+H^-	no cut	105	91.3	83.1	75.7	65.9	51.7	40.1	30.4	22.6	5.07
	$\theta < 10°$	99.5	88.6	81.6	74.9	65.5	51.6	40.1	30.4	22.6	5.07
	$\theta < 7.5°$	94.5	85.0	78.8	72.8	64.1	51.1	39.9	30.4	22.6	5.07
	$\theta < 5°$	81.8	74.5	70.0	65.3	58.5	47.9	38.3	29.7	22.4	5.07
W^-H^+	no cut	109	94.8	86.5	79.2	69.2	54.7	42.4	32.0	23.6	5.22
	$\theta < 10°$	103	92.3	85.1	78.5	68.9	54.7	42.4	32.0	23.6	5.22
	$\theta < 7.5°$	97.7	88.2	81.9	76.0	67.3	54.0	42.1	31.9	23.6	5.22
	$\theta < 5°$	84.4	77.0	72.3	67.8	61.2	50.1	39.9	30.9	23.1	5.19

Table 11: *Muon fluxes at Earth for different annihilation channels and for annihilation in the Sun. A neutralino mass of $m_{\tilde{\chi}}$ = 150 GeV is used. Values in paranthesis are calculated from less than 100 events and have thus large errors. In each channel* 10^5 *events are simulated.*

Channel	θ cut	Φ_μ [$\times 10^{-35}$ m^{-2}(parent pair)$^{-1}$] E_μ^{det} [GeV] $>$									
		0	3	5	7	10	15	20	25	30	50
$c\bar{c}$	no cut	13.3	10.6	9.05	7.68	6.10	4.19	2.89	1.99	1.27	(0.29)
	$\theta < 10°$	11.9	10.0	8.80	7.58	6.08	4.19	2.89	1.99	1.27	(0.29)
	$\theta < 7.5°$	10.9	9.32	8.29	7.27	5.92	4.15	2.89	1.99	1.27	(0.29)
	$\theta < 5°$	8.75	7.69	6.93	6.25	5.26	3.87	2.77	1.94	1.26	(0.29)
$b\bar{b}$	no cut	42.8	35.8	31.8	28.4	23.9	17.6	12.9	9.28	6.83	(1.8)
	$\theta < 10°$	39.2	34.2	30.9	28.0	23.7	17.6	12.9	9.28	6.83	(1.8)
	$\theta < 7.5°$	36.3	32.2	29.5	26.9	23.2	17.4	12.8	9.28	6.83	(1.8)
	$\theta < 5°$	30.5	27.6	25.7	23.8	21.0	16.3	12.3	8.98	6.73	(1.8)
$t\bar{t}$	no cut	181	164	153	143	130	110	93.3	79.0	67.1	32.1
	$\theta < 10°$	175	161	151	142	130	110	93.2	79.0	67.1	32.1
	$\theta < 7.5°$	169	156	148	140	128	109	93.1	79.0	67.1	32.1
	$\theta < 5°$	153	143	136	130	120	104	89.9	77.2	66.0	32.0
$\tau^+\tau^-$	no cut	227	209	199	188	174	152	131	113	97.0	48.5
	$\theta < 10°$	222	207	197	187	173	151	131	113	97.0	48.5
	$\theta < 7.5°$	217	203	194	184	171	151	131	112	96.9	48.5
	$\theta < 5°$	201	189	182	174	162	144	127	110	95.3	48.3
W^+W^-	no cut	291	274	262	252	237	215	195	177	160	104
	$\theta < 10°$	287	272	261	251	237	215	195	177	160	104
	$\theta < 7.5°$	282	268	258	249	235	214	195	177	160	104
	$\theta < 5°$	268	255	246	238	227	208	191	174	158	104
Z^0Z^0	no cut	334	314	302	291	272	246	223	201	179	114
	$\theta < 10°$	330	312	300	290	271	246	223	201	179	114
	$\theta < 7.5°$	324	308	297	287	269	245	223	200	179	114
	$\theta < 5°$	307	292	283	275	259	237	218	197	177	114
$H_1^0H_3^0$	no cut	43.9	34.5	29.5	25.3	20.1	14.1	9.85	6.99	4.81	(1.1)
	$\theta < 10°$	38.4	32.4	28.5	24.9	20.0	14.1	9.85	6.99	4.81	(1.1)
	$\theta < 7.5°$	34.7	29.9	26.7	23.8	19.5	13.9	9.83	6.99	4.81	(1.1)
	$\theta < 5°$	27.7	24.5	22.4	20.3	17.2	12.9	9.33	6.73	4.68	(1.1)
$Z^0H_1^0$	no cut	153	138	129	122	110	95.6	82.5	71.7	62.1	32.0
	$\theta < 10°$	147	135	128	121	110	95.5	82.5	71.7	62.1	32.0
	$\theta < 7.5°$	142	131	125	118	109	94.8	82.1	71.6	62.1	32.0
	$\theta < 5°$	130	121	116	111	103	90.8	79.8	70.0	61.2	31.9
$Z^0H_2^0$	no cut	197	182	173	166	154	136	122	108	96.5	57.3
	$\theta < 10°$	192	180	172	165	154	136	122	108	96.5	57.3
	$\theta < 7.5°$	187	176	169	163	152	135	122	108	96.4	57.3
	$\theta < 5°$	175	166	160	155	146	131	119	106	95.3	57.2
W^+H^-	no cut	189	173	162	152	139	120	102	88.0	73.7	35.8
	$\theta < 10°$	183	170	161	151	139	120	102	88.0	73.7	35.8
	$\theta < 7.5°$	177	165	157	148	137	119	102	87.8	73.7	35.8
	$\theta < 5°$	162	152	145	138	129	114	98.5	85.9	72.6	35.8
W^-H^+	no cut	185	169	159	150	136	117	101	86.3	73.5	37.5
	$\theta < 10°$	180	166	157	149	136	117	101	86.3	73.5	37.5
	$\theta < 7.5°$	174	162	154	146	134	117	101	86.1	73.5	37.5
	$\theta < 5°$	160	150	143	137	127	112	97.7	84.5	72.6	37.5

Table 12: *Muon fluxes at Earth for different annihilation channels and for annihilation in the Sun. A neutralino mass of* $m_{\tilde{\chi}} = 200$ *GeV is used. Values in paranthesis are calculated from less than 100 events and have thus large errors. In each channel* 10^5 *events are simulated.*

Channel	θ cut	Φ_μ [$\times 10^{-35}$ m^{-2}(parent pair)$^{-1}$] E_μ^{det} [GeV] $>$									
		0	3	5	7	10	15	20	25	30	50
$c\bar{c}$	no cut	17.8	14.8	13.0	11.6	9.87	7.35	5.71	4.14	3.02	(0.80)
	$\theta < 10°$	16.1	14.1	12.7	11.4	9.83	7.35	5.71	4.14	3.02	(0.80)
	$\theta < 7.5°$	14.9	13.2	12.1	11.0	9.62	7.27	5.68	4.14	3.02	(0.80)
	$\theta < 5°$	12.6	11.4	10.6	9.87	8.88	6.93	5.55	4.09	3.00	(0.80)
$b\bar{b}$	no cut	56.4	47.9	43.3	39.3	34.0	26.6	20.5	16.1	12.6	4.15
	$\theta < 10°$	52.6	46.2	42.4	38.8	33.8	26.6	20.5	16.1	12.6	4.15
	$\theta < 7.5°$	49.5	44.0	40.8	37.6	33.1	26.3	20.4	16.1	12.6	4.15
	$\theta < 5°$	42.6	38.5	36.1	33.8	30.4	24.9	19.7	15.7	12.4	4.15
$t\bar{t}$	no cut	254	235	222	211	195	172	152	134	118	69.7
	$\theta < 10°$	248	231	221	210	195	172	152	134	118	69.7
	$\theta < 7.5°$	241	226	217	207	193	171	152	134	118	69.7
	$\theta < 5°$	223	211	203	195	184	165	148	132	117	69.6
$\tau^+\tau^-$	no cut	311	291	278	266	248	222	197	177	157	94.9
	$\theta < 10°$	307	288	277	265	247	222	197	177	157	94.9
	$\theta < 7.5°$	301	283	273	261	245	221	197	176	157	94.9
	$\theta < 5°$	283	268	259	249	235	213	192	173	155	94.7
W^+W^-	no cut	375	357	345	333	318	294	271	249	230	160
	$\theta < 10°$	372	355	344	333	317	294	271	249	230	160
	$\theta < 7.5°$	368	351	341	330	316	293	270	249	230	160
	$\theta < 5°$	352	338	329	319	306	286	265	245	227	159
Z^0Z^0	no cut	439	417	403	390	371	342	314	287	262	181
	$\theta < 10°$	434	414	402	389	371	342	314	287	262	181
	$\theta < 7.5°$	428	410	398	386	369	341	314	287	262	181
	$\theta < 5°$	410	394	384	373	357	332	308	283	259	180
$H_1^0H_3^0$	no cut	63.9	53.1	47.1	41.6	34.8	25.9	19.8	14.7	11.1	3.66
	$\theta < 10°$	58.1	50.7	45.9	41.0	34.7	25.9	19.8	14.7	11.1	3.66
	$\theta < 7.5°$	54.0	47.9	43.8	39.7	33.9	25.7	19.8	14.7	11.1	3.66
	$\theta < 5°$	45.2	41.0	38.1	35.1	30.8	24.2	19.1	14.4	11.0	3.66
$Z^0H_1^0$	no cut	221	205	195	185	173	154	137	123	109	69.7
	$\theta < 10°$	216	203	194	185	173	154	137	123	109	69.7
	$\theta < 7.5°$	211	199	191	183	171	153	137	123	109	69.7
	$\theta < 5°$	197	188	181	173	164	148	133	121	108	69.6
$Z^0H_2^0$	no cut	255	238	226	217	203	184	166	152	138	94.2
	$\theta < 10°$	250	235	225	216	203	184	166	152	138	94.2
	$\theta < 7.5°$	245	232	222	214	202	183	166	152	138	94.2
	$\theta < 5°$	233	221	213	206	195	179	163	150	137	94.1
W^+H^-	no cut	267	248	237	227	213	192	170	151	134	83.0
	$\theta < 10°$	261	245	235	226	213	192	170	151	134	83.0
	$\theta < 7.5°$	255	241	232	223	211	191	170	151	134	83.0
	$\theta < 5°$	238	227	219	212	202	185	165	148	132	82.9
W^-H^+	no cut	269	251	239	229	215	191	171	153	137	85.6
	$\theta < 10°$	263	248	238	228	214	191	171	153	137	85.6
	$\theta < 7.5°$	257	243	234	226	212	190	171	153	137	85.6
	$\theta < 5°$	242	231	224	216	205	186	168	151	136	85.5

Table 13: *Muon fluxes at Earth for different annihilation channels and for annihilation in the Sun. A neutralino mass of $m_{\tilde{\chi}}$ = 250 GeV is used. Values in paranthesis are calculated from less than 100 events and have thus large errors. In each channel 10^5 events are simulated.*

Channel	θ cut	Φ_μ [$\times 10^{-35}$ m^{-2}(parent pair)$^{-1}$] E_μ^{det} [GeV] $>$									
		0	3	5	7	10	15	20	25	30	50
$c\bar{c}$	no cut	25.2	21.8	19.8	18.0	15.5	12.3	10.0	8.21	6.56	(2.5)
	$\theta < 10°$	23.4	21.0	19.4	17.8	15.4	12.3	10.0	8.21	6.56	(2.5)
	$\theta < 7.5°$	22.1	20.1	18.8	17.3	15.2	12.2	10.0	8.20	6.56	(2.5)
	$\theta < 5°$	19.1	17.7	16.8	15.7	14.0	11.6	9.69	8.05	6.48	(2.5)
$b\bar{b}$	no cut	82.8	73.1	67.6	62.5	55.6	46.2	38.9	32.3	27.1	13.5
	$\theta < 10°$	78.8	71.4	66.7	62.0	55.4	46.1	38.9	32.3	27.1	13.5
	$\theta < 7.5°$	75.2	68.7	64.6	60.5	54.5	45.8	38.8	32.2	27.1	13.5
	$\theta < 5°$	66.8	61.8	58.7	55.4	50.8	43.7	37.6	31.6	26.8	13.5
$t\bar{t}$	no cut	383	361	348	334	316	288	263	240	217	145
	$\theta < 10°$	377	358	346	333	316	288	263	240	217	145
	$\theta < 7.5°$	370	353	342	330	314	286	263	240	217	145
	$\theta < 5°$	350	336	327	317	303	279	258	237	215	145
$\tau^+\tau^-$	no cut	483	460	445	431	412	381	350	321	295	203
	$\theta < 10°$	479	457	443	430	411	380	350	321	295	203
	$\theta < 7.5°$	473	453	440	427	409	379	350	321	294	203
	$\theta < 5°$	453	435	424	412	397	370	343	317	291	202
W^+W^-	no cut	514	494	481	469	454	425	401	378	352	270
	$\theta < 10°$	511	492	480	469	454	424	401	378	352	270
	$\theta < 7.5°$	507	489	478	467	453	424	401	378	352	270
	$\theta < 5°$	493	477	467	457	444	417	396	374	349	270
Z^0Z^0	no cut	600	576	562	548	526	495	464	436	410	318
	$\theta < 10°$	596	573	560	547	526	495	464	436	410	318
	$\theta < 7.5°$	590	569	556	544	524	493	463	436	410	318
	$\theta < 5°$	571	553	541	531	512	484	456	432	407	317
$H_1^0H_3^0$	no cut	102	88.4	80.6	73.4	64.3	51.5	41.9	34.6	28.5	14.1
	$\theta < 10°$	95.6	85.7	79.3	72.7	64.1	51.5	41.9	34.6	28.5	14.1
	$\theta < 7.5°$	90.4	82.1	76.5	70.8	63.0	51.1	41.8	34.6	28.5	14.1
	$\theta < 5°$	78.4	72.3	68.2	64.0	58.0	48.1	40.1	33.5	27.9	14.0
$Z^0H_1^0$	no cut	349	331	320	310	296	273	254	235	219	162
	$\theta < 10°$	344	329	318	310	295	273	254	235	219	162
	$\theta < 7.5°$	339	325	315	307	294	272	254	235	219	162
	$\theta < 5°$	324	312	304	297	286	267	250	232	217	161
$Z^0H_2^0$	no cut	363	344	334	323	306	282	261	244	227	168
	$\theta < 10°$	358	342	332	322	305	282	261	244	227	168
	$\theta < 7.5°$	353	338	329	319	303	281	261	243	227	168
	$\theta < 5°$	339	326	319	310	296	276	257	241	226	168
W^+H^-	no cut	390	369	357	344	326	300	274	251	230	166
	$\theta < 10°$	384	366	355	342	326	300	274	251	230	166
	$\theta < 7.5°$	377	361	351	339	323	299	273	250	230	166
	$\theta < 5°$	359	345	336	326	313	291	268	247	228	165
W^-H^+	no cut	413	391	378	365	347	319	296	272	251	181
	$\theta < 10°$	407	388	376	364	347	319	296	272	251	181
	$\theta < 7.5°$	400	383	372	361	345	318	295	272	251	181
	$\theta < 5°$	383	369	360	350	336	312	291	269	250	180

Table 14: *Muon fluxes at Earth for different annihilation channels and for annihilation in the Sun. A neutralino mass of $m_{\tilde{\chi}}$ = 350 GeV is used. Values in paranthesis are calculated from less than 100 events and have thus large errors. In each channel* 10^5 *events are simulated.*

Channel	θ cut	Φ_μ [$\times 10^{-35}$ m^{-2}(parent pair)$^{-1}$] E_μ^{det} [GeV] >									
		0	3	5	7	10	15	20	25	30	50
$c\bar{c}$	no cut	36.9	33.0	30.5	28.2	25.6	21.2	17.3	14.2	12.2	5.80
	$\theta < 10°$	35.0	32.1	30.1	28.0	25.4	21.2	17.3	14.2	12.2	5.80
	$\theta < 7.5°$	33.1	30.7	29.0	27.2	24.9	20.9	17.1	14.2	12.2	5.80
	$\theta < 5°$	29.5	27.7	26.3	25.0	23.2	19.9	16.5	13.9	12.0	5.78
$b\bar{b}$	no cut	115	103	96.5	90.3	81.8	70.0	59.5	50.8	44.0	24.6
	$\theta < 10°$	110	101	95.3	89.7	81.6	69.9	59.5	50.8	44.0	24.6
	$\theta < 7.5°$	106	97.9	92.9	87.8	80.5	69.4	59.3	50.7	44.0	24.6
	$\theta < 5°$	96.2	89.6	85.6	81.6	75.7	66.4	57.6	49.7	43.4	24.6
$t\bar{t}$	no cut	524	499	482	467	445	411	380	353	328	246
	$\theta < 10°$	517	496	480	466	444	411	380	353	328	246
	$\theta < 7.5°$	510	490	476	463	442	410	379	353	328	246
	$\theta < 5°$	491	474	462	450	431	402	374	350	326	246
$\tau^+\tau^-$	no cut	668	643	626	606	580	546	512	478	447	340
	$\theta < 10°$	664	640	624	604	579	546	511	478	447	340
	$\theta < 7.5°$	659	636	621	602	577	544	511	478	447	340
	$\theta < 5°$	640	620	605	588	565	536	504	473	443	340
W^+W^-	no cut	637	619	607	594	574	546	518	493	472	386
	$\theta < 10°$	634	617	606	594	574	546	518	493	472	386
	$\theta < 7.5°$	630	614	603	592	572	545	517	493	472	386
	$\theta < 5°$	617	602	592	581	563	538	512	489	469	385
Z^0Z^0	no cut	752	732	718	704	683	651	623	595	568	468
	$\theta < 10°$	748	730	716	703	683	651	623	595	568	468
	$\theta < 7.5°$	743	726	713	701	681	650	622	595	568	468
	$\theta < 5°$	727	711	699	688	671	643	617	591	565	467
$H_1^0H_3^0$	no cut	162	145	135	126	113	96.8	83.0	71.7	61.2	36.9
	$\theta < 10°$	155	142	133	125	113	96.8	83.0	71.7	61.2	36.9
	$\theta < 7.5°$	149	138	130	122	111	96.1	82.8	71.6	61.2	36.9
	$\theta < 5°$	136	126	120	114	105	92.3	80.5	70.4	60.6	36.9
$Z^0H_1^0$	no cut	473	454	441	427	411	383	360	339	320	259
	$\theta < 10°$	467	451	439	426	410	383	360	339	320	259
	$\theta < 7.5°$	461	447	435	424	408	382	360	339	319	259
	$\theta < 5°$	446	434	424	414	400	377	357	337	318	259
$Z^0H_2^0$	no cut	476	454	442	429	412	388	365	341	321	255
	$\theta < 10°$	471	451	440	428	412	388	365	341	321	255
	$\theta < 7.5°$	465	447	437	426	410	388	364	341	321	255
	$\theta < 5°$	449	433	424	415	401	382	360	338	320	255
W^+H^-	no cut	526	501	486	473	454	420	395	369	342	265
	$\theta < 10°$	520	498	485	472	454	420	395	369	342	265
	$\theta < 7.5°$	513	493	481	469	451	419	394	368	342	265
	$\theta < 5°$	495	477	466	457	441	411	389	365	339	265
W^-H^+	no cut	575	551	535	520	501	468	438	413	388	309
	$\theta < 10°$	568	548	533	518	501	468	438	413	388	309
	$\theta < 7.5°$	562	543	529	516	499	467	438	413	388	309
	$\theta < 5°$	544	527	515	503	489	459	433	409	385	308

Table 15: *Muon fluxes at Earth for different annihilation channels and for annihilation in the Sun. A neutralino mass of $m_{\tilde{\chi}}$ = 500 GeV is used. In each channel* 10^5 *events are simulated.*

A.2 Muon fluxes from neutralino annihilations in the Earth

Channel	θ cut	Φ_μ [$\times 10^{-25}$ m^{-2}(parent pair)$^{-1}$] E_μ^{det} [GeV] >									
		0	3	5	7	10	15	20	25	30	50
$c\bar{c}$	no cut	0.139	0.0748	0.0478	0.0302	0.0153	(0.0040)	(0.00065)	(0)	(0)	0
	$\theta < 10°$	0.0821	0.0550	0.0387	0.0262	0.0143	(0.0039)	(0.00065)	(0)	(0)	0
	$\theta < 7.5°$	0.0570	0.0400	0.0289	0.0201	0.0118	(0.0031)	(0.00065)	(0)	(0)	0
	$\theta < 5°$	0.0308	0.0231	0.0172	0.0123	0.00736	(0.0021)	(0.00043)	(0)	(0)	0
$b\bar{b}$ †	no cut	0.458	0.282	0.200	0.140	0.0785	0.0262	0.00749	(0.0014)	(0.000099)	0
	$\theta < 10°$	0.300	0.217	0.167	0.123	0.0724	0.0253	0.00725	(0.0013)	(0.000099)	0
	$\theta < 7.5°$	0.218	0.163	0.130	0.0980	0.0599	0.0218	0.00639	(0.0012)	(0.000099)	0
	$\theta < 5°$	0.118	0.0912	0.0740	0.0574	0.0364	0.0138	0.00414	(0.00088)	(0.000055)	0
$\tau^+\tau^-$	no cut	1.41	1.07	0.872	0.706	0.507	0.276	0.137	0.0529	(0.016)	0
	$\theta < 10°$	1.11	0.901	0.764	0.638	0.472	0.266	0.134	0.0522	(0.016)	0
	$\theta < 7.5°$	0.882	0.727	0.626	0.531	0.404	0.232	0.119	0.0475	(0.016)	0
	$\theta < 5°$	0.524	0.437	0.380	0.325	0.254	0.150	0.0789	0.0305	(0.011)	0

Table 16: *Muon fluxes at the Earth's surface for different annihilation channels and for annihilation in the Earth. A neutralino mass of $m_{\tilde{\chi}} = 50$ GeV is used. Values in paranthesis are calculated from less than 100 events and have thus large errors. In each channel* 10^5 *events are simulated except in † where* 10^6 *events are simulated.*

Channel	θ cut	Φ_μ [$\times 10^{-25}$ m^{-2}(parent pair)$^{-1}$] E_μ^{det} [GeV] > 0	3	5	7	10	15	20	25	30	50
$c\bar{c}$	no cut	0.484	0.352	0.283	0.226	0.156	0.0893	0.0462	(0.024)	(0.011)	(0)
	$\theta < 10°$	0.387	0.309	0.260	0.213	0.152	0.0887	0.0459	(0.024)	(0.011)	(0)
	$\theta < 7.5°$	0.319	0.262	0.226	0.191	0.139	0.0835	0.0442	(0.024)	(0.011)	(0)
	$\theta < 5°$	0.194	0.161	0.144	0.126	0.0955	0.0598	0.0349	(0.020)	(0.010)	(0)
$b\bar{b}$ †	no cut	1.58	1.23	1.03	0.866	0.660	0.416	0.250	0.148	0.0806	(0.0042)
	$\theta < 10°$	1.33	1.11	0.964	0.827	0.644	0.412	0.249	0.147	0.0806	(0.0042)
	$\theta < 7.5°$	1.13	0.962	0.850	0.741	0.588	0.387	0.238	0.143	0.0784	(0.0042)
	$\theta < 5°$	0.759	0.658	0.590	0.524	0.428	0.294	0.190	0.116	0.0648	(0.0034)
$\tau^+\tau^-$	no cut	5.38	4.68	4.26	3.85	3.29	2.49	1.88	1.37	0.959	0.172
	$\theta < 10°$	5.00	4.45	4.09	3.73	3.21	2.46	1.86	1.36	0.956	0.172
	$\theta < 7.5°$	4.53	4.06	3.76	3.45	3.01	2.34	1.79	1.32	0.939	0.170
	$\theta < 5°$	3.32	3.02	2.82	2.59	2.29	1.83	1.43	1.07	0.773	0.146
W^+W^-	no cut	7.04	6.22	5.73	5.27	4.66	3.76	2.92	2.22	1.64	0.371
	$\theta < 10°$	6.67	5.99	5.56	5.15	4.58	3.73	2.90	2.22	1.64	0.371
	$\theta < 7.5°$	6.09	5.50	5.14	4.79	4.29	3.54	2.79	2.15	1.60	0.368
	$\theta < 5°$	4.57	4.16	3.90	3.67	3.33	2.80	2.26	1.76	1.31	0.318
Z^0Z^0	no cut	8.15	7.20	6.61	6.05	5.26	4.12	3.12	2.29	1.60	0.198
	$\theta < 10°$	7.67	6.90	6.39	5.89	5.17	4.07	3.10	2.28	1.60	0.198
	$\theta < 7.5°$	6.99	6.35	5.91	5.48	4.85	3.87	2.98	2.21	1.56	0.197
	$\theta < 5°$	5.19	4.75	4.45	4.16	3.72	3.02	2.39	1.81	1.30	0.180
$Z^0H_2^0$	no cut	5.39	4.73	4.34	3.97	3.49	2.82	2.20	1.69	1.27	0.301
	$\theta < 10°$	5.01	4.53	4.20	3.87	3.43	2.80	2.19	1.69	1.27	0.301
	$\theta < 7.5°$	4.60	4.19	3.92	3.63	3.25	2.68	2.12	1.64	1.24	0.299
	$\theta < 5°$	3.44	3.17	2.99	2.80	2.53	2.12	1.71	1.35	1.04	0.249

Table 17: *Muon fluxes at the Earth's surface for different annihilation channels and for annihilation in the Earth. A neutralino mass of $m_{\tilde{\chi}}$ = 100 GeV is used. Values in paranthesis are calculated from less than 100 events and have thus large errors. In each channel* 10^5 *events are simulated except in † where* 10^6 *events are simulated.*

Channel	θ cut	Φ_μ [$\times 10^{-25}$ m^{-2}(parent pair)$^{-1}$] E_μ^{det} [GeV] >									
		0	3	5	7	10	15	20	25	30	50
$c\bar{c}$	no cut	0.965	0.771	0.659	0.559	0.437	0.286	0.188	0.117	0.0712	(0.0026)
	$\theta < 10°$	0.845	0.714	0.627	0.541	0.430	0.284	0.188	0.117	0.0712	(0.0026)
	$\theta < 7.5°$	0.746	0.642	0.573	0.502	0.405	0.275	0.182	0.116	0.0712	(0.0026)
	$\theta < 5°$	0.535	0.466	0.423	0.377	0.317	0.223	0.151	0.101	0.0613	(0.0026)
$b\bar{b}$	no cut	3.00	2.50	2.20	1.95	1.61	1.18	0.840	0.596	0.433	(0.095)
	$\theta < 10°$	2.71	2.35	2.12	1.90	1.59	1.18	0.839	0.596	0.433	(0.095)
	$\theta < 7.5°$	2.44	2.15	1.96	1.77	1.51	1.14	0.828	0.594	0.432	(0.095)
	$\theta < 5°$	1.82	1.63	1.50	1.38	1.20	0.940	0.700	0.508	0.376	(0.087)
$t\bar{t}$	no cut	8.11	7.07	6.43	5.88	5.09	4.03	3.12	2.32	1.70	0.283
	$\theta < 10°$	7.60	6.79	6.26	5.76	5.02	4.00	3.11	2.32	1.70	0.283
	$\theta < 7.5°$	7.02	6.34	5.88	5.45	4.79	3.87	3.04	2.28	1.68	0.283
	$\theta < 5°$	5.50	5.03	4.70	4.40	3.93	3.26	2.62	1.99	1.50	0.262
$\tau^+\tau^-$	no cut	11.9	10.8	10.2	9.57	8.64	7.23	6.03	4.99	4.09	1.71
	$\theta < 10°$	11.5	10.6	10.0	9.44	8.57	7.21	6.02	4.98	4.09	1.71
	$\theta < 7.5°$	10.9	10.1	9.59	9.09	8.29	7.03	5.91	4.91	4.04	1.70
	$\theta < 5°$	9.05	8.44	8.05	7.67	7.08	6.11	5.22	4.40	3.67	1.60
W^+W^-	no cut	17.1	15.9	15.2	14.5	13.4	11.8	10.3	8.90	7.75	4.08
	$\theta < 10°$	16.7	15.7	15.0	14.3	13.3	11.8	10.3	8.89	7.74	4.08
	$\theta < 7.5°$	16.1	15.1	14.6	13.9	13.0	11.5	10.1	8.80	7.69	4.06
	$\theta < 5°$	13.6	12.9	12.4	11.9	11.2	10.0	8.93	7.86	6.95	3.78
Z^0Z^0	no cut	20.6	19.1	18.2	17.3	16.1	14.2	12.4	10.8	9.28	4.77
	$\theta < 10°$	20.1	18.8	17.9	17.2	16.0	14.1	12.4	10.8	9.28	4.77
	$\theta < 7.5°$	19.3	18.1	17.3	16.7	15.6	13.8	12.2	10.7	9.19	4.75
	$\theta < 5°$	16.3	15.4	14.8	14.3	13.5	12.0	10.7	9.45	8.20	4.35
$Z^0H_1^0$	no cut	5.58	4.77	4.26	3.83	3.23	2.42	1.76	1.23	0.812	(0.078)
	$\theta < 10°$	5.16	4.54	4.12	3.74	3.18	2.40	1.76	1.22	0.812	(0.078)
	$\theta < 7.5°$	4.70	4.18	3.81	3.50	3.01	2.31	1.71	1.20	0.798	(0.078)
	$\theta < 5°$	3.58	3.23	2.98	2.76	2.42	1.91	1.45	1.04	0.706	(0.072)
$Z^0H_2^0$	no cut	12.5	11.5	10.8	10.2	9.32	8.11	7.07	6.14	5.33	2.73
	$\theta < 10°$	12.1	11.2	10.6	10.1	9.25	8.07	7.06	6.14	5.32	2.73
	$\theta < 7.5°$	11.6	10.8	10.3	9.77	9.02	7.92	6.96	6.08	5.28	2.72
	$\theta < 5°$	9.70	9.16	8.78	8.39	7.81	6.96	6.19	5.45	4.79	2.52
W^+H^-	no cut	7.81	6.85	6.29	5.74	5.00	3.95	3.07	2.33	1.74	0.406
	$\theta < 10°$	7.32	6.59	6.13	5.63	4.94	3.94	3.06	2.33	1.74	0.406
	$\theta < 7.5°$	6.79	6.17	5.77	5.34	4.73	3.81	3.00	2.29	1.73	0.405
	$\theta < 5°$	5.39	4.95	4.68	4.36	3.92	3.23	2.61	2.04	1.57	0.378
W^-H^+	no cut	8.32	7.32	6.68	6.15	5.38	4.26	3.32	2.53	1.93	0.407
	$\theta < 10°$	7.83	7.05	6.50	6.03	5.32	4.24	3.31	2.53	1.92	0.407
	$\theta < 7.5°$	7.27	6.62	6.15	5.74	5.10	4.11	3.25	2.49	1.91	0.407
	$\theta < 5°$	5.68	5.22	4.88	4.60	4.15	3.42	2.77	2.17	1.69	0.380

Table 18: *Muon fluxes at the Earth's surface for different annihilation channels and for annihilation in the Earth. A neutralino mass of $m_{\tilde{\chi}}$ = 150 GeV is used. Values in paranthesis are calculated from less than 100 events and have thus large errors. In each channel* 10^5 *events are simulated.*

Channel	θ cut	Φ_μ [$\times 10^{-25}$ m^{-2}(parent pair)$^{-1}$] E_μ^{det} [GeV] >									
		0	3	5	7	10	15	20	25	30	50
$c\bar{c}$	no cut	1.60	1.34	1.19	1.08	0.891	0.662	0.492	0.350	0.243	(0.061)
	$\theta < 10°$	1.47	1.27	1.16	1.05	0.879	0.659	0.490	0.349	0.243	(0.061)
	$\theta < 7.5°$	1.34	1.18	1.08	0.990	0.841	0.641	0.482	0.346	0.242	(0.061)
	$\theta < 5°$	1.06	0.948	0.881	0.820	0.711	0.559	0.431	0.313	0.224	(0.060)
$b\bar{b}$	no cut	5.04	4.41	4.04	3.68	3.19	2.53	1.98	1.56	1.20	0.373
	$\theta < 10°$	4.71	4.24	3.93	3.61	3.15	2.52	1.98	1.56	1.20	0.373
	$\theta < 7.5°$	4.39	3.99	3.73	3.45	3.04	2.47	1.94	1.54	1.19	0.373
	$\theta < 5°$	3.52	3.25	3.06	2.88	2.58	2.15	1.73	1.40	1.10	0.356
$t\bar{t}$	no cut	16.1	14.7	13.8	13.0	11.9	10.2	8.78	7.52	6.38	3.17
	$\theta < 10°$	15.6	14.4	13.6	12.9	11.8	10.2	8.78	7.52	6.38	3.17
	$\theta < 7.5°$	14.9	13.8	13.2	12.5	11.5	10.0	8.68	7.47	6.35	3.17
	$\theta < 5°$	12.8	12.0	11.5	11.0	10.2	9.03	7.96	6.94	5.96	3.06
$\tau^+\tau^-$	no cut	21.1	19.6	18.7	17.8	16.6	14.7	12.8	11.2	9.76	5.29
	$\theta < 10°$	20.6	19.3	18.5	17.7	16.5	14.6	12.8	11.2	9.76	5.29
	$\theta < 7.5°$	20.0	18.8	18.0	17.3	16.2	14.4	12.7	11.1	9.70	5.29
	$\theta < 5°$	17.5	16.5	15.9	15.3	14.5	13.1	11.6	10.3	9.03	5.07
W^+W^-	no cut	31.4	29.8	28.8	27.8	26.5	24.2	22.1	20.1	18.3	12.0
	$\theta < 10°$	31.0	29.6	28.6	27.7	26.4	24.2	22.1	20.1	18.3	12.0
	$\theta < 7.5°$	30.3	29.0	28.1	27.2	26.0	23.9	21.9	19.9	18.2	11.9
	$\theta < 5°$	27.4	26.3	25.6	24.8	23.8	22.0	20.3	18.7	17.1	11.4
Z^0Z^0	no cut	36.7	34.8	33.5	32.4	30.7	28.1	25.6	23.1	20.8	13.4
	$\theta < 10°$	36.2	34.5	33.3	32.3	30.6	28.0	25.5	23.1	20.8	13.4
	$\theta < 7.5°$	35.4	33.8	32.7	31.8	30.2	27.8	25.3	23.0	20.7	13.4
	$\theta < 5°$	31.9	30.5	29.6	28.8	27.5	25.5	23.4	21.4	19.4	12.7
$H_1^0H_3^0$	no cut	3.80	3.08	2.69	2.34	1.92	1.38	0.976	0.683	0.491	0.130
	$\theta < 10°$	3.37	2.89	2.58	2.28	1.90	1.37	0.975	0.683	0.491	0.130
	$\theta < 7.5°$	3.03	2.64	2.39	2.14	1.82	1.34	0.965	0.680	0.491	0.130
	$\theta < 5°$	2.32	2.06	1.89	1.73	1.51	1.15	0.852	0.625	0.462	0.127
$Z^0H_1^0$	no cut	14.5	13.3	12.5	11.8	10.8	9.35	8.10	7.03	6.08	3.35
	$\theta < 10°$	14.0	13.0	12.3	11.7	10.8	9.33	8.09	7.03	6.08	3.35
	$\theta < 7.5°$	13.5	12.6	12.0	11.4	10.6	9.19	8.00	6.97	6.05	3.34
	$\theta < 5°$	11.6	10.9	10.4	9.99	9.34	8.24	7.26	6.40	5.61	3.18
$Z^0H_2^0$	no cut	22.2	20.8	20.0	19.2	18.0	16.3	14.7	13.3	12.1	7.81
	$\theta < 10°$	21.7	20.5	19.8	19.1	17.9	16.2	14.7	13.3	12.1	7.81
	$\theta < 7.5°$	21.1	20.0	19.4	18.7	17.6	16.1	14.6	13.3	12.1	7.78
	$\theta < 5°$	18.8	18.0	17.5	16.9	16.0	14.7	13.5	12.4	11.3	7.44
W^+H^-	no cut	17.8	16.4	15.6	14.7	13.6	11.8	10.2	8.78	7.47	3.88
	$\theta < 10°$	17.3	16.2	15.4	14.6	13.5	11.7	10.2	8.78	7.46	3.88
	$\theta < 7.5°$	16.7	15.6	14.9	14.2	13.2	11.6	10.1	8.71	7.43	3.88
	$\theta < 5°$	14.3	13.5	13.0	12.5	11.7	10.4	9.14	7.96	6.85	3.69
W^-H^+	no cut	16.1	14.9	14.0	13.3	12.2	10.6	9.19	7.96	6.90	3.69
	$\theta < 10°$	15.6	14.6	13.9	13.2	12.2	10.6	9.18	7.95	6.90	3.69
	$\theta < 7.5°$	15.0	14.1	13.5	12.8	11.9	10.4	9.10	7.90	6.88	3.69
	$\theta < 5°$	13.0	12.3	11.8	11.3	10.6	9.43	8.31	7.32	6.43	3.55

Table 19: *Muon fluxes at the Earth's surface for different annihilation channels and for annihilation in the Earth. A neutralino mass of* $m_{\tilde{\chi}} = 200$ *GeV is used. Values in paranthesis are calculated from less than 100 events and have thus large errors. In each channel* 10^5 *events are simulated.*

Channel	θ cut	Φ_μ [$\times 10^{-25}$ m^{-2}(parent pair)$^{-1}$] E_μ^{det} [GeV] $>$									
		0	3	5	7	10	15	20	25	30	50
$c\bar{c}$	no cut	2.37	2.06	1.86	1.69	1.47	1.13	0.892	0.676	0.524	0.201
	$\theta < 10°$	2.23	1.98	1.81	1.67	1.46	1.13	0.891	0.676	0.523	0.201
	$\theta < 7.5°$	2.08	1.87	1.72	1.59	1.40	1.10	0.879	0.670	0.520	0.201
	$\theta < 5°$	1.71	1.55	1.45	1.35	1.21	0.983	0.803	0.621	0.488	0.198
$b\bar{b}$	no cut	7.44	6.66	6.17	5.71	5.11	4.22	3.46	2.83	2.31	0.995
	$\theta < 10°$	7.10	6.48	6.05	5.64	5.08	4.20	3.45	2.83	2.31	0.995
	$\theta < 7.5°$	6.72	6.18	5.80	5.43	4.93	4.12	3.42	2.81	2.30	0.995
	$\theta < 5°$	5.66	5.27	4.99	4.73	4.35	3.71	3.14	2.61	2.18	0.969
$t\bar{t}$	no cut	26.2	24.5	23.4	22.4	20.9	18.6	16.6	14.8	13.1	8.03
	$\theta < 10°$	25.6	24.2	23.2	22.2	20.8	18.6	16.6	14.8	13.1	8.03
	$\theta < 7.5°$	24.9	23.6	22.7	21.8	20.5	18.4	16.5	14.7	13.0	8.01
	$\theta < 5°$	22.3	21.3	20.6	19.9	18.8	17.1	15.5	13.9	12.4	7.79
$\tau^+\tau^-$	no cut	32.6	30.9	29.8	28.6	27.0	24.4	22.0	19.8	17.7	11.1
	$\theta < 10°$	32.2	30.6	29.6	28.4	26.9	24.4	22.0	19.8	17.7	11.1
	$\theta < 7.5°$	31.5	30.0	29.0	28.0	26.5	24.1	21.9	19.7	17.7	11.1
	$\theta < 5°$	28.7	27.5	26.7	25.8	24.6	22.6	20.6	18.7	16.9	10.9
W^+W^-	no cut	49.0	47.0	45.8	44.5	42.7	39.7	37.1	34.5	32.1	23.5
	$\theta < 10°$	48.6	46.8	45.6	44.4	42.6	39.6	37.1	34.5	32.1	23.5
	$\theta < 7.5°$	47.9	46.2	45.0	43.9	42.2	39.4	36.9	34.4	32.0	23.5
	$\theta < 5°$	44.8	43.4	42.4	41.4	39.9	37.4	35.2	33.0	30.9	22.9
Z^0Z^0	no cut	58.7	56.3	54.7	53.2	51.1	47.6	44.2	41.1	37.9	27.4
	$\theta < 10°$	58.2	56.0	54.5	53.1	51.0	47.6	44.2	41.1	37.9	27.4
	$\theta < 7.5°$	57.3	55.3	53.8	52.5	50.5	47.2	44.0	40.9	37.8	27.4
	$\theta < 5°$	53.5	51.8	50.5	49.4	47.7	44.9	42.0	39.2	36.4	26.8
$H_1^0H_3^0$	no cut	6.32	5.41	4.86	4.38	3.77	2.95	2.31	1.81	1.39	0.542
	$\theta < 10°$	5.85	5.18	4.73	4.30	3.73	2.94	2.31	1.81	1.39	0.542
	$\theta < 7.5°$	5.43	4.88	4.50	4.13	3.62	2.89	2.28	1.80	1.39	0.542
	$\theta < 5°$	4.42	4.04	3.76	3.49	3.14	2.59	2.09	1.67	1.31	0.523
$Z^0H_1^0$	no cut	25.4	23.9	22.9	22.0	20.7	18.7	16.9	15.4	13.9	9.27
	$\theta < 10°$	24.9	23.6	22.8	21.9	20.6	18.7	16.9	15.4	13.9	9.27
	$\theta < 7.5°$	24.3	23.1	22.4	21.6	20.4	18.5	16.8	15.3	13.9	9.26
	$\theta < 5°$	22.1	21.1	20.5	19.9	18.9	17.4	15.9	14.6	13.3	9.06
$Z^0H_2^0$	no cut	32.9	31.3	30.2	29.2	27.8	25.7	23.7	21.9	20.1	14.2
	$\theta < 10°$	32.4	31.0	30.0	29.0	27.7	25.7	23.7	21.9	20.1	14.2
	$\theta < 7.5°$	31.7	30.4	29.5	28.6	27.4	25.4	23.5	21.8	20.1	14.2
	$\theta < 5°$	29.2	28.2	27.4	26.7	25.6	24.0	22.4	20.8	19.3	13.8
W^+H^-	no cut	30.6	28.8	27.7	26.5	25.0	22.7	20.6	18.5	16.6	11.1
	$\theta < 10°$	30.1	28.5	27.5	26.4	24.9	22.6	20.5	18.5	16.6	11.1
	$\theta < 7.5°$	29.3	27.9	27.0	26.0	24.6	22.4	20.4	18.4	16.6	11.1
	$\theta < 5°$	26.5	25.3	24.5	23.7	22.6	20.8	19.1	17.3	15.8	10.8
W^-H^+	no cut	27.0	25.3	24.3	23.3	22.0	19.8	17.8	16.1	14.5	9.44
	$\theta < 10°$	26.5	25.0	24.1	23.2	21.9	19.8	17.8	16.1	14.5	9.44
	$\theta < 7.5°$	25.8	24.5	23.7	22.8	21.6	19.6	17.7	16.0	14.5	9.43
	$\theta < 5°$	23.5	22.5	21.8	21.1	20.1	18.4	16.8	15.3	13.9	9.21

Table 20: *Muon fluxes at the Earth's surface for different annihilation channels and for annihilation in the Earth. A neutralino mass of* $m_{\tilde{\chi}}$ = *250 GeV is used. In each channel* 10^5 *events are simulated.*

Channel	θ cut	Φ_μ [$\times 10^{-25}$ m^{-2}(parent pair)$^{-1}$] E_μ^{det} [GeV] $>$									
		0	3	5	7	10	15	20	25	30	50
$c\bar{c}$	no cut	4.16	3.73	3.47	3.23	2.90	2.38	1.96	1.59	1.33	0.635
	$\theta < 10°$	3.99	3.64	3.41	3.20	2.88	2.37	1.96	1.59	1.33	0.635
	$\theta < 7.5°$	3.81	3.50	3.30	3.11	2.82	2.34	1.94	1.58	1.33	0.635
	$\theta < 5°$	3.32	3.09	2.94	2.80	2.57	2.17	1.83	1.52	1.29	0.630
$b\bar{b}$	no cut	13.5	12.4	11.7	11.1	10.1	8.84	7.65	6.67	5.71	3.17
	$\theta < 10°$	13.1	12.2	11.6	11.0	10.1	8.82	7.65	6.67	5.71	3.17
	$\theta < 7.5°$	12.7	11.9	11.3	10.8	9.92	8.74	7.61	6.64	5.70	3.17
	$\theta < 5°$	11.4	10.7	10.3	9.84	9.15	8.17	7.20	6.36	5.50	3.11
$t\bar{t}$	no cut	51.1	48.6	47.0	45.6	43.4	40.0	36.9	34.0	31.6	22.7
	$\theta < 10°$	50.4	48.2	46.8	45.4	43.3	40.0	36.9	34.0	31.6	22.7
	$\theta < 7.5°$	49.6	47.5	46.2	44.9	42.9	39.8	36.8	33.9	31.5	22.7
	$\theta < 5°$	46.4	44.7	43.5	42.5	40.8	38.1	35.4	32.9	30.7	22.4
$\tau^+\tau^-$	no cut	63.9	61.4	59.7	58.0	55.7	51.8	48.4	45.0	41.8	30.5
	$\theta < 10°$	63.4	61.1	59.5	57.9	55.6	51.8	48.3	45.0	41.8	30.5
	$\theta < 7.5°$	62.7	60.4	58.9	57.4	55.1	51.5	48.1	44.9	41.7	30.5
	$\theta < 5°$	59.2	57.2	55.9	54.6	52.7	49.5	46.6	43.6	40.7	30.1
W^+W^-	no cut	91.5	88.6	86.9	85.1	82.5	78.2	73.9	69.9	66.6	53.6
	$\theta < 10°$	91.1	88.4	86.7	85.0	82.4	78.2	73.9	69.9	66.6	53.6
	$\theta < 7.5°$	90.4	87.8	86.2	84.5	82.1	77.9	73.7	69.8	66.5	53.6
	$\theta < 5°$	86.9	84.5	83.2	81.6	79.4	75.6	71.8	68.1	65.1	52.9
Z^0Z^0	no cut	112	108	106	104	101	96.1	91.4	86.5	82.0	66.0
	$\theta < 10°$	111	108	106	104	101	96.0	91.4	86.5	82.0	66.0
	$\theta < 7.5°$	110	107	105	103	101	95.7	91.2	86.3	81.9	66.0
	$\theta < 5°$	106	104	102	100	97.6	93.2	89.0	84.6	80.4	65.3
$H_1^0H_3^0$	no cut	12.5	11.2	10.4	9.72	8.72	7.34	6.19	5.24	4.42	2.35
	$\theta < 10°$	11.9	10.9	10.3	9.63	8.68	7.33	6.19	5.24	4.42	2.35
	$\theta < 7.5°$	11.4	10.5	9.94	9.36	8.50	7.23	6.14	5.22	4.41	2.35
	$\theta < 5°$	9.91	9.19	8.80	8.36	7.69	6.66	5.76	4.97	4.25	2.32
$Z^0H_1^0$	no cut	56.6	54.3	53.0	51.6	49.7	56.6	43.8	41.2	38.7	30.0
	$\theta < 10°$	56.1	54.0	52.8	51.5	49.7	46.5	43.8	41.2	38.7	30.0
	$\theta < 7.5°$	55.4	53.5	52.3	51.1	49.4	46.4	43.7	41.1	38.7	30.0
	$\theta < 5°$	52.6	50.9	49.9	48.9	47.4	44.7	42.3	40.0	37.8	29.5
$Z^0H_2^0$	no cut	64.1	61.7	60.4	59.0	56.7	53.5	50.1	47.1	44.4	35.1
	$\theta < 10°$	63.5	61.4	60.2	58.8	56.7	53.5	50.1	47.1	44.4	35.1
	$\theta < 7.5°$	62.8	60.8	59.7	58.4	56.3	53.3	50.0	47.0	44.4	35.1
	$\theta < 5°$	59.9	58.2	57.2	56.1	54.3	51.5	48.6	45.8	43.4	34.6
W^+H^-	no cut	64.9	62.1	60.3	58.7	56.4	52.9	49.5	46.3	43.2	33.0
	$\theta < 10°$	64.2	61.7	60.0	58.5	56.3	52.9	49.5	46.3	43.2	33.0
	$\theta < 7.5°$	63.4	61.0	59.5	58.1	55.9	52.7	49.4	46.2	43.2	33.0
	$\theta < 5°$	59.8	57.7	56.4	55.2	53.3	50.5	47.6	44.7	41.9	32.4
W^-H^+	no cut	55.4	53.0	51.5	50.1	48.0	44.8	42.0	39.2	36.6	27.9
	$\theta < 10°$	54.8	52.7	51.3	50.0	47.9	44.7	42.0	39.2	36.6	27.9
	$\theta < 7.5°$	54.1	52.1	50.9	49.5	47.6	44.5	41.9	39.1	36.6	27.9
	$\theta < 5°$	51.5	49.8	48.7	47.6	45.9	43.2	40.8	38.3	35.9	27.6

Table 21: *Muon fluxes at the Earth's surface for different annihilation channels and for annihilation in the Earth. A neutralino mass of $m_{\tilde{\chi}}$ = 350 GeV is used. In each channel* 10^5 *events are simulated.*

Channel	θ cut	Φ_μ [$\times 10^{-25}$ m^{-2}(parent pair)$^{-1}$] E_μ^{det} [GeV] >									
		0	3	5	7	10	15	20	25	30	50
$c\bar{c}$	no cut	7.52	6.96	6.61	6.28	5.78	5.00	4.38	3.84	3.39	1.99
	$\theta < 10°$	7.33	6.86	6.54	6.24	5.76	4.99	4.38	3.84	3.39	1.99
	$\theta < 7.5°$	7.12	6.69	6.40	6.13	5.68	4.95	4.36	3.83	3.39	1.99
	$\theta < 5°$	6.49	6.14	5.90	5.69	5.32	4.70	4.20	3.72	3.31	1.98
$b\bar{b}$	no cut	24.5	23.1	22.1	21.2	20.0	18.1	16.2	14.6	13.2	8.60
	$\theta < 10°$	24.1	22.8	21.9	21.1	19.9	18.0	16.2	14.5	13.2	8.60
	$\theta < 7.5°$	23.5	22.4	21.6	20.8	19.7	17.9	16.1	14.5	13.1	8.60
	$\theta < 5°$	21.8	20.9	20.2	19.6	18.6	17.1	15.5	14.1	12.8	8.51
$t\bar{t}$	no cut	101	97.6	95.4	93.3	90.5	85.2	80.8	76.4	71.8	57.4
	$\theta < 10°$	100	97.2	95.1	93.1	90.3	85.2	80.8	76.4	71.8	57.4
	$\theta < 7.5°$	99.2	96.4	94.4	92.6	89.9	84.9	80.6	76.3	71.7	57.4
	$\theta < 5°$	95.5	93.2	91.4	89.8	87.4	82.9	79.1	75.1	70.8	57.0
$\tau^+\tau^-$	no cut	123	119	117	114	111	106	101	95.5	90.6	72.5
	$\theta < 10°$	123	119	117	114	111	106	100	95.5	90.6	72.5
	$\theta < 7.5°$	122	118	116	114	110	105	100	95.4	90.5	72.5
	$\theta < 5°$	118	115	113	111	108	103	98.5	93.9	89.4	72.1
W^+W^-	no cut	186	182	179	177	173	167	161	154	149	127
	$\theta < 10°$	185	182	179	176	173	167	161	154	149	127
	$\theta < 7.5°$	185	181	179	176	173	166	160	154	149	127
	$\theta < 5°$	181	178	175	173	170	164	158	153	147	127
Z^0Z^0	no cut	217	213	209	206	201	194	185	178	172	147
	$\theta < 10°$	217	212	209	206	201	194	185	178	172	147
	$\theta < 7.5°$	216	211	208	205	201	193	185	178	171	147
	$\theta < 5°$	211	207	204	202	197	190	183	176	170	146
$H_1^0H_3^0$	no cut	25.0	23.2	22.1	21.1	19.5	17.3	15.4	13.7	12.3	7.81
	$\theta < 10°$	24.4	22.9	21.9	21.0	19.4	17.3	15.4	13.7	12.3	7.81
	$\theta < 7.5°$	23.7	22.4	21.5	20.6	19.2	17.2	15.3	13.7	12.3	7.81
	$\theta < 5°$	21.6	20.5	19.8	19.1	18.0	16.3	14.7	13.2	11.9	7.69
$Z^0H_1^0$	no cut	116	113	111	109	105	101	95.7	91.3	87.2	73.1
	$\theta < 10°$	115	112	110	108	105	101	95.7	91.3	87.2	73.1
	$\theta < 7.5°$	114	112	110	108	105	100	95.5	91.2	87.1	73.1
	$\theta < 5°$	111	109	107	106	103	98.6	94.2	90.1	86.2	72.7
$Z^0H_2^0$	no cut	125	121	119	117	114	109	104	99.4	95.7	80.9
	$\theta < 10°$	124	121	119	117	114	109	104	99.4	95.7	80.9
	$\theta < 7.5°$	123	120	118	116	113	109	104	99.3	95.6	80.9
	$\theta < 5°$	120	117	115	114	111	107	102	98.1	94.6	80.4
W^+H^-	no cut	135	131	129	126	123	117	111	106	102	83.4
	$\theta < 10°$	134	131	129	126	123	117	111	106	102	83.4
	$\theta < 7.5°$	133	130	128	126	122	117	111	106	101	83.3
	$\theta < 5°$	130	127	125	122	119	114	109	105	100	82.8
W^-H^+	no cut	110	107	105	103	99.4	94.7	90.3	86.3	82.3	68.4
	$\theta < 10°$	109	106	104	102	99.3	94.7	90.3	86.3	82.3	68.4
	$\theta < 7.5°$	109	106	104	102	99.0	94.5	90.2	86.2	82.2	68.4
	$\theta < 5°$	106	103	101	99.6	97.0	92.8	88.9	85.1	81.4	68.1

Table 22: *Muon fluxes at the Earth's surface for different annihilation channels and for annihilation in the Earth. A neutralino mass of $m_{\tilde{\chi}}$ = 500 GeV is used. In each channel* 10^5 *events are simulated.*

B Manual for NUMU 1.0

NUMU 1.0 is a program that takes care of the whole chain of processes from the annihilation products in the Sun or the Earth to detectable muons in the ice (of e.g. AMANDA). There should not be much need of running it oneself since the results of a lot of runs are tabulated in appendix A, but a description of the program is nevertheless included and the program may be obtained upon request. For those who wants to run the program without deeper knowledge of the way the program does the things it does, it is enough to read sec. B.1 below. The sections following that one are devoted for those who wants to know how to program works and/or modify it.

Since the NUMU 1.0 program uses JETSET 7.3 and PYTHIA 5.6 [24] one has to link it with the JETSET library. It also uses PDFLIB for the new GRV structure functions [23] and this package also has to be linked to the program. The HBOOK package also has to be linked with the program since data are written to HBOOK files. All these packages are found in the CERNLIB package.

B.1 How to run NUMU 1.0

When running the program one has to enter which annihilation channel to study, what mass of the neutralino to use, if annihilation in the Earth also should be considered and how many events to simulate. One also has the option of getting full or limited output on the screen and on NTUPLEs (which are like big arrays that can be analysed with PAW). If full output to the screen is chosen, event listings are printed as well as simulation information. Some variables for each found neutrino are written to NTUPLEs in the file `numu.hbook`. If limited output to NTUPLEs is chosen only the most important ones are written to the file. Otherwise more variables are written which can be used for interesting checks and figures. The variables written to the NTUPLEs are explained in the common block SUDAT and EADAT in sec. B.2. At the end of each run, the muon fluxes (i.e. those found in appendix A) with certain cuts (in E_μ^{det} and θ) are printed.

If one wants to change the cuts in E_μ^{det} and θ one has to change EMUTH and ANGTH in the common block FLUXES as explained in sec. B.3.

A typical run can look something like this (some output, especially from PYTHIA and JETSET are not shown):

```
**********************************************************************
***                           NUMU 1.0                             ***
***                   Written by Joakim Edsjo.                     ***
***                         December 1993                          ***
***                                                                ***
***                   E-mail: edsjo@tsl.uu.se                      ***
**********************************************************************

You can look at           12 different channels:
 1  c    c~    for neutralino masses above    1.4 GeV.
 2  b    b~    for neutralino masses above    5.0 GeV.
 3  t    t~    for neutralino masses above  150.0 GeV.
 4  tau- tau+  for neutralino masses above    1.8 GeV.
 5  W+   W-    for neutralino masses above   80.0 GeV.
 6  Z0   Z0    for neutralino masses above   91.2 GeV.
 7  H10  H30   for neutralino masses above  175.0 GeV.
 8  Z0   H10   for neutralino masses above  145.6 GeV.
 9  Z0   H20   for neutralino masses above   80.6 GeV.
```

```
10  W+   H-    for neutralino masses above  140.0 GeV.
11  W-   H+    for neutralino masses above  140.0 GeV.
12  g    g     for neutralino masses above    0.0 GeV.

Which channel do you want to simulate? 2
What neutralino mass should be used [GeV]? 150
Do you want to consider annihilation in the Earth as well (y or n)? n
How many events should be simulated? 100000
(If you choose more than 100000 events the number
 has to be a multiple of 100000.)
Do you want full output on the screen (y or n)? y
Do you want full output on NTUPLEs (y or n)? n

Generation of neutrinos in the sun has started...


                   The Lund Monte Carlo - JETSET version 7.3
                   **  Last date of change:   3 Nov 1992  **



                           Event listing (summary)

   I  particle/jet KS     KF orig    p_x      p_y      p_z       E        m

   1  (b)          14      5    0    0.000    0.000  149.917  150.000    5.000
   2  (b~)         14     -5    0    0.000    0.000 -149.917  150.000    5.000
   3  (CMshower)   11     94    1    0.000    0.000    0.000  300.000  300.000
   4  (b)          14      5    3    0.000    0.000  139.753  153.561   63.641
   5  (b~)         14     -5    3    0.000    0.000 -139.753  146.439   43.743
   6  (b)          14      5    4  -14.190  -23.187   47.988   55.468    5.909
   7  (g)          14     21    4   14.190   23.187   91.765   98.093   21.504
   8  (b~)         13     -5    5   -5.327   -5.488 -137.204  137.508    5.000
   9  (g)          14     21    5    5.327    5.488   -2.549    8.931    3.843
  10  (b)          13      5    6  -13.406  -22.816   46.086   53.378    5.000
  11  (g)          13     21    6   -0.784   -0.370    1.901    2.090    0.000
  12  (g)          14     21    7    9.560   11.879   23.369   28.092    3.248
  13  (g)          14     21    7    4.630   11.308   68.396   70.001    8.534
  14  (g)          14     21    9    5.552    4.521   -1.573    7.539    1.761
  15  (g)          13     21    9   -0.225    0.967   -0.975    1.392    0.000
  16  (g)          13     21   12    7.371   10.623   20.797   24.489    0.000
  17  (g)          13     21   12    2.189    1.255    2.572    3.603    0.000
  18  (g)          14     21   13   -0.311    7.873   45.029   45.785    2.556
  19  (g)          14     21   13    4.941    3.435   23.367   24.216    2.051
  20  (g)          13     21   14    5.147    4.031   -0.877    6.596    0.000
  21  (g)          13     21   14    0.404    0.491   -0.696    0.943    0.000
  22  (g)          13     21   18    0.252    0.521    6.877    6.901    0.000
  23  (g)          14     21   18   -0.563    7.352   38.153   38.884    1.401
  24  (g)          13     21   19    0.866    0.315    2.070    2.266    0.000
  25  (g)          14     21   19    4.075    3.120   21.297   21.951    1.388
  26  (g)          13     21   23   -0.880    6.286   30.759   31.407    0.000
  27  (g)          13     21   23    0.317    1.066    7.394    7.477    0.000
  28  (g)          13     21   25    2.291    1.234    8.360    8.756    0.000
  29  (g)          13     21   25    1.784    1.887   12.936   13.194    0.000
  30  (b~)       A 12     -5    8   -5.327   -5.488 -137.204  137.508    5.000
  31  (g)        I 12     21   20    5.147    4.031   -0.877    6.596    0.000
  32  (g)        I 12     21   21    0.404    0.491   -0.696    0.943    0.000
  33  (g)        I 12     21   15   -0.225    0.967   -0.975    1.392    0.000
  34  (g)        I 12     21   16    7.371   10.623   20.797   24.489    0.000
  35  (g)        I 12     21   17    2.189    1.255    2.572    3.603    0.000
  36  (g)        I 12     21   22    0.252    0.521    6.877    6.901    0.000
```

37	(g)	I	12	21	26	-0.880	6.286	30.759	31.407	0.000
38	(g)	I	12	21	27	0.317	1.066	7.394	7.477	0.000
39	(g)	I	12	21	24	0.866	0.315	2.070	2.266	0.000
40	(g)	I	12	21	28	2.291	1.234	8.360	8.756	0.000
41	(g)	I	12	21	29	1.784	1.887	12.936	13.194	0.000
42	(g)	I	12	21	11	-0.784	-0.370	1.901	2.090	0.000
43	(b)	V	11	5	10	-13.406	-22.816	46.086	53.378	5.000
44	(string)		11	92	30	0.000	0.000	0.000	300.000	300.000
45	(B*0)		11	513	44	-5.002	-4.767	-129.634	129.928	5.335
46	pi+		1	211	44	-0.119	-0.383	-2.909	2.940	0.140
47	(pi0)		11	111	44	0.376	0.036	-0.963	1.043	0.135
48	(omega)		11	223	44	-0.036	-0.302	-1.781	1.969	0.783
49	(Lambda~0)		11	-3122	44	-0.035	0.927	-0.984	1.753	1.116
50	pi-		1	-211	44	0.398	0.072	-0.620	0.753	0.140
51	(Sigma*0)		11	3214	44	1.888	1.195	-1.046	2.820	1.365
52	n~0		1	-2112	44	0.991	1.460	-0.889	2.188	0.940
53	(Lambda0)		11	3122	44	1.174	0.401	-0.052	1.669	1.116
54	(K*0)		11	313	44	0.846	1.728	-0.192	2.134	0.904
55	(K~0)		11	-311	44	0.478	1.276	2.859	3.206	0.498
56	K+		1	321	44	0.805	1.170	1.522	2.139	0.494
57	pi-		1	-211	44	5.936	7.951	15.945	18.780	0.140
58	pi+		1	211	44	1.838	0.418	2.518	3.149	0.140
59	(rho0)		11	113	44	-0.021	0.550	2.673	2.833	0.762
60	(rho-)		11	-213	44	-0.188	4.280	20.775	21.229	0.849
61	(eta')		11	331	44	0.286	1.415	6.009	6.254	0.958
62	pi+		1	211	44	0.786	0.709	7.004	7.085	0.140
63	K-		1	-321	44	0.117	1.539	4.489	4.772	0.494
64	(K*+)		11	323	44	1.583	1.548	15.605	15.788	0.916
65	K-		1	-321	44	0.217	0.616	2.706	2.828	0.494
66	(K*+)		11	323	44	0.250	-0.024	2.076	2.273	0.891
67	(rho-)		11	-213	44	0.870	0.461	6.360	6.471	0.680
68	(eta')		11	331	44	0.106	0.328	2.297	2.512	0.957
69	(B*~0)		11	-513	44	-13.545	-22.604	46.234	53.483	5.335
70	(B0)		11	511	45	-5.009	-4.763	-129.620	129.911	5.279
71	gamma		1	22	45	0.007	-0.004	-0.014	0.017	0.000
72	gamma		1	22	47	0.130	0.063	-0.471	0.492	0.000
73	gamma		1	22	47	0.245	-0.026	-0.492	0.551	0.000
74	pi+		1	211	48	0.075	-0.194	-0.575	0.627	0.140
75	pi-		1	-211	48	-0.094	-0.157	-0.146	0.273	0.140
76	(pi0)		11	111	48	-0.017	0.049	-1.060	1.070	0.135
77	n~0		1	-2112	49	-0.025	0.704	-0.699	1.367	0.940
78	(pi0)		11	111	49	-0.010	0.222	-0.286	0.386	0.135
79	(Lambda0)		11	3122	51	1.362	0.742	-0.787	2.066	1.116
80	(pi0)		11	111	51	0.527	0.453	-0.259	0.754	0.135
81	p+		1	2212	53	1.054	0.326	-0.134	1.455	0.938
82	pi-		1	-211	53	0.120	0.075	0.081	0.215	0.140
83	K+		1	321	54	0.784	1.319	-0.385	1.657	0.494
84	pi-		1	-211	54	0.062	0.409	0.193	0.477	0.140
85	(K_S0)		11	310	55	0.478	1.276	2.859	3.206	0.498
86	pi-		1	-211	59	-0.223	0.627	1.827	1.949	0.140
87	pi+		1	211	59	0.202	-0.077	0.846	0.884	0.140
88	pi-		1	-211	60	-0.450	3.533	16.887	17.259	0.140
89	(pi0)		11	111	60	0.262	0.746	3.888	3.970	0.135
90	gamma		1	22	61	0.013	0.569	2.723	2.781	0.000
91	(rho0)		11	113	61	0.273	0.846	3.286	3.472	0.683
92	(K0)		11	311	64	0.885	1.149	11.568	11.669	0.498
93	pi+		1	211	64	0.698	0.399	4.038	4.119	0.140
94	(K0)		11	311	66	0.066	0.228	1.558	1.652	0.498
95	pi+		1	211	66	0.184	-0.252	0.518	0.621	0.140
96	pi-		1	-211	67	0.611	0.243	2.328	2.423	0.140
97	(pi0)		11	111	67	0.259	0.218	4.032	4.049	0.135
98	pi+		1	211	68	0.143	0.074	0.426	0.476	0.140
99	pi-		1	-211	68	-0.095	-0.045	0.398	0.435	0.140

```
100  (eta)         11    221   68    0.059    0.300    1.473    1.601    0.549
101  (B~0)         11   -511   69  -13.414  -22.338   45.815   52.970    5.279
102  gamma          1     22   69   -0.131   -0.266    0.418    0.513    0.000
103  (D*_s+)       11    433   70   -2.398   -3.754  -95.117   95.245    2.113
104  (D-)          11   -411   70   -2.611   -1.009  -34.502   34.666    1.869
105  gamma          1     22   76    0.049    0.057   -0.672    0.676    0.000
106  gamma          1     22   76   -0.066   -0.008   -0.388    0.393    0.000
107  gamma          1     22   78   -0.023    0.128   -0.255    0.287    0.000
108  gamma          1     22   78    0.013    0.094   -0.030    0.100    0.000
109  p+             1   2212   79    1.216    0.720   -0.629    1.809    0.938
110  pi-            1   -211   79    0.146    0.023   -0.158    0.257    0.140
111  gamma          1     22   80    0.407    0.295   -0.231    0.553    0.000
112  gamma          1     22   80    0.119    0.158   -0.028    0.200    0.000
113  pi-            1   -211   85    0.215    0.329    1.224    1.293    0.140
114  pi+            1    211   85    0.263    0.947    1.635    1.913    0.140
115  gamma          1     22   89    0.063    0.302    1.260    1.297    0.000
116  gamma          1     22   89    0.199    0.444    2.628    2.673    0.000
117  pi-            1   -211   91   -0.088    0.679    2.075    2.190    0.140
118  pi+            1    211   91    0.361    0.167    1.211    1.283    0.140
119  K_L0           1    130   92    0.885    1.149   11.568   11.669    0.498
120  K_L0           1    130   94    0.066    0.228    1.558    1.652    0.498
121  gamma          1     22   97    0.195    0.167    2.256    2.271    0.000
122  gamma          1     22   97    0.064    0.051    1.776    1.778    0.000
123  gamma          1     22  100    0.284    0.114    0.995    1.041    0.000
124  gamma          1     22  100   -0.225    0.186    0.478    0.560    0.000
125  (D+)          11    411  101  -12.438  -21.772   42.224   49.143    1.869
126  pi-            1   -211  101   -0.487    0.035    1.051    1.167    0.140
127  (pi0)         11    111  101   -0.490   -0.601    2.541    2.660    0.135
128  (D_s+)        11    431  103   -2.430   -3.701  -92.384   92.511    1.969
129  gamma          1     22  103    0.032   -0.053   -2.734    2.734    0.000
130  mu-            1     13  104   -0.204   -0.018   -0.764    0.798    0.106
131  nu_mu~         1    -14  104   -0.922   -0.457   -9.422    9.478    0.000
132  K+             1    321  104   -0.735   -0.396  -10.048   10.095    0.494
133  pi-            1   -211  104   -0.547   -0.238   -9.377    9.396    0.140
134  (pi0)         11    111  104   -0.203    0.099   -4.892    4.899    0.135
135  K-             1   -321  125   -8.235  -13.187   25.861   30.178    0.494
136  pi+            1    211  125   -1.424   -3.558    6.202    7.292    0.140
137  pi+            1    211  125   -2.779   -5.027   10.161   11.673    0.140
138  gamma          1     22  127   -0.154   -0.255    1.147    1.185    0.000
139  gamma          1     22  127   -0.336   -0.346    1.394    1.475    0.000
140  mu+            1    -13  128   -0.120   -0.243   -1.906    1.928    0.106
141  nu_mu          1     14  128   -0.212   -0.763  -18.205   18.222    0.000
142  (phi)         11    333  128   -2.098   -2.695  -72.273   72.361    1.009
143  gamma          1     22  134   -0.170    0.127   -4.417    4.423    0.000
144  gamma          1     22  134   -0.033   -0.028   -0.474    0.476    0.000
145  K+             1    321  142   -0.928   -1.361  -34.825   34.867    0.494
146  K-             1   -321  142   -1.169   -1.335  -37.448   37.494    0.494
                 sum:   0.00          0.000    0.000    0.000  300.000  300.000


Number of generated events =        1000
Number of generated events =        2000
Number of generated events =        3000
          .
          .
          .
Number of generated events =       99000
Number of generated events =      100000

Simulation of neutrino interactions in the sun has started...

                         The Lund Monte Carlo - PYTHIA version 5.6
                         **  Last date of change:  16 Apr 1993  **
```

```
***************** PYINIT: initialization of PYTHIA routines *****************

==============================================================================
I                                                                            I
I          PYTHIA will be initialized for nu_mu on p+ fixed target          I
I                    at    150.000 GeV/c lab-momentum                        I
I                                                                            I
I          corresponding to     16.804 GeV center-of-mass energy             I
I                                                                            I
==============================================================================

  *****  PDFLIB Version:  4.13  Released on  931013  at  22.45  in the
 CERN Program Library     W5051  *****
  *****  Library compiled on       931022 at        1933  *****
  Warning : NON standard settings, TMAS value =    150.0000000000000
   set by user !!


  Nucleon PDFs :  Ngroup =           5,   Nset =           3
 ,  for GRV Set HO Structure Functions

----------------------------------------------------------------------------

******** PYMAXI: summary of differential cross-section maximum search ********

          ==========================================================
          I                                      I                 I
          I  ISUB  Subprocess name               I  Maximum value  I
          I                                      I                 I
          ==========================================================
          I                                      I                 I
          I   10   f + f' -> f + f' (QFD)        I    8.2728E-10   I
          I                                      I                 I
          ==========================================================

********************** PYINIT: initialization completed **********************
 Neutrino on proton finished...
 Neutrino on neutron finished...
 Anti neutrino on proton finished...
 Anti neutrino on neutron finished...

 Simulation of neutrino interactions in the ice has started...

Now simulating in the energy range   0.0 to    7.7 GeV.

                            Event listing (summary)

   I  particle/jet KS     KF orig    p_x      p_y      p_z       E        m

   1  mu-           1     13    0   -0.960   -0.605    1.622    1.982    0.106
   2  pi+           1    211    0    0.623    0.745    1.463    1.761    0.140
   3  p+            1   2212    0    0.110    0.023    2.246    2.437    0.938
   4  gamma         1     22    0    0.025   -0.066    0.052    0.087    0.000
   5  gamma         1     22    0    0.202   -0.098    0.447    0.500    0.000
                  sum:  1.00         0.000    0.000    5.829    6.768    3.438


 Neutrino on proton finished...
 Neutrino on neutron finished...
 Anti neutrino on proton finished...
 Anti neutrino on neutron finished...

Now simulating in the energy range   7.7 to   12.3 GeV.
 Neutrino on proton finished...
 Neutrino on neutron finished...
```

```
 Anti neutrino on proton finished...
 Anti neutrino on neutron finished...

Now simulating in the energy range  12.3 to   24.8 GeV.
 Neutrino on proton finished...
 Neutrino on neutron finished...
 Anti neutrino on proton finished...
 Anti neutrino on neutron finished...

Now simulating in the energy range  24.8 to   58.6 GeV.
 Neutrino on proton finished...
 Neutrino on neutron finished...
 Anti neutrino on proton finished...
 Anti neutrino on neutron finished...

Now simulating in the energy range  58.6 to  150.0 GeV.
 Neutrino on proton finished...
 Neutrino on neutron finished...
 Anti neutrino on proton finished...
 Anti neutrino on neutron finished...

 Simulation in the ice finished...

 SUMMARY
  Annihilation channel:  2
  Generated particles: b    b~
  Neutralino mass =  150.0
  Number of events  =  100000
  Number of found muon neutrinos =   48254
  Number of neutrinos after int. =   45933

  Annihilation in the Sun
  =======================
  Flux at Earth per parent pair [1E-35 m-2]

  Theta <  10.0 degrees
  Emudet >   0.0 GeV  ->  Flux =    26.010     based on   16525 events.
  Emudet >   3.0 GeV  ->  Flux =    22.107     based on   10796 events.
  Emudet >   5.0 GeV  ->  Flux =    19.430     based on    7841 events.
  Emudet >   7.0 GeV  ->  Flux =    17.018     based on    5668 events.
  Emudet >  10.0 GeV  ->  Flux =    13.818     based on    3512 events.
  Emudet >  15.0 GeV  ->  Flux =    9.8446     based on    1809 events.
  Emudet >  20.0 GeV  ->  Flux =    6.9008     based on     976 events.
  Emudet >  25.0 GeV  ->  Flux =    4.7899     based on     542 events.
  Emudet >  30.0 GeV  ->  Flux =    3.5085     based on     321 events.
  Emudet >  50.0 GeV  ->  Flux =   0.63038     based on      38 events.

  Theta <   7.5 degrees
  Emudet >   0.0 GeV  ->  Flux =    23.647     based on   11471 events.
  Emudet >   3.0 GeV  ->  Flux =    20.505     based on    8636 events.
  Emudet >   5.0 GeV  ->  Flux =    18.324     based on    6780 events.
  Emudet >   7.0 GeV  ->  Flux =    16.290     based on    5182 events.
  Emudet >  10.0 GeV  ->  Flux =    13.431     based on    3355 events.
  Emudet >  15.0 GeV  ->  Flux =    9.7471     based on    1782 events.
  Emudet >  20.0 GeV  ->  Flux =    6.8710     based on     971 events.
  Emudet >  25.0 GeV  ->  Flux =    4.7899     based on     542 events.
  Emudet >  30.0 GeV  ->  Flux =    3.5085     based on     321 events.
  Emudet >  50.0 GeV  ->  Flux =   0.63038     based on      38 events.

  Theta <   5.0 degrees
  Emudet >   0.0 GeV  ->  Flux =    18.914     based on    6815 events.
  Emudet >   3.0 GeV  ->  Flux =    16.732     based on    5517 events.
  Emudet >   5.0 GeV  ->  Flux =    15.212     based on    4650 events.
  Emudet >   7.0 GeV  ->  Flux =    13.839     based on    3858 events.
  Emudet >  10.0 GeV  ->  Flux =    11.776     based on    2731 events.
  Emudet >  15.0 GeV  ->  Flux =    9.0268     based on    1603 events.
```

```
Emudet >  20.0 GeV  ->  Flux =    6.5706     based on     918 events.
Emudet >  25.0 GeV  ->  Flux =    4.6976     based on     531 events.
Emudet >  30.0 GeV  ->  Flux =    3.4869     based on     319 events.
Emudet >  50.0 GeV  ->  Flux =   0.63038     based on      38 events.

No cut in theta
Emudet >   0.0 GeV  ->  Flux =    29.203     based on   45933 events.
Emudet >   3.0 GeV  ->  Flux =    23.399     based on   13648 events.
Emudet >   5.0 GeV  ->  Flux =    20.108     based on    8697 events.
Emudet >   7.0 GeV  ->  Flux =    17.329     based on    5911 events.
Emudet >  10.0 GeV  ->  Flux =    13.912     based on    3562 events.
Emudet >  15.0 GeV  ->  Flux =    9.8587     based on    1813 events.
Emudet >  20.0 GeV  ->  Flux =    6.9008     based on     976 events.
Emudet >  25.0 GeV  ->  Flux =    4.7899     based on     542 events.
Emudet >  30.0 GeV  ->  Flux =    3.5085     based on     321 events.
Emudet >  50.0 GeV  ->  Flux =   0.63038     based on      38 events.
```

B.2 Subroutines, functions and common blocks

In the following, the subroutines, functions and common blocks of NUMU 1.0 is described as well as the main program.

PROGRAM **NUMU**

Purpose: To simulate the whole chain of processes from the annihilation products in the Sun or the Earth to detectable muons in the ice (of e.g. AMANDA)

Output: Muon fluxes with cuts in E_μ^{det} and θ are printed on the screen (or the log-file) after each run. More detailed information is written to NTUPLEs (which is a kind of big arrays in HBOOK that can be processed further by PAW) and histograms in the file `numu.hbook`.

Procedure: Parameters of PYTHIA and JETSET are modified and running information is read in from the user. The file `numu.hbook` is opened where NTUPLES and histograms are declared. The simulation is made and information written to the screen and the file.

SUBROUTINE **INFO**(CHN, ECM, NEV, OP, EA, NTF)

Purpose: To read in simulation information from the user.

Output:

- CHN The annihilation channel to simulate.
- ECM Twice the neutralino mass in GeV.
- NEV Number of events to simulate.
- OP Full output on the screen during the simulation (.TRUE.) or not (.FALSE.).
- EA If annihilation in the Earth also should be considered (.TRUE.) or not (.FALSE.).
- NTF If full output to NTUPLEs should be written (.TRUE.) or not (.FALSE.).

SUBROUTINE **MODPYT**

Purpose: Set some general switches of PYTHIA and JETSET and define the Higgs bosons and the top quark as explained in sec. 2.1.

SUBROUTINE **GENEVT**(CHN, NEV)

Purpose: To administer the hadronisation of annihilation products in the Sun, their interactions with the solar medium, the neutrino interactions with the Sun on the way out of it and the interaction of neutrinos with the ice (in e.g. AMANDA).

Input:
- CHN — The annihilation channel to simulate.
- NEV — Number of events to simulate.

Output: The resulting energy spectra historgrams and NTUPLES are written to a HBOOK file `numu.hbook` (taken care of DATSAV) and the fluxes are stored in the common block FLUXES.

Procedure: The hadronisation, decay and interactions of hadrons in the Sun are taken care of GENNU. The neutrino interactions on the way out of the Sun are simulated with PYTHIA in NUINT. The interactions in the ice at the detector are taken care of MUSIM, where the neutrino interactions are simulated with PYTHIA and the resulting muon energy is calculated.

Calls to: GENNU, INIT, NUINT, MUSIM, DATRES and DATSAV.
HFN of HBOOK.

SUBROUTINE **GENNU**(CHN, ECM)

Purpose: To simulate the hadronisation and/or decay of annihilation products in the Sun and the interactions of the products in the solar medium to get the resulting neutrino energy as it leaves the core of the Sun.

Input:
- CHN — The annihilation channel to simulate.
- ECM — Center of mass energy (GeV) for the parent pairs which is equal to twice the neutralino mass.

Output: The resulting data about the produced neutrino is stored in NUDAT in the common block NEUTRINO.

Procedure: The hadronisation and/or decay are simulated with JETSET 7.3 and the interactions of the heavy hadrons are taken care of HADINT.

Calls to: HADINT
LU2ENT, LUSHOW, LUEXEC and LULIST of JETSET

SUBROUTINE **HADINT**(I, ENU, WH, NHI)

Purpose: To calculate the interactions of annihilation products in the Sun, especially the energy loss of heavy hadrons.

Input:
- I — The line number in the event record where the neutrino of interest is.
- ENU — The neutrino energy in GeV as obtained from JETSET,i.e. without heavy hadron interactions taken care of.
- WH — Where the interactions are to be considered. WH='SU' for the Sun and 'EA' for the Earth.

Output:
- ENU — Neutrino energy (in GeV) after correction for heavy hadron interactions. The energy is put to -1.0 GeV if any of the parents in the chain of parents, from which the neutrino originated, has been stopped.
- NHI — The total number of interactions that all parent hadrons of a neutrino have participated in.

Procedure: The mean free path and the probability for interaction is calculated. If an interaction takes place, the energy loss of the heavy hadron is calculated with the method described in sec. 3.2.

Calls to: PTYPE

INTEGER FUNCTION **PTYPE**(KF)

Purpose: To determine of what kind the particle with particle code KF is, i.e. to determine the strength of the interactions between the particle and the surrounding medium in the core of the Sun or the Earth.

Output: On output PTYPE is a value between 0 and 5 where each number corresponds to a certain group of particles according to the following:

PTYPE=0 Particles that interact so strongly with the suraounding medium that they they can be assumed to be stopped before decay and hence they can be neglected as high energy muon neutrino producers.

PTYPE=1 b-mesons that may interact before decay.

PTYPE=2 c-mesons that may interact before decay.

PTYPE=3 b-baryons that may interact before decay.

PTYPE=4 c-baryons that may interact before decay.

PTYPE=5 Particles that decay fast enough so that their interactions can be neglected.

Remarks: Called by HADINT.

SUBROUTINE **INIT**(ENU, TARG, LIN, ITYP)

Purpose: To initialize PYTHIA.

Input:

ENU Maximum neutrino energy in GeV.

TARG Target nucleon, +1 for proton and 0 for neutron.

LIN Particle code for incoming lepton, +14 for muon neutrino and -14 for anti muon neutrino.

ITYP Type of interaction to simulate, 'NC' for neutral currents and 'CC' for charged currents.

Procedure: Set switches and initialize PYTHIA.

Calls to: PYINIT of PYTHIA.

SUBROUTINE **NUINT**(ENU, KF, NNUI)

Purpose: To simulate the neutrino interactions on the way out of the Sun.

Input:

ENU Neutrino energy (in GeV) before interactions.

KF Particle code for the neutrino, +14 for muon neutrino and -14 for anti muon neutrino.

Output:

ENU Neutrino energy after interaction in GeV. The energy is put to -1.0 GeV if the neutrino is absorbed.

NNUI The number of interactions that the neutrino has participated in.

Procedure: The mean free path and the probability for interaction is calculated. If an interaction takes place and it is a neutral current, the interaction is simulated with PYTHIA from where the scattered neutrino energy is obtained. The procedure is described in sec. 4.2.

SUBROUTINE **NUINTS**(ENU, KF)

Purpose: To calculate the neutrino interactions on the way out of the Sun.

Input:

ENU Neutrino energy before interaction in GeV.

KF Particle code for the neutrino, +14 for muon neutrino and -14 for anti muon neutrino.

Output:

ENU Neutrino energy after interactions in GeV. The energy is put to -1.0 GeV if the neutrino is absorbed.

Procedure: The energy loss is assumed to be continous and the absorption process (charged current) is considered separately of the energy loss process (neutral current) according to the procedure of Ritz and Seckel [11].

Calls to: NUABS and NUSTO.

Remarks: This routine is only used for comparison with the routine NUINT.

SUBROUTINE **NUABS**(ENU, KF)

Purpose: To handle the absorption of neutrinos and antineutrinos on the way out of the Sun.

Input:

ENU Neutrino energy at the core of the Sun in GeV.

KF Particle code for the neutrino, +14 for muon neutrino and -14 for anti muon neutrino.

Output:

ENU The energy is put to -1.0 GeV if the neutrino is absorbed, otherwise it is unchanged.

Procedure: The absorption probability is calculated with the method of Ritz and Seckel [11].

Remarks: This routine is called by NUINTS and is only used for comparison with the routine NUINT.

SUBROUTINE **NUSTO**(ENU, KF)

Purpose: To calculate the energy loss of neutrinos and antineutrinos on the way out of the Sun.

Input:

ENU Neutrino energy before interactions in GeV.

KF Particle code for the neutrino, +14 for muon neutrino and -14 for anti muon neutrino.

Output:

ENU Neutrino energy after interactions in GeV.

Procedure: The energy loss is assumed to be continous and is calculated according to the procedure of Ritz and Seckel [11].

Remarks: This routine is called by NUINTS and is only used for comparison with the routine NUINT.

SUBROUTINE **MUSIM**(IEV, KFNU, WH)

Purpose: To simulate the charged current interaction in the ice, to calculate the energy of the muon at an imaginary plane in the ice and to write information to the common blocks SUDAT or EADAT.

Input:

IEV — Index to the entry of the variable NUDAT in the common block NEUTRINO to study.

KFNU — Particle code for the muon neutrino.

WH — From where the neutrino comes. WH='SU' for the Sun and 'EA' for the Earth. The difference is where the result is written and if a smearing of the angle θ should be done or not (see sec. 5.3).

Output: Muon data are written to the common block SUDAT or EADAT and the muon fluxes in the common block FLUXES are updated.

Procedure: The charged current interaction is taken care of GENMU, the muon energy at an imaginary plane is calculated with EMUDET and the contribution to the muon flux in the ice is calculated with DFLUX and if WH='EA' it is corrected with $1/D^2$ where D is the actual distance from the annihilation place to the detector obtained from MUANG. The fact that annihilation does not take place exactly in the core of the Earth (which yields the smearing of θ) is taken care of MUANG.

Calls to: GENMU, MUCREA, DFLUX, EMUDET and MUANG.
HF1 and HFN of HBOOK.

SUBROUTINE **GENMU**(ENU, EMU, THETA)

Purpose: To simulate a charged current interaction in the ice and extract relevant data for the resulting muon.

Input:

ENU — Neutrino energy in GeV.

Output:

EMU — Energy (GeV) of the outgoing muon.

THETA — The angle (degrees) between the neutrino direction and the muon direction.

Procedure: The charged current interaction is simulated with PYTHIA.

Calls to: PYEVNT, LUEDIT, LULIST and PLU of JETSET and PYTHIA.

SUBROUTINE **MUCREA**(ENU, EMU, THETA, PART)

Purpose: To create a muon from an incoming muon neutrino.

Input:

ENU — Neutrino energy in GeV.

PART — Particle code for the neutrino, +14 for muon neutrino and -14 for anti muon neutrino.

Output:

EMU — Muon energy in GeV.

THETA — Angle of the muon relative to the neutrino in degrees.

Procedure: The muon is created with an energy according to a simple parametrization of the cross section, $d\sigma/dE_\mu$.

Remarks: The routine is only used as an approximate method for low energies ($E_\nu <$ ENUMIN in the common block NEUTRINO) where the more accurate simulation, taken care of GENMU, is very time consuming.

REAL FUNCTION **DFLUX**(ENU, EMU, PART, WH)

Purpose: To calculate the contribution to the muon flux from a single muon.

Input:

ENU — Energy of the neutrino in GeV that the muon originated from.
EMU — Energy of the muon in GeV.
PART — Particle code for the neutrino, +14 for muon neutrino and -14 for anti muon neutrino.
WH — Where the neutrino comes from. WH='SU' for the Sun and 'EA' for the Earth.

Output:
DFLUX — The contribution to the muon flux in the ice from this specific event. Unit: 10^{-30} m^{-2}.

Procedure: The contribution to the flux is calculated with eq. (81).

Calls to: XSECTN and MURANG.

Remarks: The distances from the source to the detector that the routine uses are the mean distance from the core of the Sun to the core of the Earth if WH='SU' and the Earth radius if WH='SU'. In the case of the Earth where the actual distance differs quite a lot from this value a correction has to be made afterwards.

REAL FUNCTION **XSECTN**(ENU, PART, TARG, ITYP)

Purpose: To calculate the cross section for the neutral or charged current reaction $\nu + N \to \nu + X$ or $\nu + N \to \mu + X$

Input:
ENU — Incoming neutrino energy in GeV
PART — Particle code for the neutrino, +14 for muon neutrino and -14 for anti muon neutrino.
TARG — Fraction of protons in the target.
ITYP — Type of interaction, 'NC' for neutral current and 'CC' for charged current.

Output:
XSECTN — The cross section for the process in b = 10^{-24} cm^2.

Procedure: The cross section is assumed to depend linearly on the neutrino energy and the coefficients are those of sec. 4.1.

REAL FUNCTION **MURANG**(EMU)

Purpose: To calculate the range of a muon of energy EMU.

Input:
EMU — Muon energy in GeV.

Output:
MURANG — Range of the muon in cm.

Procedure: The range is calculated with eq. (68) and the numerical values of eq. (67).

REAL FUNCTION **EMUDET**(EMU)

Purpose: To calculate the energy of a muon as it reaches an imaginary plane in the ice.

Input:
EMU — Muon energy at creation in GeV

Output:
EMU — Muon energy at the plane in GeV.

Procedure: The energy of the muon is calculated with the procedure described in sec. 5.2.

SUBROUTINE **MUANG**(THETA, D, MNEU)

Purpose: To simulate the angle between a muon in the detector and the direction from the core of the Earth to the detector according to sec. 5.3.

Input:

THETA — The angle between the muon and the neutrino direction in the charged current interaction.

MNEU — The mass of the neutralino in GeV.

Output:

THETA — The angle between the muon and the direction from the core of the Earth to the detector.

D — The distance from the point of annihilation to the detector in units of the Earth radius.

Procedure: The place of annihilation in the Earth is chosen and from that the smearing and the distance D is calculated according to the procedure in sec. 5.3.

SUBROUTINE **DATRES**(IEV,WH)

Purpose: To reset the data in the common block SUDAT or EADAT to values from NUDAT(IEV,...)

Output: If WH='SU', VARS of common block SUDAT is reset and filled with values from NUDAT(IEV,...) and if WH='EA', VARE of common block EADAT is reset and filled with value from NUDAT(IEV,...).

SUBROUTINE **DATSAV**(IEV,WH)

Purpose: To save the data in the common block SUDAT or EADAT to corresponding NTUPLE and to add entries to histograms.

Output: If WH='SU' VARS is saved to NTUPLE 50 of the file `numu.hbook` and if WH='EA' VARE is saved to NTUPLE 51 of the file `numu.hbook`.

COMMON/**NEUTRINO**/NUI, NNUINT, NUF, ENUMIN, ENUMAX, ENUINI, NUDAT(100000,7), OUTPUT, EARTH

Purpose: General information about the simulation and some intermediate data.

Variables:

NUI — Number of entries in NUDAT.

NNUINT — Number of muon neutrinos and anti neutrinos that has got out of the Sun.

NUF — Number of generated muon neutrinos and anti neutrinos.

ENUMIN — Lowest neutrino energy (in GeV) for which simulation with PYTHIA takes place.

ENUMAX — Maximum possible neutrino energy (in GeV), i.e. the neutralino mass.

ENUINI — The maximum neutrino energy (in GeV) used in the initialization of PYTHIA.

NUDAT(I,J) — Data about the generated neutrinos. This variable is used to store data before processing them further and writing them to a file. Data about the I:th neutrino found is located in NUDAT(I,J) where the entries for different values of J are:

J=1 — Neutrino energy (GeV) directly after production in the Sun (energy loss of hadrons is included).

J=2 — Particle code for the parent particle of the neutrino, e.g. 511 if the neutrino originates from B^0 decay.

J=3 Particle code for the neutrino, +14 for muon neutrinos and -14 for anti muon neutrinos.
J=4 Neutrino energy (GeV) after interaction with the solar medium on the way out of the Sun. Put to -1 if the neutrino is absorbed.
J=5 Neutrino energy (GeV) directly after production in the Earth (energy loss of hadrons is included).
J=6 Total number of interactions that the parent hadrons have participated in.
J=7 The number of interactions that the neutrino has participated in on the way out of the Sun.

OUTPUT Equal to .TRUE. if event listings should be printed while running.
EARTH Equal to .TRUE. if annihilation in the Earth should be included as well.

COMMON/**FLUXES**/FLUX(4,10), FLUXE(4,10), EMUTH(10), ANGTH(3), NFL(4,10), NFLE(4,10)

Purpose: To store the calculated muon fluxes above certain thresholds.
Variables:
EMUTH(I) Thresholds for the muon energy in GeV.
ANGTH(I) Upper threshold for the angle θ, where θ is the angle between the direction of the muon and the direction from the source of neutrinos to the detector. In case of annihilation in the Earth, the actual place of annihilation is used to obtain the correct angle.
FLUX(J,I) Muon flux (10^{-30} m^{-2} parent pair^{-1}) from the Sun above the threshold specified in EMUTH(I) and with θ below that specified in ANGTH(J). In FLUX(4,I) only the energy cut is applied.
FLUXE(J,I) As above but from the core of the Earth.
NFL(J,I) Number of found neutrinos or antineutrinos on which the calculation of the fluxes in FLUX(J,I) is based.
NFLE(J,I) Number of found neutrinos or antineutrinos on which the calculation of the fluxes in FLUXE(J,I) is based.

COMMON/**ANNICH**/KF1(15), KF2(15), ACH, ACHMAX

Purpose: To store information about the different annihilation channels.
Variables:
KF1(I) Particle code for the first annihilation product in channel I.
KF2(I) Particle code for the second annihilation product in channel I.
ACH The chosen annihilation channel.
ACHMAX The number of channels available for simulation.

COMMON/**XS**/ANUP, ANUN, AANUP, AANUN, BNUP, BNUN, BANUP, BANUN

Purpose: To store information about the total charged and neutral current cross sections as calculated in sec. 4.1.
Variables:
A... Charged current cross sections coefficients, a, in $\sigma = aE_\nu$. Unit: 10^{-39} cm^2 GeV^{-1}.
B... Neutral current cross sections coefficients, b, in $\sigma = bE_\nu$. Unit: 10^{-39} cm^2 GeV^{-1}.

COMMON/**SUN**/IP, IN

Purpose: To store information about the effective thickness of the Sun as calculated in sec. 4.2.

Variables:

IP Effective thickness (in g/cm^3) of protons in the Sun according to eq. (51).

IN Effective thickness (in g/cm^3) of neutrons in the Sun according to eq. (52).

COMMON/**DET**/PFRACT, DENS

Purpose: To store information about the detector.

Variables:

PFRACT Number fraction of protons in the detector medium, e.g. $10/18 = 0.55555\ldots$ for ice.

DENS Density of the detector medium in g/cm^3.

COMMON/**SUDAT**/VARS(11)

Purpose: To store information (which eventually will be written to an NTUPLE) about one event in the Sun.

Variables:

VARS(1) Neutrino energy (in GeV) after interacions on the way out of the Sun. Put to -1.0 if the neutrino is absorbed.

VARS(2) Muon energy (in GeV) at the detector.

VARS(3) The angle θ, which is the angle of the muon relative to the direction from the Sun to the Earth.

VARS(4) The contribution to the muon flux from this event according to eq. (81).

VARS(5) Neutrino energy (in GeV) before interactions in the Sun (but with energy loss of hadrons included).

VARS(6) The particle code for the particle from which the neutrino originated.

VARS(7) The particle code for the neutrino, i.e. +14 for neutrinos and -14 for antineutrinos.

VARS(8) The muon energy (in GeV) before energy losses in the ice.

VARS(9) Number of interctions that the neutrino has participated in on the way out of the Sun.

VARS(10) The total number of interactions for all parent hadrons of the neutrino.

VARS(11) The neutrino energy (in GeV) after interactions on the way out of the Sun calculated with NUINTS. Included for comparison with VARS(1).

Remarks: These variables are written to NTUPLE 50 in the file `numu.hbook` and if full output is chosen (NTF of common block NEUTRINO equal to .TRUE.) all 11 variables are written, but if limited output is chosen, only the first four variables are written.

COMMON/**EADAT**/VARE(10)

Purpose: To store information (which eventually will be written to an NTUPLE) about one event in the Sun.

Variables:

VARE(1) Neutrino energy (in GeV) after after creation (energy loss of hadrons included).

VARE(2) Muon energy (in GeV) at the detector.

VARE(3) The angle θ, which is the angle of the muon relative to the direction from the core of the Earth to the detector.

VARE(4)	The contribution to the muon flux from this event according to eq. (81).
VARE(5)	The particle code for the particle from which the neutrino originated.
VARE(6)	The particle code for the neutrino, i.e. +14 for neutrinos and -14 for antineutrinos.
VARE(7)	The muon energy (in GeV) before energy losses in the ice.
VARE(8)	The angle β, which is the angle between the direction from the point of neutralino annihilation to the detector and the direction from the core of the Earth to the detector.
VARE(9)	The angle θ', which is the angle between the direction of the muon and the direction of the neutrino from which it is created.
VARE(10)	The distance from the point of neutralino annihilation to the detector at the surface of the Earth in units of the Earth's radius.
Remarks:	These variables are written to NTUPLE 51 of the file `numu.hbook` and if full output is chosen (NTF of common block NEUTRINO equal to .TRUE.) all 10 variables are written, but if limited output is chosen, only the first four variables are written.

BLOCK DATA **START**

Purpose: To set various common block variables to their initial values.

B.3 Implementation of new things

If one wants to change some of the constants used in the simulation, such as cross sections, characteristics of the detector, cuts in E_μ^{det} and θ etc. one only has to change the constants in the corresponding common block described above. If one wants to include new processes or more accurate ways of treating things, the routines above can be replaced with new ones with the aid of the program description above.